In-operando X-ray analysis of temperature-responsive changes in layered structure of polymer ultrathin films

Yuwei Liu

February 2020

In-operando X-ray analysis of temperature-responsive changes in layered structure of polymer ultrathin films

Yuwei Liu
Doctoral Program in Materials Science and Engineering

Submitted to the Graduate School of
Pure and Applied Sciences
in Partial Fulfillment of the Requirements
for the Degree of Doctor of Philosophy in Engineering

at the
University of Tsukuba

Table of Contents

Abstract

The revolution of the analysis technique would be one of the most activity engine for the materials science, especially the development of the in-operando analysis technique. With the recording of the states of sample in the different environments, the in-situ dynamic study of the functional material system becomes favorable, and as the development of the resolution of data recording, the kinetic study can be also conducted simultaneously. However, with the increasing requirements from the academic and industry, the developing of materials science was stranding by the barriers of technique. For example, in the semiconductor industry, many characterizing of the products cannot be conducted in their factory and have to only be conducted in the large facility, such as the synchrotron. However, the most useful information is still the states of the product during the annealing or etching in the production line. Thus, the development of the in-operando analysis technique for laboratory condition is always promising.

This time, a new in-operando X-ray reflectivity technique has been customized for the laboratory conditions, which shown great potential on the study of the ultrathin film system. With the design of the pinhole optic, the specular reflection of the full exiting angle can be received by the pixel detector simultaneously, which greatly reduced the time for data collection and avoided the mechanical motion during the measurement. Meanwhile, the frequency analysis method - Fourier transfer analysis, has been also developed for the free-model research. Both advantages have contributed the in-operando X-ray reflectivity analysis in the laboratory. Taking this as a starting point, the fundamental research on the polymer ultrathin films has been conducted. As the results, many abnormal phenomena have been confirmed in the different polymer ultrathin film system, such as the negative thermal expansion (NTE) in Polyvinyl acetate (PVAc) ultrathin film, the asymmetric swelling/ shrinking in Poly(N-isopropylacrylamide) (PNIPAM) ultrathin film, and the crystallization of the gamma phase in deposited Nylon 6 thin film, which have been never reported or discussed well in the past. In the laboratory, the systematic research has been conducted for these phenomena, and then some new hypothesis has been proposed. It is believed that these phenomena should also exist widely in other polymer ultrathin film systems, such as engineering materials that have been extensively studied.

In the PVAc ultrathin film system, the new finding has been confirmed in this amorphous material, which is one of the most common polymers with the glass transition temperature (Tg) around 31° C. In the temperature cycle between the 19 ° C and 45 ° C, two different instances of the NTE have been confirmed in this polymer ultrathin film, although it was believed that the NTE can only occur with change in the crystal structure. When the sample was kept at the 45 ° C for aging, one slow thickness decreasing has been observed. However, when the temperature below the Tg, one reversible NTE has been confirmed in the temperature cycle. It is found that not only did NTE show a dependence on the thickness of thin film, but also it would change after the different thermal treatments. In the discussion, the trilayers model has been proposed for the thermal expansion in polymer ultrathin film system. It is assumed that one interface layer can gradually formed at the rubbery state with the interface interaction. Because of the different orientation of the polymer chain in the constrained layer, the internal stress would occur with

temperature between the interface layer and its adjacent region, resulting in the additional deformation in the amorphous polymer ultrathin film.

On the other hand, one asymmetric swelling/shrinking associated with hydrophobic/ hydrophilic transition of PNIPAM has been confirmed in its ultrathin film under the atmospheric conditions, although it was generally accepted that the hydrophobic/ hydrophilic transition should be reversible and only occur with bulk water. In the temperature cycle between 15 and 60 ° C, heating and cooling resulted in some clear differences. During cooling, initially, the thickness was almost constant but began to increase when the temperature exceeded 33° C, while the reversible response was not observed during heating. With moisture control experiments, it is confirmed that the hydrophobic/hydrophilic transition can happen in the PNIPAM thin film as the temperature scanning across the lower critical solution temperature (LCST) at 33° C, causing swelling/shrinking. Considering the different mobility of the polymer chain in the boundary layers, it is proposed that the transition ability of PNIPAM can be different at the surface and interface layer. Due to hydrophobic/hydrophilic transition at the surface, the absorption of moisture shown the temperature dependence. However, the interface is always hydrophobic, and the adsorption of moisture would show any temperature dependence. Thus, the asymmetric swelling/shrinking was observed in the PNIPAM ultrathin film in temperature cycle.

Finally, we have also developed the physical evaporation deposition method for the preparation of polymer ultrathin film. The high-quality nylon 6 ultrathin film has been prepared by the molecular beam epitaxy (MBE) setup. The relationships between deposition kinetics and the structure were discussed in the results and the Raman spectroscopy suggests that organic functionalities characteristic of the nylon structure was retained. Future more, the gamma phase has been only found in this ultrathin film, which was also proposed to the kinetics of deposition process. In this nylon 6 thin film, the great swelling and the shift of T_g have been observed. It is suggested that the interface interaction and gamma phase structure contracture to this property in nylon 6 ultrathin film.

Chapter 1

Introduction

For each material system, the dynamic and kinetic properties are always the most interesting topic for the academic and industry. Just like the tone of the instrument, the unique response of the materials system can help me identify their useful for the each proposes. However, the “tone” is a series states of the instrument with stimulation. Although the complex sound signal can be easily recorded by our ears, the monitoring of the state of the material systems is always difficult. And thus, one new discipline has been developed for the analysis of dynamic and kinetic properties of material system, called the in-operando analysis. The in-operando analysis is not only important for the academic researches, such as the study of the dynamic and kinetic of materials system, but only worthwhile to the industry process, which cannot be stopped once they are started. In the past century, the in-operando analysis has long been already applied to various disciplines, such as optics, electricity, and thermodynamics, and has made great contributions to the development. However, the in-operand analysis of material systems is also not an easy process. Especially, as the requirements of materials system from industry and academic is getting higher and higher, in many cases, the developing of materials science was stranding by the barriers of this technique. For example, in the semiconductor industry, many characterizing of the products cannot be conducted in their factory and have to only be conducted in the large facility, such as the synchrotron. However, the most useful information is still the states of the product during the annealing or etching in the production

line. Thus, the development of the in-operando analysis technique for laboratory condition is always promising. In my work, a new in-operando X-ray reflectivity technique has been customized for the laboratory conditions, which shown great potential on the study of the ultrathin film system. With the design of the pinhole optic, the specular reflection of the full exiting angle can be received by the pixel detector simultaneously, which greatly reduced the time for data collection and avoided the mechanical motion during the measurement. Meanwhile, the frequency analysis method - Fourier transfer analysis, has been also developed for the free-model research. Both advantages have contributed the in-operando X-ray reflectivity analysis in the laboratory. Taking this as a starting point, the fundamental research on the polymer ultrathin films has been conducted in my PhD program.

Polymer ultrathin film system is a very interesting and susceptible system because its properties can change dramatically due to only small changes of structure or dynamics at the interface.[1–7] However, only a few researchers have realized that there are substantial changes on moving from the bulk to ultrathin films; specifically, the contribution of the surface layer and the interface layer in the system gradually increases, and, consequently, knowledge of the bulk system is not applicable to the thin-film system because the kinetical and dynamical behavior of the polymer chains can be quite different within the thin-film boundary conditions.[8–10] With the in-operando analysis, many abnormal phenomena have been confirmed in the different polymer ultrathin film systems in past, and these abnormal phenomena may have a huge impact on the engineering process. For example, the glass transition temperature (T_g), which may be considered the most important characteristic of polymer, can greatly change with the confinement effect from the interface in an ultra-thin film system.[11–14] And the de-wetting process, which is the primary factor in structure collapse and is generally accepted to occur only in the rubber state, can also happen in the glassy state in thin film systems.[15–17] But, it is a pity that these researches in this area is still. There are only few reports with experimental data in the past, and the discussions of the mechanism were also always contradictory. One of reasons is the limitation in the analysis technique. Although many powerful techniques have been already developed for the nano structure, such as transmission electron microscope (TEM), scanning electron microscope (SEM), and atomic force microscope (AFM), the in-operando analysis of the nano-layer structure was still difficult for laboratory conditions in the past.

In this doctoral thesis, the layer structure of the polymer ultrathin film with their thermal responsive behaviors have been discussed with the in-operando X-ray reflectivity analysis. Depending on the advanced multi-channel X-ray reflectometer,[18,19] some abnormal behaviors which would represent the unknown area in our knowledge of polymer ultrathin film systems have been successfully confirmed in these works.[20–23] In the following chapters, the X-ray reflectivity technique has been simply introduced first, and then three main research subjects have been presented in detail. In the polyvinyl acetate (PVAc) thin film and poly(N-isopropylacrylamide) (PNIPAM) ultrathin film, the abnormal structure change of these polymer ultrathin films has been observed with temperature scan, respectively, such as the negative thermal expansion and the asymmetric swelling/shrinking with hydrophobic/ hydrophilic transition. Meanwhile, we have also tried to develop the new method for the preparation of polymer ultrathin film. The high-quality nylon 6 ultrathin film has been prepared by the molecular beam epitaxy (MBE) setup.

The relationships between deposition kinetics and the structure of the gamma phase were discussed in the results. As discussion of the mechanism for the above phenomena, the contribution of the interface interaction has been proposed for the change in the orientation, activity energy and the mobility of the polymer chain in the boundary layers. It is suggested that these phenomena would be also widely existed in other polymer ultrathin film systems, although some of them have been already studied extensively before.

Uniaxial negative thermal expansion of polyvinyl Acetate (PVAc) thin film

In this section, it reports some experimental observation of reproducible uniaxial negative thermal expansion (u-NTE) in amorphous polyvinyl acetate (PVAc) ultra-thin film. It has been found that the mechanism of the phenomena is different from latest reports on so called negative thermal expansion (NTE) in crystal or other topological materials. It is known that PVAc exhibits glass transition at around 31 ° C. During cooling from the high-temperature side, one can observe the decrease of the thickness by monitoring interference fringes in X-ray reflectivity curve as a function of temperature. When across the glass transition, however, the thickness starts to increase, instead of reducing. In the heating process, the thickness decreases as long as the temperature is lower than that for glass transition (Tg). In the present research, such changes in thickness during repeated heating/cooling cycles have been studied systematically. To discuss the mechanism, dependence on film thickness has been investigated as well. It has been found that the present phenomena are well explained as u-NTE, which induces reduction and increase of thickness (z-direction) just by thermal expansion and shrinking in x-y directions, respectively. This would be caused and enhanced by the growth of a mechanically hard, high-density layer near the interface to the surface of hydrophilic silicon dioxide. The structural change during heating cycles is discussed in detail.

Two different instances of NTE in polyvinyl acetate (PVAc) thin films were discovered in a temperature cycle from 45 ° C to 19 ° C for the first time; and the NTE even in much thicker film such as 130 nm, was observed that might not be well understood from the past research. In the experiment, commercial PVAc thin films, with a glass transition temperature around 31 ° C, were prepared on silicon wafer by spin coating, and the structure change with temperature was studied by the multi-channel X-ray reflectometry. In the repeated temperature cycles, an increase in the thickness of PVAc thin film was confirmed in its glassy state with temperature cooling, and when the PVAc thin film was in its rubbery state, a slow decreasing in thickness was observed in the resting stage between each temperature cycles. These two different instances of NTE were confirmed as dependent on dynamics and kinetics respectively. On the other hand, another interesting finding is that performance of NTE exhibits differences with total thickness. especially in PVAc ultrathin film (of 12 nm). The thickness of the polymer ultrathin film can continue to decrease with temperature heating even in its rubber state.

In the discussion, the Tri-layer model has been first proposed in this work for the detail mechanism of NTE in polymer ultrathin film system. In the postulated model, a PVAc thin film is considered to consist of three different layers with the space distribution of polymer chain, which is called interface layer,

transition layer and normal layer. It is proposed that the boundary layer can exist and vary with the conditions of the polymer thin-film system, causing the additional deformation of the polymer thin film with temperature. In the ultrathin film system, interface interaction considerably contributes to dynamics and kinetics of the polymer chain, and one possibility is that the spatial distribution of polymer chains near the interface can gradually change in depth from 3D to 2D parallel to the surface of substrate and result in the decrease in free volume. It is proposed that the interface layer can be formed in the rubber state and then be further frozen in the glassy state with a larger coefficient of thermal expansion parallel the surface of substrate. With temperature change in its glassy state, the interface layer can contribute to the additional deformation to the up-side layer, called the transition layer, by each buried entanglement with normal thermal expansion. On the other hand, in the polymer thin film, such as the thickness of 130 nm, the bulk-like surface layer can exist, which is called the normal layer and show normal thermal expansion with temperature. In the Tri-layer model, NTE can be only related to the performance of the interface layer and transition layer. The observation of thermal expansion of PVAc thin film systems can vary with the competition between normal thermal expansion and NTE in temperature cycle.

Asymmetric change in Poly(N-isopropylacrylamide) (PNIPAM) ultrathin film with temperature cycle

In this section, the unusual behaviors of PNIPAM has been first observed in the ultrathin film system under the ambient conditions. It is proposed that the transition ability of PNIPAM would be more complicated due to the few water amounts in the environment and the different states of the polymer chain in the ultrathin film system. In the experiment, commercial PNIPAM thin films were prepared on silicon wafer by spin coating, and the structure change with temperature was studied by the customized multichannel X-ray reflectometry in different strategies. During the discrete monitoring, the thicknesses of PNIPAM ultrathin film were recorded over two months. Continuous recovery and increases in the thickness of PNIPAM ultrathin films were observed after each individual heating treatment at 70 ° C for 3 h. On the other hand, an asymmetric change in the thickness of PNIPAM ultrathin film was observed on temperature cycling between 15 and 60 ° C during the operando monitoring. In the cooling process, the thickness of PNIPAM ultrathin film was stable first, but then abruptly increased as the temperature below the LCST. In contrast, in the heating process, the thickness of PNIPAM ultrathin film monotonically decreased with increasing temperature. To clarify the contributions of different kinetic processes, moisture control monitoring, and long-term monitoring were conducted. As the results, we confirmed that the changes in thickness is resulted from the sorption of water with the transition of PNIPAM, but this asymmetric behavior is only caused by thermal treatment at ambient conditions with finite-time observation.

Finally, one model has been postulated based on the inhomogeneity of the mobility of polymer chain in the ultrathin film system. The surface layer and interface layer would have different phase transition properties, and this difference may result in the asymmetrical behavior during temperature cycling. It is proposed that the polymer chains in the surface layer of PNIAPM ultrathin film can be highly mobile, and, as the temperature rises, these polymer chains may aggregate with thermal motion completing a transition

from the hydrophilic to hydrophobic state. In contrast, the polymer chains in the interface layer would be further constrained by interfacial interactions, and the transition would be more difficult than other regions. During the temperature cycle, the surface layer would be like an automatic door which can respond to the temperature for absorption of water, whereas the interface layer would be like exit that is always open for evaporation. Therefore, it is proposed that the surface layer and interface layer dominate the absorption and desorption of water molecules in the temperature cycle, respectively, making the ultrathin film act like a "smart" pathway for the water vapor flow.

The discovering of ultrathin film forming and its property

In this section, it reports successful preparation of the thin film form of Nylon 6, well known due to its excellent physical and mechanical properties; however, the technique has been considered technically difficult thus far. Molecular beam epitaxy (MBE) apparatus was used for physical vapor deposition (PVD). The obtained thin film was studied by Raman spectra and X-ray diffraction analysis, and the results were compared with those for the Nylon 6 solid powder, used as the PVD source. It was found that the main structures were similar, but the γ phase of Nylon 6 has only been observed in the deposited film. Regarding to this phenomenon, it is proposed that the PVD process and interface interaction have had an impact on the formation of the hydrogen bond. During the deposition process, the heating temperature was set around 190 to 220 ° C, which may contribute to rapid crystallization. The interface interaction would also suppress the rearrangement of the chain for the intermolecular hydrogen bonding. Furthermore, the stacking of polymer chains would be favored in the deposition process. All factors contributed the intramolecular hydrogen bonding in γ phase crystal. On the other hand, with changing the deposition time, a variety of thicknesses ranging from 20 to 100 nm was obtained. These were studied by X-ray reflectivity analysis and scanning probe microscopy (SPM). It was noted that the deposition rate strongly influences the quality of the thin film, which may be related to the kinetics of the formation of the entanglement in the polymer system.

Finally, the temperature-stability of Nylon 6 thin film was investigated by in-operando X-ray reflectivity measurement. During the temperature scan from 10 to 70 ° C under ambient conditions, the greatest thickness reduction of 1.7% occurred when the temperature was below 28 ° C. Above 28 ° C, there was no clear change in the coefficient of thermal expansion, although the glass transition of Nylon 6 can happen around 47 ° C. Moisture control experiments revealed that some swelling can occur in the Nylon 6 thin film. The present results could suggest some interface interaction, and it is also suggested that the existence of γ phase Nylon 6 crystal might contribute to the shift of Glass transition temperature (Tg).

Reference

(1) Forrest, J. A.; Dalnoki-Veress, K.; Dutcher, J. R. Interface and Chain Confinement Effects on the Glass Transition Temperature of Thin Polymer Films. *Phys. Rev. E - Stat. Physics, Plasmas, Fluids, Relat. Interdiscip. Top.* **1997**, *56* (5), 5705–5716.

(2) Fukao, K.; Miyamoto, Y. Glass Transitions and Dynamics in Thin Polymer Films: Dielectric Relaxation of Thin Films of Polystyrene. *Phys. Rev. E* **2000**, *61* (2), 1743–1754.

(3) Pochan, D. J.; Lin, E. K.; Satija, S. K.; Wu, W. Thermal Expansion of Supported Thin Polymer Films: A Direct Comparison of Free Surface vs Total Confinement. *Macromolecules* **2001**, *34* (9), 3041–3045.

(4) Stafford, C. M.; Vogt, B. D.; Harrison, C.; Julthongpiput, D.; Huang, R. Elastic Moduli of Ultrathin Amorphous Polymer Films. *Macromolecules* **2006**, *39* (15), 5095–5099.

(5) Kline, R. J.; McGehee, M. D.; Toney, M. F. Highly Oriented Crystals at the Buried Interface in Polythiophene Thin-Film Transistors. *Nat. Mater.* **2006**, *5* (3), 222–228.

(6) Bal, J. K.; Beuvier, T.; Unni, A. B.; Chavez Panduro, E. A.; Vignaud, G.; Delorme, N.; Chebil, M. S.; Grohens, Y.; Gibaud, A. Stability of Polymer Ultrathin Films (< 7 Nm) Made by a Top-down Approach. *ACS Nano* **2015**, *9* (8), 8184–8193.

(7) Liu, Y.; Sakurai, K. Thermoresponsive Behavior of Poly (N-Isopropylacrylamide) Solid Ultrathin Film under Ordinary Atmospheric Conditions. *Chem. Lett.* **2017**, *46* (4), 495–498.

(8) Wattenbarger, M. R.; Chan, H. S.; Evans, D. F.; Dill, K. A. Surface‐induced Enhancement of Internal Structure in Polymers and Proteins. *J. Chem. Phys.* **1990**, *93* (11), 8343–8351.

(9) Gennes, P. De. Glass Transitions in Thin Polymer Films. *Macromolecules* **2000**, *205*, 201–205.

(10) Bal, J. K.; Beuvier, T.; Unni, A. B.; Chavez Panduro, E. A.; Vignaud, G.; Delorme, N.; Chebil, M. S.; Grohens, Y.; Gibaud, A. Stability of Polymer Ultrathin Films (<7 Nm) Made by a Top-Down Approach. *ACS Nano* **2015**, *9* (8), 8184–8193.

(11) Wallace, W. E.; Van Zanten, J. H.; Wu, W. L. Influence of an Impenetrable Interface on a Polymer Glass-Transition Temperature. *Phys. Rev. E* **1995**, *52* (4), R3329–R3332.

(12) DeMaggio, G. B.; Frieze, W. E.; Gidley, D. W.; Zhu, M.; Hristov, H. A.; Yee, A. F. Interface and Surface Effects on the Glass Transition in Thin Polystyrene Films. *Phys. Rev. Lett.* **1997**, *78* (8), 1524–1527.

(13) Tsui, O. K. C.; Russell, T. P.; Hawker, C. J. Effect of Interfacial Interactions on the Glass Transition of Polymer Thin Films. *Macromolecules* **2001**, *34* (16), 5535–5539.

(14) White, R. P.; Price, C. C.; Lipson, J. E. G. Effect of Interfaces on the Glass Transition of Supported and Freestanding Polymer Thin Films. *Macromolecules* **2015**, *48* (12), 4132–4141.

(15) Reiter, G. Dewetting as a Probe of Polymer Mobility in Thin Films. *Macromolecules* **1994**, *27* (11), 3046–3052.

(16) Reiter, G. Dewetting of Highly Elastic Thin Polymer Films. *Phys. Rev. Lett.* **2001**, *87* (18), 186101.

(17) Reiter, G.; Hamieh, M.; Damman, P.; Sclavons, S.; Gabriele, S.; Vilmin, T.; Raphaël, E. Residual Stresses in Thin Polymer Films Cause Rupture and Dominate Early Stages of Dewetting. *Nat. Mater.* **2005**, *4* (10), 754–758.

(18) Sakurai, K.; Mizusawa, M. X-Ray Reflectometer and the Measurement Method. 3903184, 2007.

(19) Sakurai, K.; Mizusawa, M.; Ishii, M. *Recent Novel X-Ray Reflectivity Techniques: Moving Towards Quicker Measurement to Observe Changes at Surface and Buried Interfaces*; 2007; Vol. 32.

(20) Liu, Y.; Sakurai, K. Uniaxial Negative Thermal Expansion of Polyvinyl Acetate Thin Film. *Langmuir* **2018**, *34* (38), 11272–11280.

(21) Liu, Y.; Sakurai, K. Slow Dynamics in Thermal Expansion of Polyvinyl Acetate Thin Film with Interface Layer. *Polym. J.* **2019**, No. 51, 1073–1079.

(22) Liu, Y.; Sakurai, K. Thickness Changes in Temperature-Responsive Poly(N -Isopropylacrylamide) Ultrathin Films under Ambient Conditions . *ACS Omega* **2019**, *4* (7), 12194–12203.

(23) Liu, Y.; Sakurai, K. Thermoresponsive Behavior of Poly(N-Isopropylacrylamide) Solid Ultrathin Film under Ordinary Atmospheric Conditions. *Chem. Lett.* **2017**, *46* (4), 495–498.

Chapter 2

X-ray analysis for layer structure analysis

2.1 Introduction

In this doctoral program, the X-ray reflectivity analysis, which is the research on the interference of X-rays reflected from top and bottom interfaces in the layer structure, has been used for study on the layer structures of polymer ultrathin films,[1] as shown in Figure 1. As the oscillations shown in the X-ray reflectivity curve, which called as Kiessig fringes, one can conducted the calculation for the layer structure parameters, such as thickness, roughness, and density. [2] Since the short wavelength and the high penetration of X-rays, X-ray reflectivity analysis is extremely sensitive to the layered structure along the depth of the film at an angstrom-to-nanometer and would be necessary to make damage for sample preparation, which makes this technology widely used in the characterization of ultrathin film structures. Regarding to the classical X-ray reflectometer in laboratory, it usually works with the theta/2theta scanning to collect the reflection at each angle, which usually takes 1 to 2 hours to complete the plotting of the X-ray reflectivity curve. And then, with the fitting process based on the Parratt expression, one can solve the layer structures with the assumption model. However, with requirements on the in-operando analysis for the layer structure, the deficiencies of classical technique are gradually emerging. For the theta/2theta scanning technique, it always takes too much time for data collection, and it cannot avoid the error caused by the mechanical movement during the measurement. Although some of these deficiencies can be solved in the large facility, such as the synchrotron, the in-operando X-ray reflectivity analysis is still difficulted to be conducted in the laboratory for the study of the kinetics and dynamics in ultrathin film system.

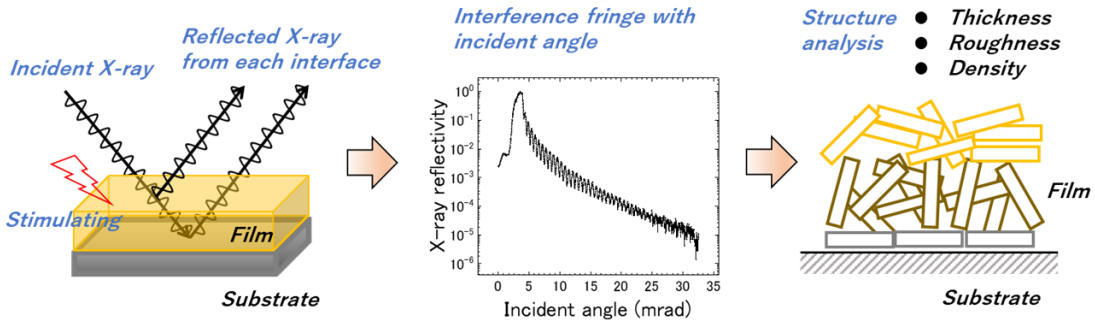

Figure 1. X-ray reflectivity analysis for the layer structure analysis. (Originally prepared for this thesis)

In my doctoral program, the customized multi-channel X-ray reflectometer have been used for the in-operando analysis in polymer ultra thin film.[3,4] The pinhole is cleverly designed into the optical path of the instrument that reflected X-ray at any angle can be collected by the pixel detector simultaneously. It not only greatly shortens the time for data collection, but also realizes static testing with this instrument. Meanwhile, the model free analysis method, Fourier transform, has been also developed for the study on change in polymer ultrathin film with the stimulation, which successfully solved the problem from the intention model. Furthermore, the temperature control system and moisture control system have been designed on the sample stage for the environment control. All such advantages make the in-operando X-ray reflectivity analysis become possible in laboratory. With the development of this technique, many abnormal phenomena have been first observed and studied in the polymer ultrathin film systems with a large number of experiments on the kinetics and dynamics in the laboratory.

2.2 X-ray reflectivity analysis for layer structure

A ray of light, when it propagates from one medium into another, will change its direction, which is called refraction of light. It is a most commonly observed phenomenon in the nature, which has been already quantitatively descripted by the Snell's law that

$$n_1 \cos a = n_2 \cos a'$$

where n1 and n2 are the refractive index of the two mediums, and α and α' are the glancing angle and exit angle as shown in Figure 2A. Regarding to the value of refractive index, it is related to the scattering property of the materials which has its own unique structure and can vary with the energy of the radiation, as shown in Figure 2B. For the visible light, the value of refractive index of most transparent materials is generally greater than 1, which can also change with the density of the materials system easily. But, with the energy increase, the value of refractive index would be less than 1 as it found to be true for X-ray that

$$n = 1 - \delta + i\beta$$

where δ is typically of the order of 10^{-5}, and β is much small than the δ. For the X-ray reflectivity analysis, when the R is much smaller than the unity, the absorption term β would be negligible. The expression of the scatter term δ can be written as

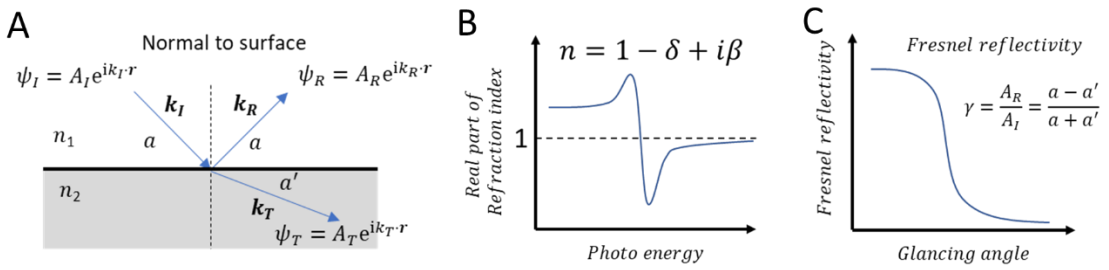

Figure 2. (A) The optical path of an incident X-ray at the interface; (B) the concept description of the real part of the refraction index with photo energy; (C) the concept description of the Fresnel reflectivity with angle. (Originally prepared for this thesis)

$$\delta = \frac{2\pi\rho_{at} f^0 \gamma_0}{k^2}$$

where ρ_{at} is the atomic density number density and f^0 is the atomic scattering factor, which are related to property of material. The scattering amplitude per electron is a constant, γ_0 = 2.82*10^{-5} Å, and the wavenumber is related to the wavelength that $k = 2\pi / \lambda$. It can be found that the δ is quite small for the polymer material with X-ray radiation (Cu Kα of 1.54 Å) of the value about 3.8*10^{-6}. Therefore, for the analysis with X-ray radiation, it generally neglected the change in the refractive index, and the scattering length density (SLD) has been used for the calculation, which's expression can be written as,

$$SLD = \frac{\rho N_A \Sigma_{i=1}^{N} b_i}{\sum_{i=1}^{N} M_i}$$

where ρ is the bulk density and M is the molecular weight. The scattering length contributions b_i for the X-ray radiation can be expressed as

$$b_i = f_i^0 \gamma_0$$

and the SLD can be converted to the x-ray refractive index by

$$\delta = \frac{\lambda^2}{2\pi} Re(SLD)$$

$$\beta = \frac{\lambda^2}{2\pi} Re(SLD)$$

With the Snell's law, the total reflection of X-ray radiation can also happen when the α' = 0, which is related a critical angle α_c that

$$n_1 \cos a_c = n_2$$

When the $\alpha < \alpha_c$, the total reflection can happen. The total reflectivity R = 1.0, and the $n_1 \cos a$ is the imaginary causing the evanescent wave. When the $\alpha > \alpha_c$, the transmission can happen with glancing angle, and reflection at the surface can be descripted by the Fresnel equations. As shown in Figrure 2A, the Fresnel Equations describe the amplitude of reflection and transition that

$$A_I + A_R = A_T$$

and

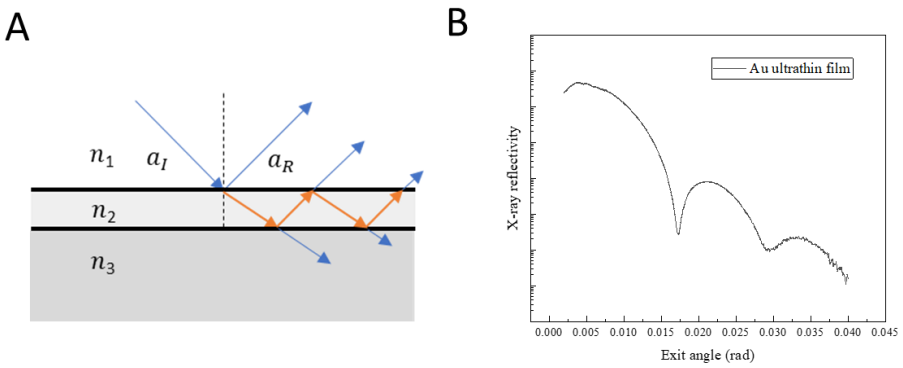

Figure 3. (A) The optical path of X-ray at one slab with infinite substrate; (B) The X-ray reflectivity curve of the Au ultrathin film. (Originally prepared for this thesis)

$$\boldsymbol{k_I}A_I + \boldsymbol{k_R}A_R = \boldsymbol{k_T}A_T$$

where we set wavenumber $k = |\boldsymbol{k_I}| = |\boldsymbol{k_R}|$, and $k*n_2/n_1 = \boldsymbol{k_T}$. Then, After the deriving with the Snell's law, one amplitude reflectivity r can be introduced that

$$r = \frac{A_R}{A_I} = \frac{a - a'}{a + a'}$$

which is called the Fresnel reflectivity that describe the direct reflection of X-ray with glancing angle at the sharp interface as shown in Figrure 2C. Then, within Born Approximation, the reflectivity can be given as

$$R = r^2 = \frac{16\pi^2}{\Delta Q^4}\left|\int \rho'_{(z)} e^{-iQz}\, dz\right|^2$$

where $\rho'_{(z)}$ is the density with the depth z, and ΔQ is change of the wavevector.

However, for the finite thickness layer structure, when the $\alpha > \alpha_c$, the reflection and transmission would not only happen at the top interface of the layer, but also at the bottom side, as shown in Figure 3A. In one single slab with the same two interfaces, the total amplitude reflection can be considered the sum of the series reflection from each interface. Thus, one phase factor e^{iQT}, which is related to the wavevector transfer $Q = 2*k*\sin\alpha$ and the thickness of slab T, would contribute the interference with the reflection angle, as shown in Figure 3B. The expression for the total reflectivity of the slab r_{slab} can be simplified to

$$\gamma_{slab} = \frac{r_{01} + r_{12}e^{iQ_1T}}{1 + r_{01}r_{12}e^{iQ_1T}},$$

where r_{01} and r_{12} represent the Fresnel reflectivity from the top and bottom side of the slab, and the Q_1 is the wavevector transfer in slab. In the more complicated cases, such as the multi-layer structure, Parratt has provided the solution by one recursion algorithm based the solution of the single slab model.[5] It defined the N layers on the top of the infinite substrate. The calculation is started from the Nth layer which is on the surface of the substrate. Then, the total reflectivity of the N^{th} layer can be calculated with the Fresnel

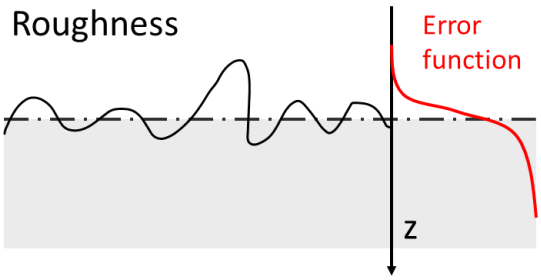

Figure 4. The roughness of the interface with error function model. (Originally prepared for this thesis)

reflectivity,

$$\gamma_{N-1,N} = \frac{\gamma'_{N-1,N} + \gamma'_{N,\infty} e^{iQ_N T}}{1 + \gamma'_{N-1,N}\gamma'_{N,\infty} e^{iQ_N T}}$$

And then, the expression for the total reflectivity (N-1)th layer can be introduced that,

$$\gamma_{N-2,N-1} = \frac{\gamma'_{N-2,N-1} + \gamma_{N-1,N} e^{iQ_{N-1} T}}{1 + \gamma'_{N-2,N-1}\gamma_{N-1,N} e^{iQ_{N-1} T}}.$$

Finally, this calculation can be recursively extended to the total reflectivity of the top layer.

On the other and, in the practical case, the roughness (or diffuse) of interface should be also considered. As shown in Figure 4, the density distribution of grated interface can be descripted as the model following the error function. In this simple model, the actual intensity reflectivity $R(Q)$ can be corrected by the factor of the interface model, expressed that,

$$R(Q) = R_F(Q)\mathrm{e}^{-Q^2\sigma^2}$$

where the $R_F(Q)$ is the idea intensity reflectivity and the σ is the rms Gaussian roughness. However, although this solution has been already widely applied in the industry and academic,
the definition and model of actual roughness is still in argument because there is still no suitable technique which can directly provide the buried interface morphology in its natural state at the different scale.

2.3 Analysis of X-ray reflectivity data

The methods for X-ray reflectivity data analysis are generally divided into two categories, model dependent analysis and model free analysis.[6,7] In the model dependent analysis method, the fitting process based on the Parratt expression was the most widely used method as the inverse processing of X-ray reflectivity data. Theoretically, depending on the presumed model, all parameters can be solved with the theoretical formula. However, in the actual experiment, there is still some potential deficiencies which may lead to error even in the perfect fitting results. One example is the measurement of unknow sample. Due to all calculation in the fitting process is based on the theoretical formula, if the reflectivity data is collected from an unknown sample, an intentional assumption on the model might lead to false results. On the other hand, even the X-ray data is collected from a known sample, it is still difficult to avoid the overfitting or underfitting

during the processes with algorithms, such as the generic algorithm and levenberg–Marquardt algorithm, which have the different sensitive to the parameter in the calculation. Furthermore, due to the difficulty in the engineering, the instrument parameters can be various in different laboratory, such resolution and the size of footprint, which would also affect the fitting result. Of course, generally, the fitting method is still reliable and widely used.

In the model free analysis method, the frequency analysis based on the Fourier transfer also show the significance on the X-ray reflectivity analysis.[8,9] Different to solution of the fitting analysis, which try to solve all paraments from X-ray reflectivity curve, the frequency analysis would only focus on the thickness, which is concluded in the phase factor in the expression of X-ray reflectivity. In the study of the unknown sample, it not only avoids the error from the intentional model, but also suppressed the contribution from the instruments itself. However, for the complexed layer structure sample, the Fourier transfer analysis would become difficult since the complicated expression in the phase factor.

For the single layer model, as the glancing angle $a >> a_c$, the absorption would be negligible, and thus the expression of the X-ray reflectivity curve can be simplified from the Parratt expression to

$$R = \frac{(\gamma'_{1,2})^2+(\gamma'_{2,3})^2-2\gamma'_{1,2}\gamma'_{2,3}cos\Delta}{1-(\gamma'_{1,2})^2-(\gamma'_{2,3})^2+(\gamma'_{1,2})^2(\gamma'_{2,3})^2}, \quad \Delta = 4\pi T\left(\sqrt{a^2-a_c^2}\,/\,\lambda\right)$$

where R is the total intensity reflection and $\gamma'_{N-1,N}$ is the Fresnel coefficient at the interface between the $(N-1)^{th}$ and N^{th} layer. Therefore, the thickness T of the single layer can be solved by the Fourier transform directly.

Then, for the double layer system, the Fourier transform analysis can be still used to solve the X-ray reflectivity curve directly. After the simplification, the expression of the X-ray reflectivity curve can be expressed as

$$R = (A\,cos\,\Delta_2 + B\,cos\,\Delta_3 + C\,cos(\Delta_2+\Delta_3) + D\,cos(\Delta_2-\Delta_3) + E/F$$

where

$$A = 2\gamma'_{1,2}\gamma'_{2,3}(1+(\gamma'_{3,4})^2)$$
$$B = 2\gamma'_{2,3}\gamma'_{3,4}(1+(\gamma'_{1,2})^2)$$
$$C = 2\gamma'_{1,2}\gamma'_{3,4}$$
$$D = 2\gamma'_{1,2}(\gamma'_{2,3})^2\gamma'_{3,4}$$
$$E = (\gamma'_{1,2})^2+(\gamma'_{2,3})^2+(\gamma'_{3,4})^2+(\gamma'_{1,2})^2(\gamma'_{2,3})^2(\gamma'_{3,4})^2$$
$$F = (1-(\gamma'_{1,2})^2)(1-(\gamma'_{2,3})^2)(1-(\gamma'_{3,4})^2)$$

In this case, the term D would be negligible, and therefore, 3 delta functions can be solved in the Fourier space, which correspond to the thickness of each layer and the sum of them. When the layer number increased to N-1, the total number of the frequency components can become N(N-1)/2. Thus, it is also possible to be used to solve the multilayer structure theoretically. However, considering the complex expression and the overlapping in the spectra, it is not recommended to use only the Fourier transform analysis to solve the multilayer structure. In the actual data analysis process in this work, the wavelength of the X-ray is constant (Cu Kα of 1.54 Å), and the critical angle a_c is read directly from the X-ray reflectivity curve. For the calculation, we selected the angle range about Q from 0.038 $Å^{-1}$ to 0.15 $Å^{-1}$, and

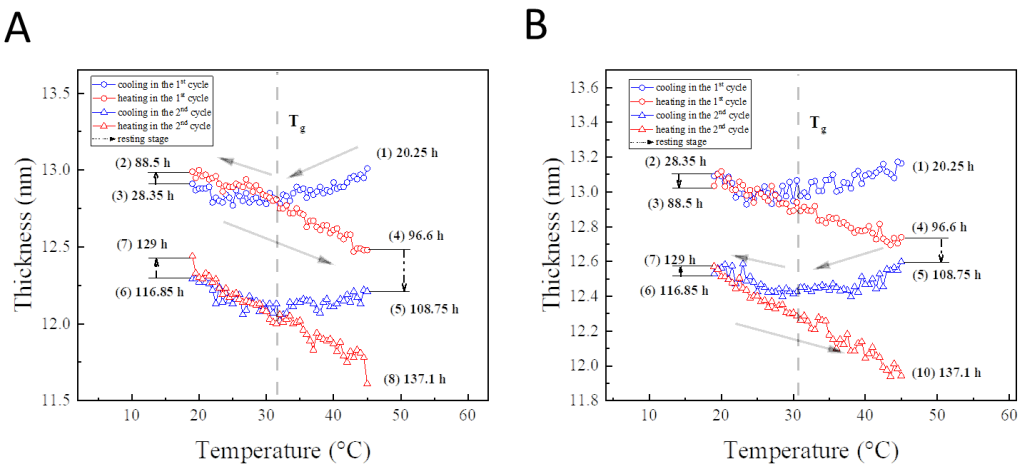

Figure 5. The thickness of PVAc ultrathin film in the temperature cycles calculated by (A) FT and (B) single layer model fitting. (Langmuir 34.38 (2018): 11272-11280)

then, after the smoothing with 500 times, the oscillation of the X-ray reflectivity curve was flattened with the base line. Finally, the thickness was calculated by the discrete Fourier transform,

$$F_n = \Sigma_{k=0}^{N-1} R_k \mathrm{e}^{-2\pi i n k/N} \quad ,$$

where F_n is the Fourier transform of the X-ray reflectivity R_k with the step number n in the thickness range, and the k is number of the plotting in the selected Q range. Generally, the resolution of the discrete Fourier transform is set around 0.1~0.5 Å.

In the model free analysis method, there would be another way based on the "visibility" of the fringes to solve the X-ray reflectivity curve, although no discussed have been reported before. During my doctoral program, it is found that, at the interface of the double layer structure which has a great contrast on the scattering length density, the "visibility" of the fingers at the high angle range in the X-ray reflectivity curve would be very sensitive to the roughness. It is proposed that this sensitivity can be related to the different contribution of the reflection from the different interfaces. Different to the general discussion on the thickness or density of the layer structure, this new method may provide a powerful way to solve the condition of the buried interface, such as the connection condition. However, the development of this new method is still in progress, and the feasibility still requires a lot of experiment to be proved. No doubt, this new analysis method should be promising way for the study of the aging process of the buried interface.

Finally, it should be noticed again that both methods can solve the X-ray reflectivity efficiently. In the actual data analysis, it is important to understand the deficiency of the analysis method used, then we could be more confident in the data analysis. In the Figure 5, two different analysis method have been compared with the same data which were collected from this PhD research work.[10,11] The experiments will be discussed in detail in Chapter 4. The thickness change of the PNIPAM ultrathin film with temperature cycles have been solved by the Fourier transfer and batch inverse fitting in Motofit.[8,9,12] By comparing the two sets of data, it can be found that the results obtained by the two calculation methods are quite close.

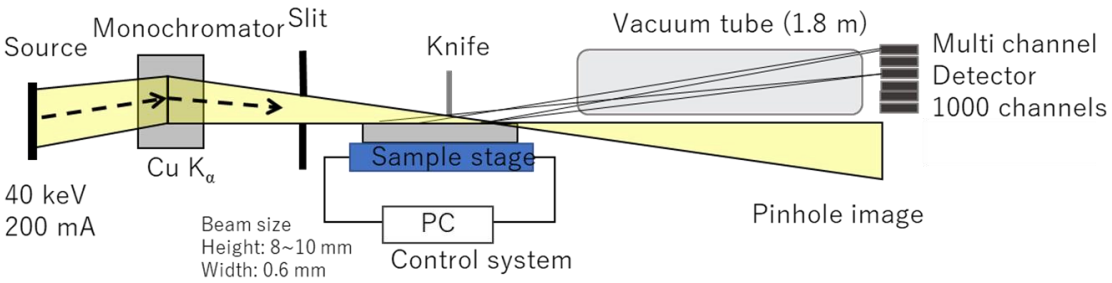

Figure 6. The schematic of the multi-channel X-ray reflectometer with its main parts. (Originally prepared for this thesis)

2.4 Multi-channel X-ray reflectometer

X-ray reflectivity analysis is quite useful method for ultra-thin film structure. As the expression discussed in the above section, the important information of ultrathin film structure, such the thickness, density and roughness are all included in the X-ray reflectivity curve. However, due to the limitations of classical technique, the in-operando X-ray reflectivity analysis was not achieved in the laboratory. But this time, through efforts in our laboratory, the in-operando X-ray reflectivity analysis of the polymer ultrathin films has been successfully conducted with the multi-channel X-ray reflectometer.

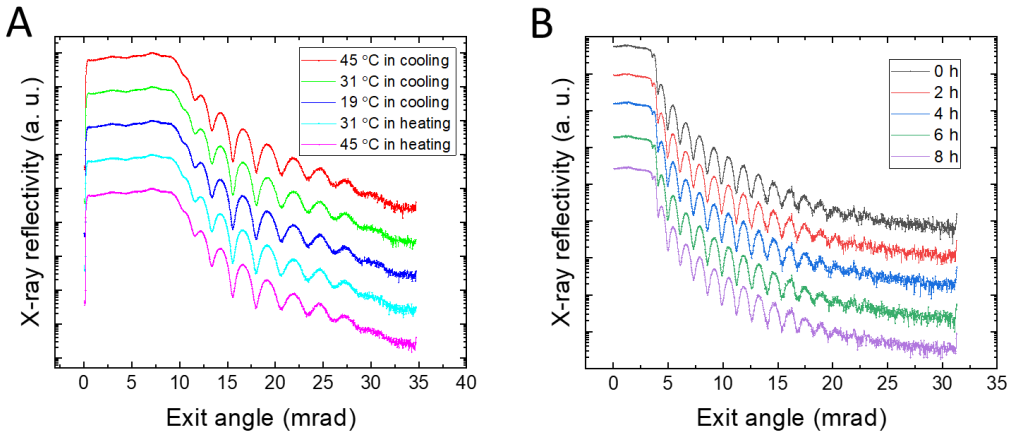

Figure 7. (A) X-ray reflectivity curves of Au and carbon thin film with temperature and time all the data is collected in 3 minutes by our multichannel reflectometry. All X-ray reflectivity curves are presented on a base-10 logarithmic scale with offset. (Langmuir 34.38 (2018): 11272-11280)

As shown in Figure 6, multi-channel X-ray reflectometer is consisting of five main parts that X-ray source, sample stage, environment control system (temperature and moisture), vacuum tube and pixel detector. The X-ray source is equipped with an 18 kW rotating anode copper (Rigaku, typical operation condition 40 kV -200 mA) and a parabolic W/Si focusing mirror. All X-rays are monochromatic (copper

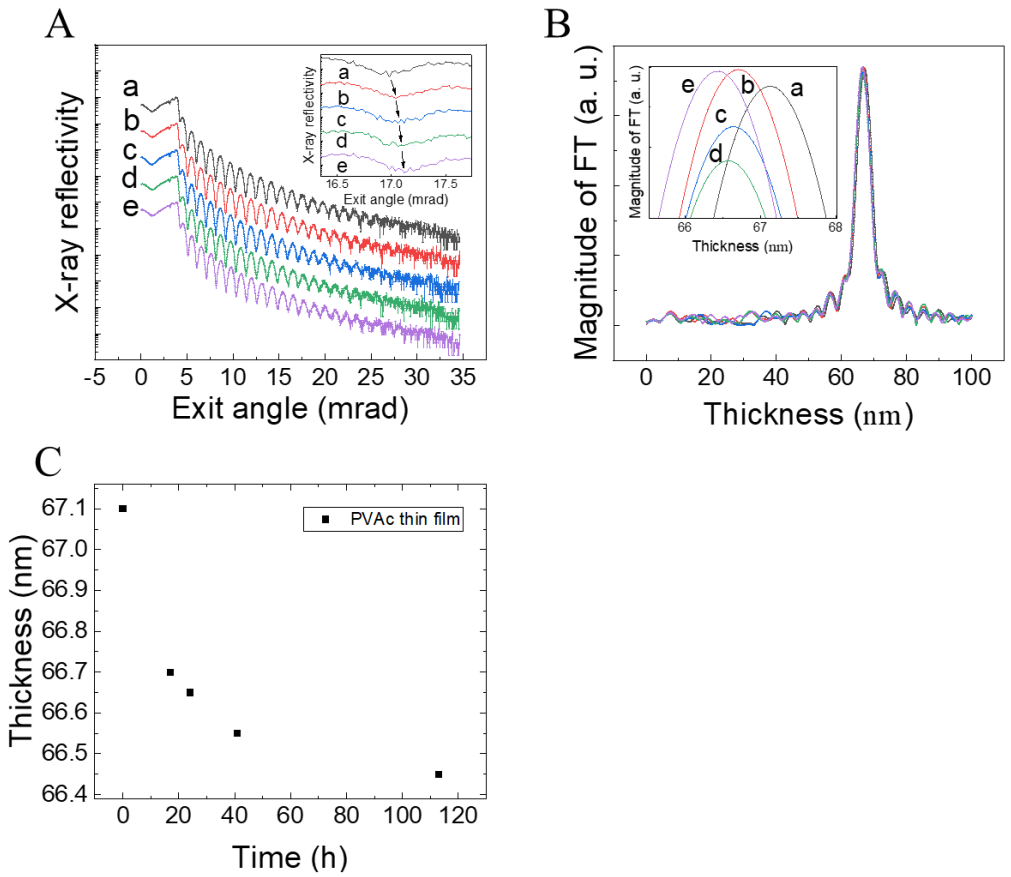

Figure 8. (A) X-ray reflectivity curves of a PVAc thin film during annealing at 45° C: a) at 0 h, b) at 17 h, c) at 24 h, d) at 41 h, and e) at 113 h — the inset graph displays the magnified fringes approximately 17 mrad. (B) The Fourier transform (FT) of the interference fringes observed in the X-ray reflectivity profiles — the inset graph displays the magnified peak of the FT magnitude with thickness. (C) The thickness change (calculated by FT) of the PVAc thin film during annealing. All X-ray reflectivity curves are presented on a base-10 logarithmic scale with an offset. (Polymer Journal 51 (2019): 1073–1079)

Kα 1.54Å) with pinhole optic and collected by a multi-channel pixel detector (1000 channel with 28 mrad detection range in optic), which is placed at nearly 1.8 m away from the sample with the vacuum tube. Because reflection from each angle can be collected by the detector simultaneously, it greatly reduced the time of data collection to the order of seconds to minutes. Meanwhile, due to there is no requirement on the angle scanning, the stability and reproducibility of this setup greatly contributes to the reliability in long-time continuous measurements. As the extension parts for environment control, the temperature control system (± 0.1 ° C) and moisture control system (± 3%) are designed on the sample stage. All advantages of the multi-channel X-ray reflectometer make the study of kinetics and dynamics of the ultrathin film system become possible in laboratory. As shown in Figure 7, the X-ray reflectivity curves of thin film system have been collected with the temperature and time, which indicated the dynamic and kinetic states of the thin film system respectively, although these data can be only collected in the synchrotron in the past.

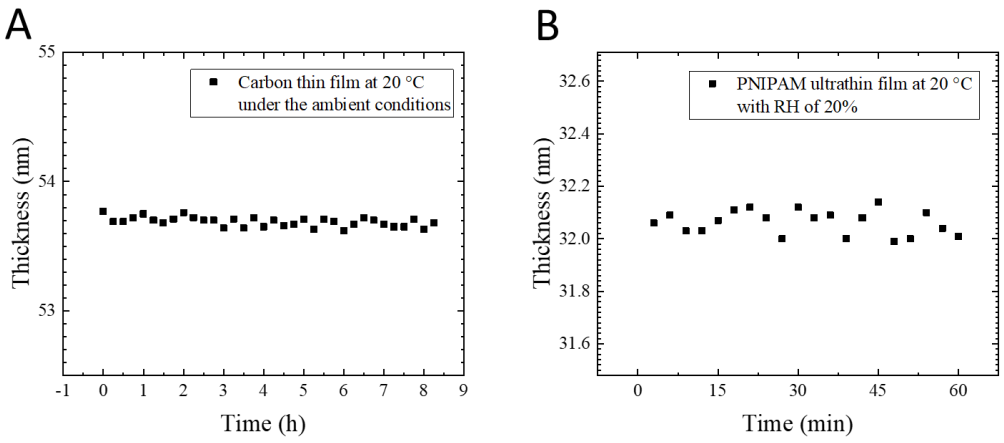

Figure 9. (A) The thickness of carbon thin film at 20 ° C under the ambient conditions and (B) the thickness of PNIPAM ultrathin film at 20 ° C with RH of 20 %. (Langmuir 34.38 (2018): 11272-11280; ACS omega 4.7 (2019): 12194-12203)

For the data analysis of X-ray reflectivity from multi-channel reflectometer analysis, the Fourier transfer analysis method has been mainly used in the doctoral program. It not only reduces the influence of the diffuse scattering intensity in the X-ray reflectivity curve but is also more suitable for the study of the unknow change in the polymer ultrathin film with environment. [10,11,13,14] As shown in Figure 8, the annealing process of the PVAc thin film have been solved by the in-operando analysis. In the Figure 8A, the X-ray reflectivity curves during the annealing were collected in at the different time during the annealing. And in the Figure 8B, the Fourier transfer of the related reflectivity data were plotted, and the main peak position pointed the thickness of the single layer structure. Finally, all thickness was plotted with time for the analysis, as shown Figure 8C, which indicated an additional slow dynamic process after the structure relaxion. With the analysis of the thickness change of PVAc during, a slow dynamic behavior has been observed in the rubbery state of PVAc thin film, and this will be discussed in detail in Chapter 3.

Finally, to prove the stability and reproducibility of X-ray reflectivity data collected by the multi-channel reflectometer, the control experiment with the different samples, carbon thin film and PNIPAM ultrathin film, have been conducted with different environment conditions. As shown in Figure 9 A, the stable sample carbon film spurted on silicon substrate, was tested at 20 ° C about 8 hours by the multi-channel reflectometer. For the results in this experiment, the carbon thin film can be expected stable without any time dependence change, which indicated the stability and reproducibility of long-time measurement with the temperature control system. On the other hand, as shown in Figure 9B, the moisture sensitive PNIPAM ultrathin film was monitored at 20 ° C with relative humidity (RH) of 20 % in 1h. For the moisture control system, it consists of three main components: a moisture controller (AHCU-2, Sansyo Co., Ltd., Japan), sample chamber (4 cm * 4 cm * 8 cm), and pump. The moisture controller adjusts the RH with air flow (humidification flow rate: 5 L/min; dehumidification flow rate: 10 L/min) from 5–80% ± 3%. The sample chamber is a semi-open plastic chamber that allows the airflow to pass in one direction. During the moisture experiments, the RH is maintained by the stream of the moisture-controlled air, and

the actual RH experienced by sample surface would be close to average RH in moisture control chamber. Because the PNIPAM ultrathin film is easy to swell, the fluctuation of the value in thickness of 0.05 nm demonstrates the reliability of a moderate control system.

2.5 Conclusion

As it is emphasized, the revolution of the analysis technique would be one of the most activity engine for the materials science, especially the development of the in-operando analysis technique. One suitable technique and analysis method would the crucial key for the starting on a new discipline. For the research on polymer ultrathin film systems, in-operando X-ray reflectivity analysis would be the most competitive candidate. Theoretically, due to the short wavelength of X-rays, the X-ray reflectivity technique is extremely sensitive to the parameters of the layer structure, especially the thickness, meanwhile it can also exhibit the changes at the buried interface. On the other hand, X-ray reflectivity technique is nondestructive, which can provide the natural information with statistics on large area in the actual environment. In my doctoral program, the multi-channel reflectometer has been built in our laboratory, and applied in the in-operando analysis of the different polymer ultrathin film systems. Depending on the outstanding performance of this novel instrument, we have successfully confirmed some physical and chemical phenomena that have been never observed in previous researches. With a large number of control experiments, it is proposed that these abnormal behaviors would been contributed by the boundary effects, which is nature of polymer ultrathin film system itself, and these intrinsic properties may widely exist in similar polymer ultrathin film systems. These researches will be discussed in the following chapters.

Reference

(1) Stoev, K. N.; Sakurai, K. Review on Grazing Incidence X-Ray Spectrometry and Reflectometry. *Spectrochimica acta, Part B: Atomic spectroscopy*. Elsevier Science B.V. January 4, 1999, pp 41–82.

(2) Kiessig, H. Interferenz von Röntgenstrahlen an Dünnen Schichten. *Ann. Phys.* **1931**, *402* (7), 769–788.

(3) Sakurai, K.; Mizusawa, M. X-Ray Reflectometer and the Measurement Method. 3903184, 2007.

(4) Sakurai, K.; Mizusawa, M.; Ishii, M. *Recent Novel X-Ray Reflectivity Techniques: Moving Towards Quicker Measurement to Observe Changes at Surface and Buried Interfaces*; 2007; Vol. 32.

(5) Parratt, L. G. Surface Studies of Solids by Total Reflection of X-Rays. *Phys. Rev.* **1954**, *95* (2), 359–369.

(6) Hamley, I. W.; Pedersen, J. S. Analysis of Neutron and X-Ray Reflectivity Data. I. Theory. *J. Appl. Crystallogr.* **1994**, *27* (pt 1), 29–35.

(7) Pedersen, J. S.; Hamley, I. W. Analysis of Neutron and X-Ray Reflectivity Data. II. Constrained Least-Squares Methods. *J. Appl. Crystallogr.* **1994**, *27* (1), 36–49.

(8) Sakurai, K.; Mizusawa, M.; Ishii, M. *Significance of Frequency Analysis in X-Ray Reflectivity: Towards Analysis Which Does Not Depend Too Much on Models*; 2008; Vol. 33.

(9) Sakurai, K.; Iida, A. Fourier Analysis of Interference Structure in X-Ray Specular Reflection from Thin Films. *Jpn. J. Appl. Phys.* **1992**, *31* (2), 113–115.

(10) Liu, Y.; Sakurai, K. Uniaxial Negative Thermal Expansion of Polyvinyl Acetate Thin Film. *Langmuir* **2018**, *34* (38), 11272–11280.

(11) Liu, Y.; Sakurai, K. Thermoresponsive Behavior of Poly (N-Isopropylacrylamide) Solid Ultrathin Film under Ordinary Atmospheric Conditions. *Chem. Lett.* **2017**, *46* (4), 495–498.

(12) Nelson, A. Co-Refinement of Multiple-Contrast Neutron/X-Ray Reflectivity Data Using MOTOFIT. *J. Appl. Crystallogr.* **2006**, *39* (2), 273–276.

(13) Liu, Y.; Sakurai, K. Slow Dynamics in Thermal Expansion of Polyvinyl Acetate Thin Film with Interface Layer. *Polym. J.* **2019**, No. 51, 1073–1079.

(14) Liu, Y.; Sakurai, K. Thickness Changes in Temperature-Responsive Poly(N -Isopropylacrylamide) Ultrathin Films under Ambient Conditions . *ACS Omega* **2019**, *4* (7), 12194–12203.

Chapter 3

Uniaxial negative thermal expansion (NTE) of polyvinyl acetate (PVAc) thin film

3.1 Introduction

In the study of the thermal mechanical properties of materials, negative thermal expansion is of the most interest.[1,2] Rather than volume increasing in heating, some materials exhibit suppression in thermal expansion, or even negative thermal expansion. Benefiting from this unusual performance, many high-precision instruments have been manufactured. However, in previous research, most instances of NTE can only exist in a few crystal materials or complex topological composites. This scarcity regrettably restricts the further development of high-precision instruments. In recent years, some researchers have occasionally observed uniaxial negative thermal expansion (NTE) in polymer ultra-thin film systems, but because of the rare reports, this discussion is still inconclusive. In 1993, William J. Orts, et al. first reported NTE in polystyrene (PS) ultra-thin film by X-ray reflectivity technique, which is based on interference analysis of reflection from each interface and extremely sensitive to the layered structure along the depth of film on angstrom to nanometer scale.[3] For the first consideration of this special observation, William J. Orts, et al. proposed that the decrease in thickness can be contributed by reducing the void near the interface. Because of the dramatic thermodynamic motion in ultra-thin film, bond constraints may lead to a temperature dependent interfacial density profile with thickness. This is a very interesting idea, but unfortunately, it is also an insufficient interpretation in follow up research, because it is accepted that the free motion of a polymer chain is limited in its glassy state. In subsequent research, Günter Reiter, et al.

mentioned isothermal thickness increasing in PS ultra-thin film again and proposed that this phenomenon can be considered as one of the byproducts of the de-wetting process.[4] In 2002, M. Mukherjee, et al. systematically studied NTE in PS ultra-thin film by synchrotron beamline, and reversible NTE was confirmed for the first time in the glassy state.[5] In 2004, Christopher L. Soles, et al. first discussed the effect of hydrophobic/hydrophilic interface on NTE in a polymer ultra-film system.[6] In this work, NTE on polycarbonate (PC) ultra-thin film was first reported, and this NTE can be different to the de-wetting process and greatly influenced by the surface energy of the substrate. In the latest related reports, T. Kanaya, et al. re-studied NTE in PS ultra-thin film, and two different NTE behaviors have been discussed in kinetics with different mechanism in their work.[7–9] Reviewing the past 25 years, experimental data on NTE has been successively updated but no detailed model can be used to explain all the phenomena in polymer thin film systems even now.

Herein, with the in-operando X-ray analysis technique in laboratory, (i) two different instances of NTE in polyvinyl acetate (PVAc) thin film in a temperature cycle from 45 °C to 19 °C were discovered for the first time, and (ii) NTE even in much thicker film such as 130 nm, was observed, that might not be well understood from the past research. In the experiment, commercial PVAc thin films, with a glass transition temperature around 31 °C,[10] were prepared on silicon wafer, and the thickness change was studied by the customized multichannel X-ray reflectometer [11,12] based on Naudon's method [13]. While the technique provides essentially the same information as ordinary X-ray reflectivity measurement based on $\theta/2\theta$ scanning, simultaneous data collection can be done in extremely short time, without any scanning, any motion of the instruments. In-operando X-ray measurements have been done by being coupled with temperature control system. In the repeated temperature cycle, an increase in the thickness of PVAc thin film was confirmed in the glassy state with temperature cooling, and a further decrease in isothermal thickness was observed in the resting stage in the rubbery state. Two different instances of NTE were confirmed as dependent on dynamics and kinetics respectively. Meanwhile, the observation of NTE also exhibits differences in total thickness, especially in PVAc ultra-thin film (of 13 nm), the thickness continues to decrease with temperature in the rubbery state. On the other hand, to avoid confusing from other external factors like bulk structure relaxing, de-wetting or crystallization, related experiments have been also conducted, like annealing monitoring and SPM measurement. All results point out that reproducible NTE exists in PVAc thin film.

As one reasonable assumption, a trilayer model has been first proposed in this work for the detail mechanism. In the postulated model, a PVAc thin film is considered to consist of three different layers, called the interface layer, transition layer and normal layer. Unlike the homogeneous properties of polymer bulk systems, interface interaction considerably contributes to dynamics and kinetics in thin film systems, and one possibility is that the spatial distribution of polymer chains gradually changes in depth from 3D to 2D parallel to the surface of substrate and free volume greatly decreases at the interface. The interface layer is proposed as it can be formed in the rubbery state and then be frozen in the glassy state with a larger coefficient of area thermal expansion, and finally contribute to the additional deformation to the up-side layer, called the transition layer, by each buried entanglement with normal thermal expansion. On

the other hand, the bulk-like surface layer, called the normal layer, can show normal thermal expansion with temperature. In the three-layer system, NTE can be thickness independent and only related to the performance of the interface layer and transition layer. The observation of thermal expansion of PVAc thin film systems can vary with the competition between normal thermal expansion and NTE.

Furthermore, based on this assumption, the extended research for state of interface layer has been studied on the PVAc thin films after the sufficient thermal treatment. The thin film (of 67 nm) was prepared on a silicon wafer with a native silicon dioxide layer. Some new phenomena were observed: in the temperature cycle between 45°C and 19°C, (i) when the PVAc thin film was kept above its T_g for sufficient time, the coefficient of thermal expansion (CTE) significantly decreased in the rubbery state at the initial state; (ii) however, after the glass transition of the PVAc thin film from the rubbery state to the glassy state, the NTE was clearly observed with cooling; and (iii) one interesting finding was that when the cooling finished and the heating started, the thermal expansion behaviors of the PVAc thin film recovered to normal, i.e., the thickness change was small in its glassy state and then abruptly increased as the temperature crossed T_g. Based on this observation, it is proposed that the interface layer might exist and vary with the conditions of the polymer thin film system, causing the unusual thickness change of the polymer thin film with temperature.

3.2 Preparation of PVAc ultrathin films

Commercial polyvinyl acetate (PVAc) powder (Sigma-Aldrich Co., USA) was used for sample preparation. The number average and weight average molecular weight are about M_n = 59k and M_w = 107k. The polydispersity, M_w/M_n, is about 1.8, which can be still considered safety for the homogeneous molecular weight distribution in polymer thin film.[14] 0.5 wt% and 4 wt% PVAc toluene solutions (Wako Chemical, Japan) were prepared, and different thickness PVAc thin films were prepared onto silicon (100) wafer (SUMCO Co., Japan, cut to the size of 15 mm × 15 mm, and then cleaned by nitric acid) by spin coating (SC-400, Oshigane Co., Ltd., Japan) with rotation 40 s at 4000 rpm. After spinning, the annealing was conducted at 45°C with 12 h and more than 113 h for the control experiments of the study on the assumed interface layer.

3.3 In-operando analysis of PVAc ultrathin films in temperature cycle

To study the thickness change of PVAc thin films with temperature, the thin films were monitored by the multichannel X-ray reflectometer in temperature cycles from 45°C to 19°C, which made real-time static data collection in the laboratory possible.[15–18] The temperature scan strategy was set at 2°C/step, 1 °C/step and 0.5 °C/step for control experiments, and each step took 9 min, including the temperature changing stage (~0.5 min) and suspending stage (~8.5 min). The valuable data collection was started at the fourth minute and stopped at the seventh minute of each step to avoid temperature fluctuations. In the study of each sample, the same experiment was repeated twice to the confirm reproducibility. And the resting stage

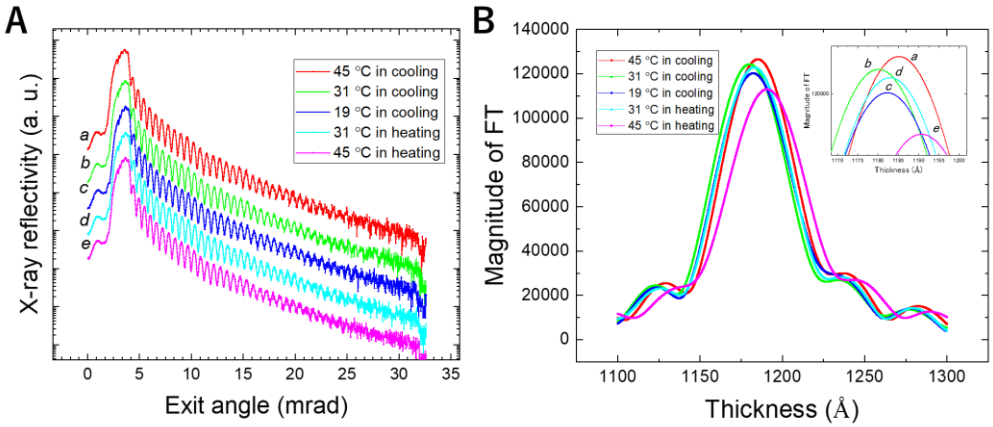

Figure 1. (A) X-ray reflectivity curves of PVAc thin film (of 120 nm) in the 1st temperature cycle and (B) Fourier transform of interference fringes observed in the X-ray reflectivity profiles: *a*) initial state at 45 °C; *b*) glass transition state at 31 °C in cooling; *c*) final state at 19 °C in cooling; *d*) glass transition state at 31 °C in heating; *e*) final state at 45 °C in heating. All X-ray reflectivity curves are presented on a base-10 logarithmic scale with offset. The insert graph in figure (B) displays the magnified peak of magnitude of FT wtih thickness. (Langmuir 34.38 (2018): 11272-11280)

was added between each temperature cycle for the static study. The different resting stage of 12 hours and 96 hours were set for the control experiments of the study on the assumed interface layer. For the thickness analysis, all X-ray reflectivity data were preferentially analyzed by Fourier transform (with a Q_z range of 0.03–0.16 nm^{-1}).[12,19] As the support analysis, scanning probe microscope (SPM) measurement (SPM-9500J3, Shimadzu Co., Ltd., Japan) was conducted with a dynamic scan model for soft surface morphology analysis, and all results were flattened by plane fitting.

3.4 Uniaxial negative thermal expansion of polyvinyl acetate thin film

3.4.1 *Observation of NTE in PVAc thin film of 120 nm*

In the experiment, the thickness changes of PVAc thin film (of 120 nm) were studied first, in temperature cycles between 45 °C to 19 °C by multi-channel X-ray reflectometer. In Figure 1 A, the X-ray reflectivity curves of the initial, glass transition and final states are presented with offset. Browsing the X-ray reflectivity curves from *a* to *e*, the stable oscillation of the Kiessig fringe can be easily confirmed, which indicates the stable reflection condition with sharp interface in the temperature cycle.[20,21] Meanwhile, a minimum of the contrast in the fringes at an angle of approximately 20 mrad can be found at the X-ray reflectivity curves in Figure 1 A, which may be considered to indicate the second spatial frequency in the PVAc thin film. But, it should be noted that the amplitude of the fringe oscillation in our reflectivity have been influenced by the diffuse scattering, because there is not slits in front of the detector. Therefore, in the data analysis, we prefer to avoid the discussion on the amplitude at the low angle range, even those

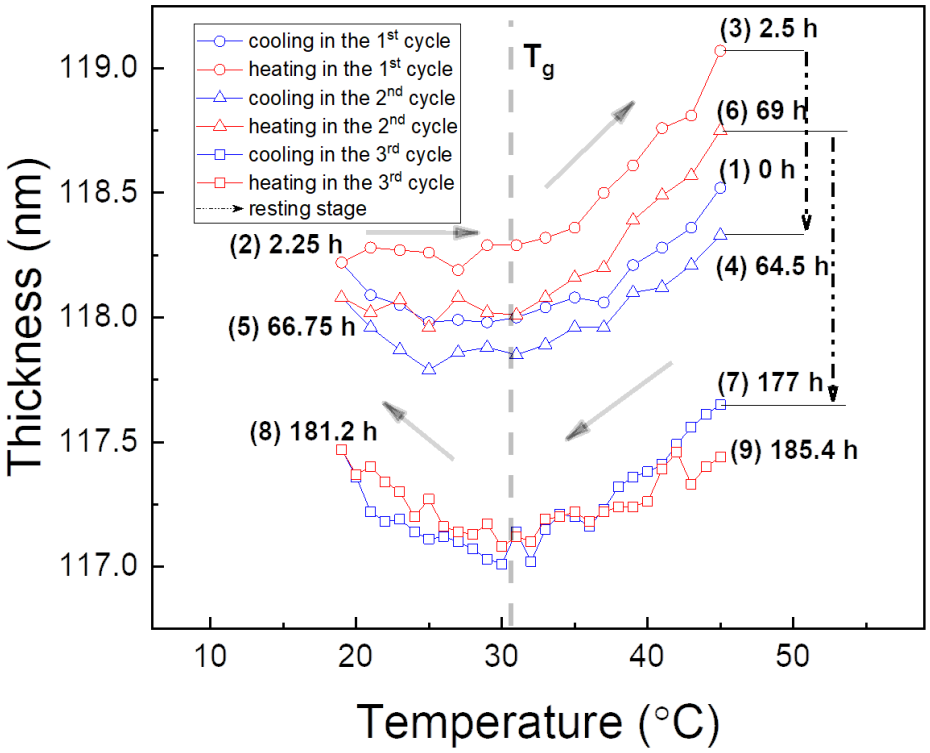

Figure 2. Thickness change (calculated by FT) of PVAc thin film (of 120 nm) in temperature cycles between 45 °C and 19 °C: (1) start of the 1st cooling run; (2) end/start of the 1st cooling/heating run; (3) end of the 1st heating run; (4) start of the 2nd cooling run; (5) end/start of the 2nd cooling/heating run; (6) end of the 2nd heating run; (7) start of the 3rd cooling run; (8) end/start of the 3rd cooling/heating run; (9) end of the 3rd heating run. The 1st and 2nd temperature cycles were set at 2 °C/steps; the 3rd temperature cycle was at 1 °C/steps. Each step took 9 min. (Langmuir 34.38 (2018): 11272-11280)

related discussion looks positive for our assumption. Then, the thickness change of PVAc thin film was further studied from the frequency in these oscillations in the long angle range. The free model analysis with Fourier transform has been used in the analysis of thickness change in this work.[22] In Figure 1 B, the Fourier transform of oscillations extracted from all the above X-ray reflectivity curves are presented, where the peak indicates the frequency component of oscillation and agrees with the layer thickness.[23,24] During the Fourier analysis, the Q_z range of 0.03 – 0.16 nm^{-1} has been employed and the final data are evaluated in the curve plotted with the step of 0.01 nm. The achievements on the thickness determination are influenced by both instrumental and sample conditions. For quite thick sample (such as several hundred nm), the analysis of high-frequency fringes is crucial, leading to the requirement for angular divergence (the distance and the detector pixel size in the case of multichannel X-ray reflectometry). For extremely thin cases, as the interference fringe is slow, the wide q range is the key for the determination. The present setup and the condition are suitable for 10~150 nm range. In such thickness range, the method gives good sensitivity for tiny changes of thickness of 0.1 nm or even smaller. Therefore, such quite small scale as 0.01 nm is used for showing thickness, it does not mean the spatial resolution (in the depth direction)

is 0.01 nm. As shown in Figure 1B, the main peak position of Fourier transform curves gradually changes with temperature indicating the change of thickness of PVAc film, In the temperature cycle between 45 ºC to 19 ºC, PVAc thin film starts with a thickness of 118.51 nm at 45 ºC after annealing and goes to 118.0 nm and 118.22 nm at 31 ºC and 19 ºC respectively in cooling. Then, upon heating again, the thickness of PVAc thin film changes to 118.29 nm at 31 ºC and finally gets to 119.07 nm at 45 ºC in the end. Considering the stable performance of control sample at constant temperature and the natural thermal expansion behaviors of PVAc with temperature cycle, it is important to see carefully the changes in the thickness, even if it is fairly small. In the cooling process from 31 ºC to 19 ºC, the thickness of PVAc thin film increases 0.22 nm but does not decrease, which may respond to previous reports on negative thermal expansion in polymer ultra-thin film, even though this thickness is already much thicker than their expectations.[6,25–28]

To further confirm this unusual thermo-responsive behavior, the 2nd experiment was done with the same conditions in the 1st temperature cycle and added the 3rd cycle with the slower speed in 1 ºC/steps. One point that should be noted is that these experiments are conducted on the same sample without moving any of the parts, and hence in-situ observation can be promised in these measurements. In Figure 2, the thickness of each state in three temperature cycles are presented as a whole. Looking at the thickness change tendency in the three cycles, one unusual thickness increase can be clearly confirmed in each cooling process. And when focused on the turning points, one more interesting finding is that all switch temperatures are around the glass transition temperature of around 31 ºC. That is to say, NTE has been observed on PVAc thin film (of 120 nm) in its glassy state with cooling, which might be considered the first observation of NTE in amorphous polymer films above 100 nm. Furthermore, when comparing this NTE behavior between the first two cycles and the third cycle, one important change can be found in that NTE in the glassy state becomes clearer and more symmetric in cooling and heating with a slow temperature scan. In the tentative discussion for the above finding, it is convinced that this usual NTE in the glassy state of PVAc thin film is kinetically different from the normal thermal expansion but also temperature dependence. Meanwhile, one can see another instance of NTE at the resting stage between each cycle. A substantial decrease in the isothermal thickness of PVAc thin film can be easily confirmed in its rubbery state after normal thermal expansion. The thickness of PVAc thin film decreases 0.77% (0.74 nm) at the 1st resting stage for 62 h. and 1.08% (1.1 nm) at the 2nd resting stage for 108 h. Obviously, one non-linear kinetic process dominated the observation of NTE in PVAc thin film in the rubbery state. As a preliminary summary for the above discussion, two usual NTE behaviors have been observed in PVAc thin film (of 120 nm) with its glassy/rubbery state in a repeated temperature cycle. Looking back at 30 years of NTE research on polymer ultra-thin films, nearly all the reports and tentative theory indicate that this unusual phenomenon of amorphous polymer film can only exist with a thickness equal to or below the radius of gyration in its glassy state. However, in this work, hitherto inconceivable data have been presented with repeat experiment and stable performance. The discussion of NTE in polymer ultra-thin films may be re-expanded again.

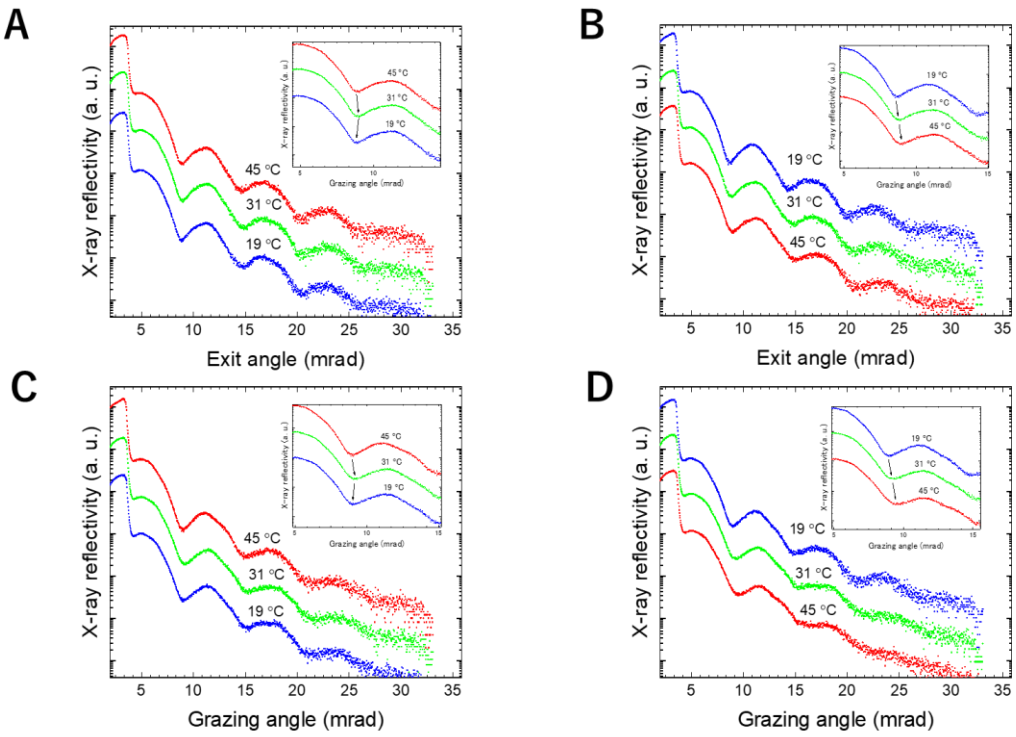

Figure 3. X-ray reflectivity curves of PVAC ultra-thin film (of 13 nm) in the 1st cooling (A), 1st heating (B), 2nd cooling (C) and 2nd heating (D): the states at 45 °C, 31 °C, and 19 °C are presented on a base-10 logarithmic scale with offset. The insert graph in each figure displays the magnified X-ray reflectivity with exit angle. (Langmuir 34.38 (2018): 11272-11280)

3.4.2 *Observation of NTE in PVAc ultrathin film of 13 nm*

In the second attempt, the same experiment was repeated on PVAc ultra-thin film (of 13 nm). To promise the enough time for the hysteresis of polymer thin film, which can be confirmed in the Figure 2, the temperature cycles were set at 0.5 °C/step, and additional resting stage was added between cooling and heating in each temperature cycle. On the other hand, to further confirm the influence from annealing, all states during annealing were also recorded. Considering the greatly influence of free surface and constrained interface, these unusual NTE can be expected more prominent in the ultra-thin film systems. In Figure 3, some X-ray reflectivity curves of PVAc ultra-thin film (of 13 nm) in temperature cycle are presented. Browsing all Kiessig fringes in Figure 3A-D, the frequency change of oscillation can be clearly observed, as shown in the insert graphic, which implies greater change in PVAc ultra-thin film (of 13 nm) with temperature change. In Figure 3A, the frequency of oscillation deceases with cooling from 45 °C to 31 °C, and then increases at 19 °C. The same tendency can be also found in Figure 3 C. Both exhibit the same behaviors as PVAc thin film (of 120 nm) indicated the same NTE in the glassy state of PVAc ultra-thin film (of 13 nm) in cooling process. But in Figures 3 B and D, the frequency of oscillation continues decreasing from 19 °C to 45 °C, indicating continued decrease in thickness of PVAc ultra-thin film (of 13

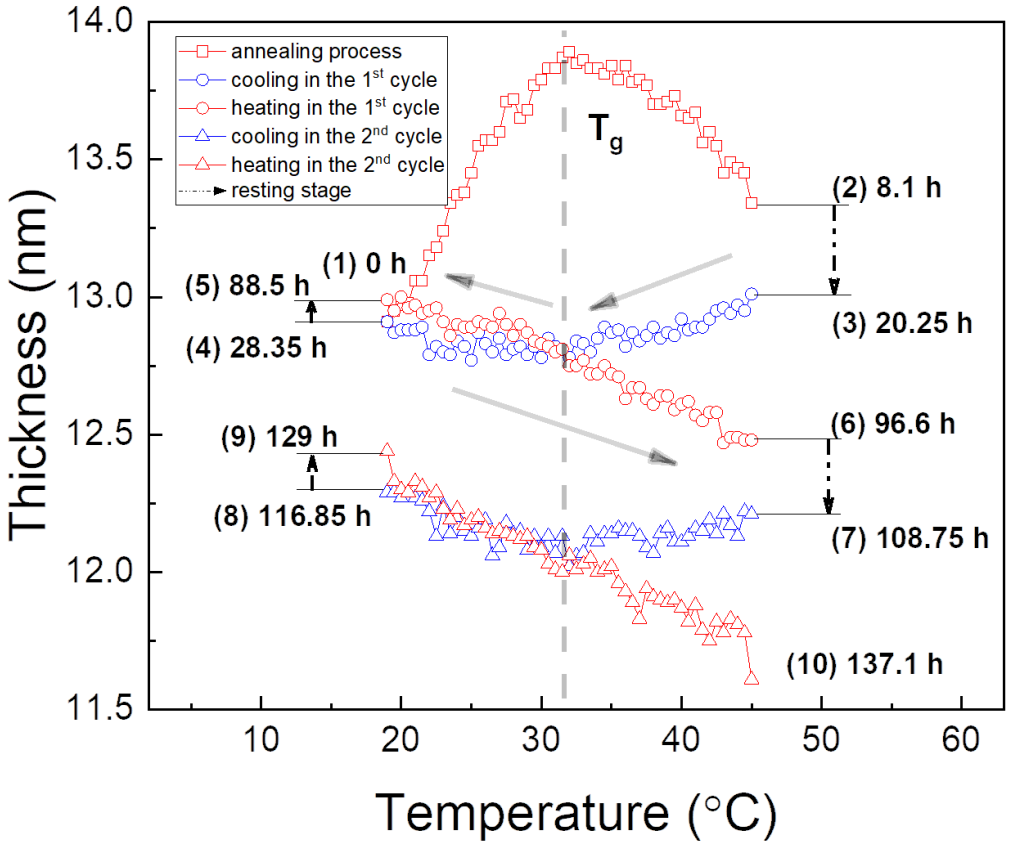

Figure 4. Thickness change (calculated by FT) of PVAc ultra-thin film (of 13 nm) in annealing and temperature cycles: (1) start of the annealing; (2) end of the annealing; (3) start of the 1st cooling run; (4) end of the 1st cooling run; (5) start of the 1st heating run; (6) end of the 1st heating run; (7) start of the 2nd cooling run; (8) end of the 2nd cooling; (9) start of the 2nd heating run; (10) end of the 2nd heating run. All temperature scan rates were set at 0.5 °C/steps. Each step took 9 min. (Langmuir 34.38 (2018): 11272-11280)

nm) in the heating process. Unlike the observation in PVAc thin film (of 120 nm), this different would be considered the origin of NTE in PVAc thin film system.

To give more detail on these processes, all X-ray reflectivity curves obtained from PVAc ultra-thin film (of 13 nm), including the annealing process, have been calculated by Fourier transform, and thickness change with temperature is presented in the Figure 4. Just as expected, in the experiment of PVAc ultra-thin film, all instances of NTE become clearer and more stable. As shown in Figure 4, the different behaviors between annealing and temperature cycle can be easily distinguished. In the annealing process, thickness greatly increases in its glassy state and suddenly decreases after glass transition, which displays a different tendency to thickness change in the following process. In the temperature cycle, reversible NTE can be confirmed in the glassy state, and another continued decrease in thickness is first observed in the rubbery state with heating. Unlike the isothermal decrease in thickness in the thicker film in the rubbery

Table 1. Experimentally obtained thermal expansion coefficients of PVAc film at each stage in temperature cycle. (Langmuir 34.38 (2018): 11272-11280)

Sample	Process	Coefficient of thermal expansion (ppm K^{-1})			
		Cooling		Heating	
		Rubbery state	Glassy state	Glassy state	Rubbery state
PVAc (120 nm)	1st cycle	301	-120	23	464
	2nd cycle	281	-80	-30	444
	3rd cycle	348	-196	-255	197
PVAc (13 nm)	1st cycle	879	-488	-983	-1750
	2nd cycle	612	-1260	-2250	-1970

state, this monotonous NTE becomes more extreme in the thinner film. Meanwhile, the resting state in the glassy and rubbery state in the thinner film have been compared. In the 1st resting stage between cooling and heating at 19 ºC for 64 h, the thickness only increases 0.62% (0.08 nm), but in the resting stage between two temperature cycles at 45 ºC for 12 h, thickness decreases 1.52% (0.2 nm). The large difference indicates the different mechanism of NTE in the glassy and rubbery state respectively. In the present research, X-ray reflectivity data have been analyzed by Fourier analysis. Although Fourier analysis is much more suitable in the determination of thickness during the temperature change in the present work, than the conventional whole pattern fitting procedures using the Parratt's recursive formula. However, the comparison with typical fitting analysis would be also interesting. The results of the analysis through the conventional whole pattern fitting have been presented in the Chapter 2, Figure 5. Roughly speaking, the tendency of the thickness change in the heating/cooling cycles is consistent. As a simple summary for the above finding, reversible NTE and monotonous NTE in PVAc ultra-thin film can be also observed in its glassy and rubbery state respectively, and they become clearer and more stable with decrease in thickness.

On the other hand, the coefficients of thermal expansion (CTE) of different PVAc film have also been calculated for analysis. Considering the unusual thickness change with temperature in short range, all change processes were treated in linear relationship and glass transition temperature is set at 31 ºC to simplify calculation. In Table 1, all CTE are presented. Comparing the data in each glassy state, it has been found that NTE in PVAc ultra-thin film (of 13 nm) can be more prominent. Meanwhile, another inconspicuous feature that can be noted is that NTE becomes clearer with repeated temperature cycle. Even though this feature is weak and ambiguous, it might also imply some mechanism in the unusual phenomena

3.4.3 *Unexplained experimental phenomena with existing model*

Reviewing the reports related to NTE in amorphous polymer systems, it is generally accepted that these

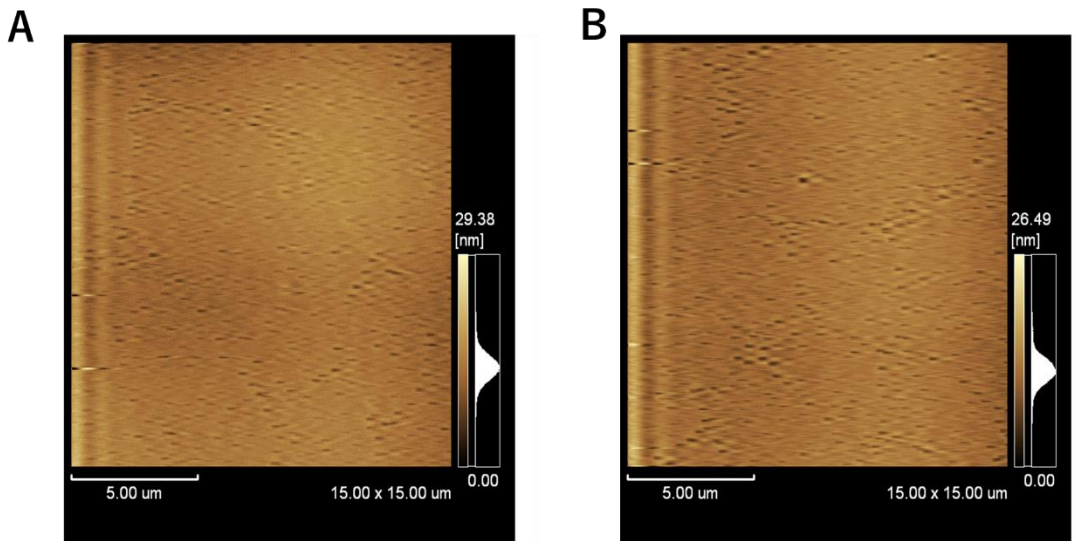

Figure 5. SPM images of PVAc ultra-thin film after annealing (A), and two temperature cycles (B). Measurements were conducted in dynamic scan model for soft surface morphology analysis, and all results were flattened by plane fitting. (Langmuir 34.38 (2018): 11272-11280)

phenomena can just be the byproduct of other common structural change processes like de-wetting, structural relaxation and lateral expansion/contraction, and hence existing theories or models are always coarse and cannot work well widely. In the research from Günter Reiter, et al., who first observed de-wetting of PS ultra-thin film below T_g, also observed the isothermal increase in thickness with roughness in its glassy state. In this elastic model, isotherm expansion in polymer film can occur with a pinhole growing in the de-wetting process in constant volume [4,29]. However, this model is not suitable for our finding. In our work, reversible NTE and monotonous NTE have been observed in PVAc thin films with temperature in its glassy and rubbery state respectively, and the fringes of X-ray reflectivity curve are always kept perfectly with temperature cycle. Both phenomena exhibit different behaviors to the de-wetting process. Meanwhile, the surface morphologies of PVAc ultra-thin film are further studied with SPM measurement. In the experiment, new PVAc ultra-thin film (of 13 nm) was prepared and treated in same process as described above. The SPM images of surface morphology after annealing and two temperature cycles are compared in the Figure 5. As illustrated in Figure 5A, some small pinholes with radius of ~100 nm can be found on the surface after annealing, and this morphology is generally considered as the initial state of de-wetting or the result of evaporation of solvent in spin coating polymer. However, these freely distributed pinholes do not change too much even after two temperature cycles as illustrated in Figure 5B. These SPM images demonstrate the stable surface morphology of PVAc ultrathin films in our experiment, which indicates that the instances of NTE in our experiment do not originate from the de-wetting process, even though some initial de-wetting step may exist in our experiment.

On the other hand, in the latest reports, the NTE in PS ultra-thin film systems is caused by two different kinetics processes was proposed by T. Kanaya, et al. In their experiment, one fast temperature dependent

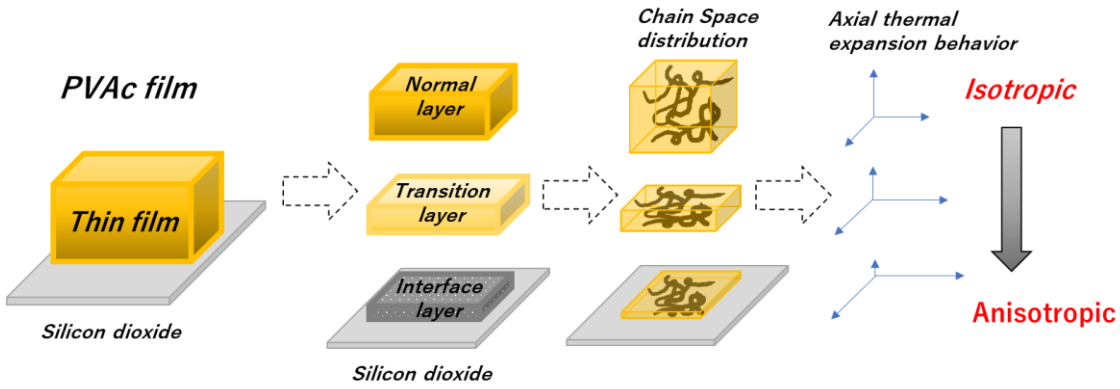

Figure 6. Postulated trilayer model in PVAc thin film: interface layer, transition layer and normal layer. The special distribution of polymer chain can be influenced by the interface interaction. The interface layer is proposed that it can form in rubbery state in 2D distribution, and then be frozen in glassy state. The transition layer is the adjunct layer of interface layer with buried entanglement. The normal layer is the remaining layer which can be considered the same as bulk. (Langmuir 34.38 (2018): 11272-11280)

NTE has been observed below T_g in heating without annealing, and another slow abnormal isothermal change in thickness has been found at the resting stage in temperature cycle. In the related interpretation, T. Kanaya suggested that two NTEs in PS ultra-thin film can be assigned to structural relaxation and lateral expansion/contraction respectively. [7–9] For the fast NTE, the volume of unrelaxed polymer materials can decrease with heating below T_g, and this behavior can disappear after efficient annealing.[30] For the slow NTE, additional deformation of polymer ultra-thin film can occur with different lateral thermal expansion between substrate and supported film, and then a slow isothermal recovery process is proposed with sliding motion only in an ultra-thin film system.[31] Without doubt, this postulated model in NTE of polymer ultra-thin film is creative and inspired, but any detailed discussion will be evolved with new finding. In our work, two different instances of NTE in PVAc thin film system have been also observed. One temperature dependent NTE in the glassy state has been confirmed with repeated experiment after annealing, and both instances of NTEs can exist in film with a thickness of more than 100 nm. In T. Kanaya's model, temperature dependent NTE from structural relaxation should only exist in heating and disappear after annealing, and lateral expansion/contraction can only result in isothermal contraction/expansion of thickness but not NTE with temperature. Such monotonous NTE observed in the rubbery state sometimes have has been understood simply as a kind of annealing process, because it includes typical transition from non-equilibrium to equilibrium states. As shown in Fig. 2 (the process, (3) to (4) and (6) to (7)), the slow negative thermal expansion process, which has been found in the rubbery state, is re-accelerated after the completion of one temperature cycle. Because the thickness decreasing process in the rubbery state starts again, one would understand that the process differs from general annealing. The transition from non-equilibrium to equilibrium states consists of several different kinetic process. In the early stage, the transition would be very fast, and then it becomes extremely slow. When finishing one temperature cycle, one would see the polymer thin film has changed, and does not

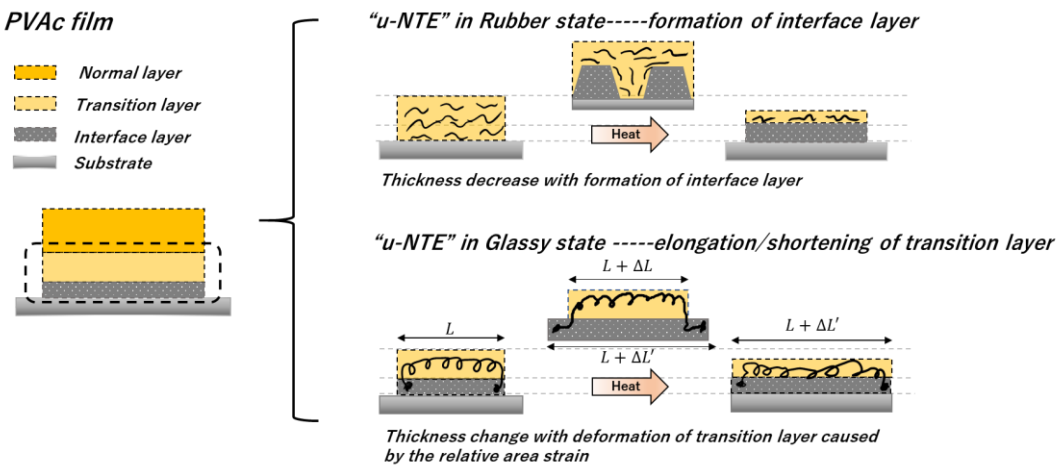

Figure 7. Conceptual sketch of two different types of NTE took place in PVAc thin film system: the NTE in rubbery state can occur with the formation of interface layer; the NTE in glassy state can occur with the additional elongation/shortening of transition layer. (Langmuir 34.38 (2018): 11272-11280)

come back to the initial state anymore. However, even after this stage, the thickness reduction process at rubbery state starts again. The monotonous NTE observed in the rubbery state is no doubt a kind of transition from non-equilibrium to equilibrium states, but it is rather complicated to understand simply as annealing. In addition to above, the conclusion that NTE can only exist in polymer film with thickness equal to or below radius of gyration would be discussed again.

3.4.4 *Modeling of NTE in PVAc thin films*

Depending on our observation, the trilayer model is first proposed to point out the mechanism of NTE in PVAc thin film systems. In this postulated model, PVAc thin film is considered to consist of three different layers, called the interface layer, transition layer and normal layer as illustrated in Figure 6. In the polymer thin film systems, the effect of the interface becomes more significant. As one possible result, the spatial distribution of polymer chains gradually changes in depth from 3D to 2D parallel to the surface of substrate and free volume greatly decreases at the interface. In other words, with axial thermal expansion, the behaviors of polymer thin film can gradually change with depth from isotropic to anisotropic. Consequently, this special layer is defined as the interface layer, which holds horizontal chain distribution and larger area density. In the temperature cycle, the interface layer is proposed to form in the rubbery state and then be frozen in the glassy state with glass transition. One important point that must be stressed here is that the interface layer is not a separate layer. Because of buried entanglements in the polymer system, the adjacent layer above the interface layer can be also affected by the interface layer. As such, this adjacent layer is defined as the transition layer, which has the same property as bulk but can be easily influenced by the interface layer. Finally, the remaining layer which can be considered the same as bulk is defined as normal layer. In the trilayer model, the observation of thermal expansion in PVAc thin film systems can vary with competition between each layer.

In the rubbery state, monotonous NTE can occur with formation of the interface layer with temperature

cycle as illustrated in Figure 7. In general, the total volume of amorphous polymer consists of the occupied volume of chains and minimum free volume (with a fraction of about 2.5~12%) between each chain.[32,33] In the rubbery state, rotation of the polymer chain becomes active, and free volume can greatly change with temperature. In the practical sample, especially for spin coating thin film systems, the free volume hole can tend to be more than expected even after annealing. And this special reality provides the possibility for our model. As shown in Figure 2 and Figure 4, the thickness of PVAc thin film decreases at the resting/heating stage in the rubbery state, which indicates the decrease in free volume in thin film systems. As all experiments were conducted after a long annealing time, clearly this change is not a kind of structural relaxation in the bulk phase, and should be more specific to thin film systems. In the rubbery state of PVAc thin film, touching event between Kuhn segments and substrate can increase with temperature and time. Considering the interface interaction (like hydrogen bond or van der Waals' force), the buried "free surface layer" might be fixed at interface with touching events resulting in the anisotropic distribution of polymer chain in horizontal and larger area density. As a result, in our observation, total thickness gradually decreases with interface layer increase in the rubbery state. It is important to note that this process is dominated by kinetics but not dynamics. Temperature only determines the possibility of touching event with molecular vibration, and steric effect dominates the equilibrium state of main chain distribution. As observed in Figure 2 and Figure 4, NTE in the rubbery state gradually weakens and finally disappears in the cooling process, but with the abnormal deformation in the glass state, NTE revives in the rubbery state in new resting/heating stage. On the other hand, it should be also noted this process can be influenced by thickness. As shown in Figure 4, the prominent NTE in the rubbery state can relate to an alternative collective sliding motion in polymer ultra-thin film with thickness equal to or below radius of gyration, which require weaker free volume and can even occur in the glassy state.[31,34]

In the glassy state, another reversible NTE can result from deformation of the transition layer with normal thermal expansion as illustrated in Figure 7. Following the above assumption of formation of the interface layer in the rubbery state, this anisotropic layer can be frozen in the glassy state with glass transition. Different to the rotation of main chain in the rubbery state, in the glassy state, only the local vibration can exist in polymer materials, which means that total volume can only change with the occupied volume of polymer chain but not the free volume. Therefore, interface layer, which consist of the horizontal polymer chain and few free volume, is proposed to have the larger CTE in horizontal directions. During normal thermal expansion in the glassy state, the interface layer can make a larger lateral deformation compared to the transition layer, and then contribute additional stress to it with buried entanglements. Finally, this stress forces the additional lateral deformation of the transition layer causing thickness decrease in constant volume. Different to the isothermal recovery process in lateral expansion/contraction model, the NTE in the glassy state in our model is temperature dependent and follows the anisotropic normal thermal expansion in the interface layer. Furthermore, the most important point is that this motion can be thickness independent. The performance of NTE in the glassy state can relate to the property of the interface layer and the mobility of the transition layer. Comparing the opposite conclusions in previous research, it has been proposed that the difference stems from the experimental

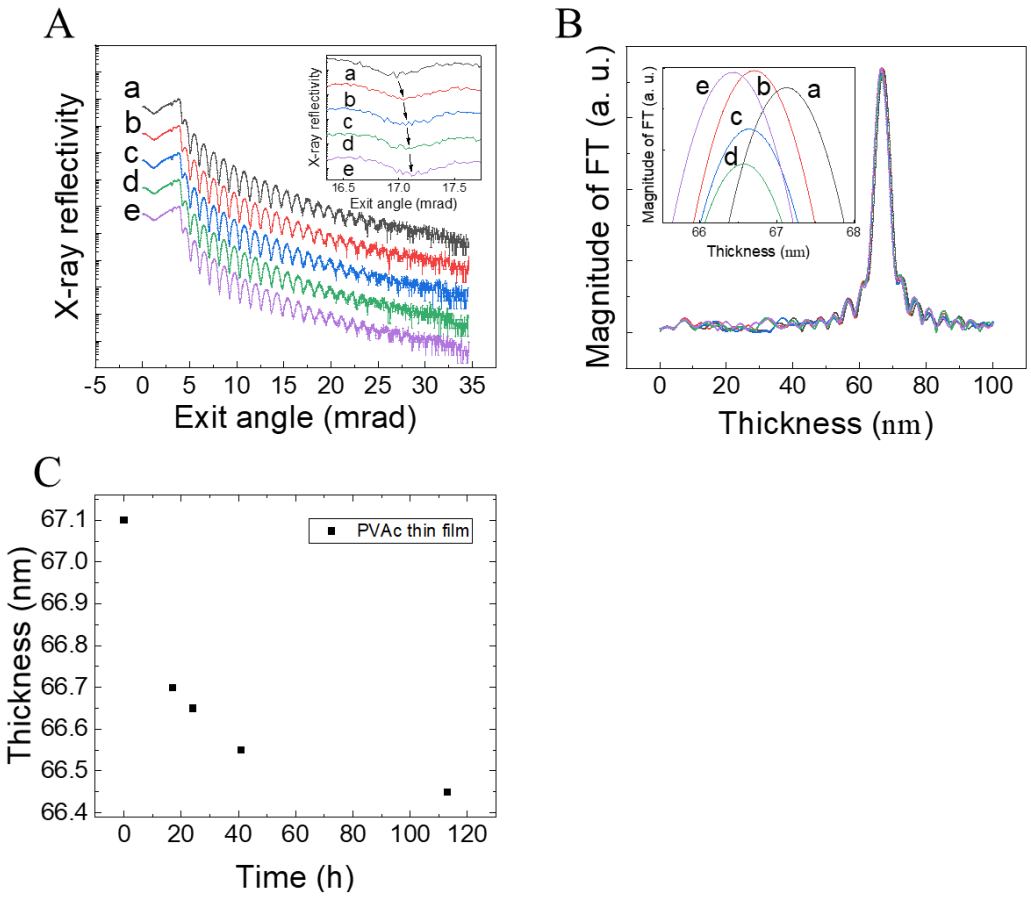

Figure 8. (A) X-ray reflectivity curves of a PVAc thin film during annealing at 45°C: a) at 0 h (black), b) at 17 h (red), c) at 24 h (blue), d) at 41 h (green), and e) at 113 h (purple) — the inset graph displays the magnified fringes approximately 17 mrad. (B) The Fourier transform (FT) of the interference fringes observed in the X-ray reflectivity profiles — the inset graph displays the magnified peak of the FT magnitude with thickness. (C) The thickness change (calculated by FT) of the PVAc thin film during annealing. All X-ray reflectivity curves are presented on a base-10 logarithmic scale with an offset. (Polymer Journal 51 (2019): 1073–1079)

sample and pre-treatment. Just as suggested above, the formation of the interface layer determines whether NTE occurs. Unlike previously well studied cases, such as the PS ultra-thin film, PVAc apparently exhibits stronger interaction with the native silicon dioxide layer of the Si substrate, leading to the negative thermal expansion even for thick film (120 nm). Much lower T_g of PVAc also indicates the higher mobility of polymer chains. Those features would support the formation of the interface layer.

For the research on multi-layer structure of polymer thin film, the concept of a multilayer structure was verified by a research group of Kanaya measuring T_g at different depth positions in a polymer thin film using neutron reflectometry.[35–37] In these experiment, deuterated and hydrogenated polystyrene (d-PS and h-PS) and poly (methyl methacrylate) (d-PMMA and h-PMMA) were stacked by floating method in multilayer structure, and these isolated layers structure promised the performance in the depth dependence. In their works, the different T_g have been confirmed in each sub-layer in the multilayer

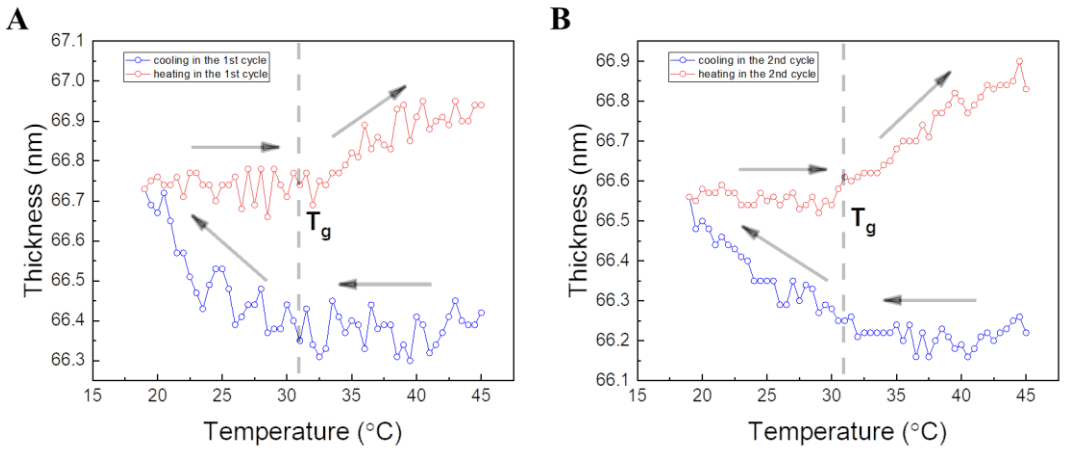

Figure 9, (A) Thickness change (calculated by FT) of a PVAc thin film during the first temperature cycle between 45°C and 19°C and (B) after heating at 45°C for four days: the thickness change (calculated by FT) of the PVAc thin film in the second temperature cycle between 45°C and 19°C. (Polymer Journal 51 (2019): 1073–1079)

polymer thin film. The T_g at the surface layer is always smaller than the T_g reported in the bulk, and it can gradually recover to the bulk value with depth increasing. However, one more interesting finding is that the T_g of bottom sub-layer greatly exceed above the experiment temperature range. These researches proved the great contribution of interface/surface effect on polymer thin film system, which cause the different mobility with depth distribution. However, the "single polymer thin film" must be more complex because of the existing of entanglement in the thin film system. But no doubt that we can still believe that the competition between interface and surface effect can contribute multilayer even in the "single polymer thin film". In our research, we have observed the NTE in PVAc thin film systems and propose the multilayer model which would be agreed by the discussion from the research group of Kanaya. On the other hand, we have also known that the negative thermal expansion would be difficult to be observed in the free-standing polymer thin film.[34] It implies that the negative thermal expansion would be caused by cooperation between the interface affection and entanglement in our spin coated PVAc thin film system.

3.4.5 *Variable interface layer in PVAc thin film with temperature cycle*

In this section, to clarify the relationship between the NTE and fine structural changes that are not yet known in the polymer thin-film system, first, the thickness change from annealing was confirmed. In Figure 8A, the collected X-ray reflectivity curves for the PVAc thin film during the annealing process (at 0, 17, 24, 41, and 113 h) are presented with an offset. Browsing the Kiessig fringes from a to e, the clear amplitude of the oscillation indicates the stable interface conditions during the annealing (at 45°C). Meanwhile, the decrease in the frequency of oscillation can also be confirmed in the insert graph, which indicates a decrease in the thickness of the PVAc thin film. As shown in Figure 8B, all X-ray reflectivity data were preferentially analyzed in a Q_z range of 0.03-0.16 nm^{-1} and the Fourier transform of the X-ray reflectivity fringes are plotted with a step of 0.05 nm. As shown in the inset graph in Figure 8B, the

Table 2. Experimentally obtained thermal expansion coefficients of the PVAc film at each stage of the temperature cycles. (Polymer Journal 51 (2019): 1073–1079)

Sample	Process	Coefficient of thermal expansion (ppm/K)			
		Cooling		Heating	
		Rubbery state	Glassy state	Glassy state	Rubbery state
PVAc	1st cycle	24	-417	13	232
(60 nm)	2nd cycle	-11	-334	-11	311

thickness of the PVAc thin film gradually decreases during the annealing. In Figure 8C, the thickness of the PVAc thin film is plotted against time for 113 hours. Noticeably, the thickness decrease of the PVAc thin film during the annealing can be considered to include two steps: the rapid thickness decreases in the first 17 h and the slow thickness decrease during the next 100 h. However, these two steps cannot be simply decided into the two kinetics processes because the sorting out of all the kinetics during annealing with only five data plots is impossible. Within the first 17 h, the thickness decreases rapidly by 0.6% from 67.1 to 66.7 nm, which could be related to the evaporation of residual toluene and the disappearance of free holes in spin-coated polymer thin films with annealing.[30] In the general prethermal treatment, the annealing can be completed with the directional creep of the polymer chain from the bulk area towards the inner free hole, which is considered fast and irreversible, similar to the first step shown in Figure 8C. During the next 100 h, the thickness decreases slowly, only by 0.4% from 66.7 to 66.45 nm, which was rarely noticed or studied in the past. In related reports, Kanaya suggested that this ultra-slow thickness decrease is a type of thickness recovery process caused by the different CTEs between the polymer thin film and its substrate.[25,26,38] And in this work, it is proposed to the formation of interface layer. As a result, the total thickness gradually decreases with the increase in the interface layer in the rubbery state. This slow thickness decrease can still be suspected of including other monotonous kinetics processes, such as the evaporation of residual toluene. However, in the following experiment results, it is shown that these monotonous kinetics processes do not contribute to the new findings in this experiment because there is no decay in the behaviors of PVAc ultrathin films with the temperature cycle.

In Figure 9, the thickness change of the PVAc thin film during the temperature cycle between 45°C and 19°C is presented. The temperature scan started at 45°C, varied up to 19°C, and then returned back to 45°C. This process was repeated twice to confirm the performance. An asymmetric and reproducible thickness change of the PVAc thin film is observed in the temperature cycle. In the cooling process, the thickness of the PVAc thin film can remain stable at first when the temperature is higher than T_g, which is reported to be 31°C in the bulk system, and then the thickness increase can occur abruptly as the

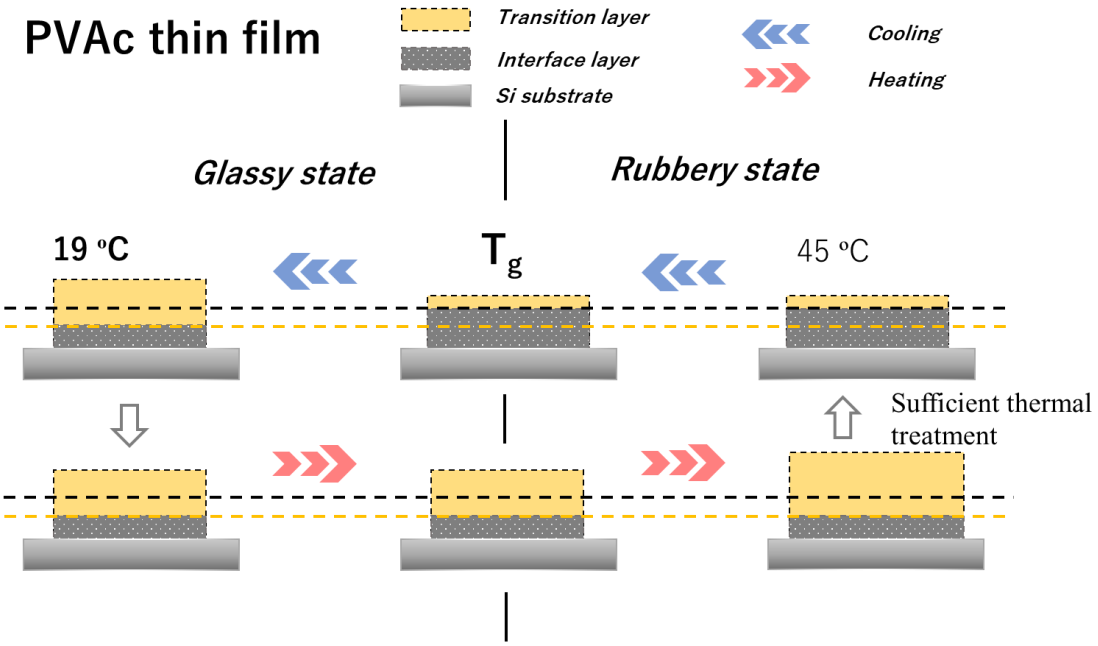

Figure 10. Conceptual sketch of the unusual thickness change in a PVAc thin-film system with sufficient thermal treatment; the interface layer can gradually grow and dominate the thickness change of the PVAc thin film during the cooling when the temperature is above Tg. When the temperature is below Tg, an NTE can occur with the additional deformation of the transition layer. Some part of the interface layer transforms into the transition layer. When the cooling ends and heating begins, the transition layer dominates the thickness change of the PVAc thin film. As the temperature returns to a value above Tg, the interface layer gradually grows again. (Polymer Journal 51 (2019): 1073–1079)

temperature crosses the T_g with further cooling. The NTE can be confirmed in the PVAc thin films in the glassy state with cooling, and another interesting find is that there is no thickness change of the PVAc thin film in its rubbery state with cooling. Furthermore, in the heating process, the behavior of the thickness change is reversed and appears similar to that of the bulk. The thickness of the PVAc thin film remains stable at the low-temperature side and then increases quickly at the high-temperature side. The CTE of the PVAc thin film was calculated and is presented in Table 2. Considering the thickness change for the short temperature range, all processes were treated as having a linear relationship, and the T_g value was set to 31°C to simplify the calculation. Table 2 shows that, in the heating process, the CTEs of the PVAc thin films are close to zero in the glassy state and approximately 230–310 ppm/K in the rubbery state, which are less than half the CTE of the PVAc bulk.[37] As is evident, the tendency of the thermal expansion of the PVAc thin film is the same as that of the bulk state in the heating process, but the CTE is suppressed. Finally, another point that is noteworthy is that the initial thicknesses of the PVAc thin films are close prior to each temperature scan, which can respond to the second step in Figure 8 that a slow isothermal thickness decrease can occur when the sample is kept at 45°C.

In the studies on the interface interaction between a polymer thin film and substrate, Kanaya confirmed that the T_g in the polymer thin-film system can change with depth, and near the interface between the

polymer and substrate, only a limited thickness change in the bottom sublayer can be observed within the experimental temperature range.[35–37] As shown in Figure 9, similar behaviors of PVAc thin films can be confirmed in the cooling process when the temperature is more than 31°C, and it is assumed that an interface layer dominates the performance of the PVAc thin films in this cooling process. As the temperature becomes less than T_g, the CTE of polymers can be exclusively governed by the vibrational contribution; therefore, the interface layer, which contains more atomic bonds, has a larger CTE in horizontal directions than it does in its adjacent layer (the transition layer). In this experiment, the interface layer grows slowly with sufficient thermal treatment at 45°C, and its CTE is suppressed by the interface interaction in the rubbery state. As shown in Figure 10, no thickness change in the rubbery state with cooling is observed. When the temperature is below the T_g, the PVAc ultrathin film could be further frozen with the anisotropic structure formed in the rubbery state, and the different CTE in the horizontal direction between the interface layer and transition layer could produce an additional internal stress by normal thermal expansion with temperature. Therefore, the transition layer would be forced by the interface layer, causing an additional deformation in the vertical direction, and the NTE would occur. Meanwhile, the interface layer could also be influenced by the stress, causing the 2D to 3D changes in the polymer chains. During the NTE with cooling, the influence of the interface layer on the CTE of the PVAc ultrathin film could gradually decline with the loosening of the interface layer. In the heating process, because of the transformation from the interface layer to the transition layer, the difference in CTEs between the interface layer and the transition layer become small, and the thickness change of the PVAc thin film is dominated by the performance of the transition layer, the CTE of which would be close to that of the bulk. Considering the remaining interface layer, the observed CTE must be lower than that in the bulk system. Therefore, suppressed thermal expansion of the PVAc thin film is observed in the heating process. However, this new state of the PVAc thin film would be unstable in its rubbery state, and the slow formation of an interface layer would occur again with heating to more than T_g. Finally, a slightly decrease in the thickness of the PVAc thin film is observed at the initial state of the second temperature cycle, together with the similar thickness change with the temperature cycle. Obviously, the interface layer state should vary in the different cases. Because the interface can gradually grow with time in the rubbery state and transform to a transition layer with an NTE in the glassy state, the interface layer state can be greatly affected by the interface interaction, mobility of polymer chains, thermal treatment, and initial state of the polymer thin film itself. In this study, the NTE of the PVAc ultrathin film is observed exclusively with cooling, but this result does not imply that the NTE can only occur with cooling. In the proposed model, the NTE of the polymer ultrathin film can occur with different CTEs between the interface layer and transition layer, while the difference in CTEs can also gradually decline with the NTE process, causing the disappearance of the NTE with the temperature change in the glassy state.

Finally, some researchers may suspect that the free surface layer in the polymer ultrathin film affects the NTE behaviors. In related reports,[35–37] it was confirmed that the existence of a free end chain can cause the high mobility of a surface layer and decease T_g. However, even in the studies for a free-standing PS thin film, which has two free surface layers, there is no report on NTE, which indicates that enthalpic

terms at the free surface layer cannot be the main factor behind the NTE observed in the experiments reported here.[34] Therefore, it is proposed that even though the free surface layer is crucial in the polymer ultrathin-film system, the effect of the free surface layer on the NTE is not significant.

3.5 Conclusion

It has been found that the polymer with such low T_g exhibits unusual NTE when it becomes the thin film form. So far, the NTE has been known only in extremely thin film cases. In the present studies, it has been experimentally found that NTE definitely takes place during heating/cooling cycles between 19 ºC and 45 ºC, not only in ultrathin 13 nm film but also in quite thick 120 nm film. Because of this new discovery, it has become important to reconsider and discuss further the origin of NTE in polymer thin film systems. With the use of a multi-channel X-ray reflectometry, fast reversible NTE has been confirmed in the glassy state in both thickness samples, and another slow monotonous NTE has been also confirmed in the rubbery state with complex kinetics which not only depend on thin film thickness but also can be re-accelerated with temperature cycle. Meanwhile, analysis of latent reasons, like bulk structural relaxation, de-wetting or crystallization has also been experimentally discussed. As one reasonable explanation, the trilayer model was first proposed to give the detail mechanism for NTE in polymer thin film systems. In the postulated model, the interface layer can form with interface interaction contributing monotonous NTE in the rubbery state. In the glassy state, the frozen interface layer can also elongate or shorten the transition layer with normal thermal expansion causing reversible NTE in the glassy state. Meanwhile, the interface layer can also transform to transition layer with this reaction force. After the loss of the interface layer in the glassy state, the thermally responsive behaviors of the polymer thin film can recover to normal in the process. Finally, the normal layer can be independent of the previous two layers but also contribute to the observation of thickness change in polymer thin film. Unlike crystal or other topological materials, one complex NTE structure can be simply built in PVAc thin film systems.

Reference

(1) Takenaka, K. Negative Thermal Expansion Materials: Technological Key for Control of Thermal Expansion. *Science and Technology of Advanced Materials*. February 2012.

(2) Evans, J. S. O. Negative Thermal Expansion Materials. *Journal of the Chemical Society - Dalton Transactions*. Royal Society of Chemistry October 7, 1999, pp 3317–3326.

(3) Orts, W. J.; van Zanten, J. H.; Wu, W.; Satija, S. K. Observation of Temperature Dependent Thicknesses in Ultrathin Polystyrene Films on Silicon. *Phys. Rev. Lett.* **1993**, *71* (6), 867.

(4) Reiter, G. Dewetting as a Probe of Polymer Mobility in Thin Films. *Macromolecules* **1994**, *27* (11), 3046–3052.

(5) Mukherjee, M.; Bhattacharya, M.; Sanyal, M. K.; Geue, T.; Grenzer, J.; Pietsch, U. Reversible Negative Thermal Expansion of Polymer Films.

(6) Soles, C. L.; Douglas, J. F.; Jones, R. L.; Wu, W. L. Unusual Expansion and Contraction in Ultrathin Glassy Polycarbonate Films. *Macromolecules* **2004**, *37* (8), 2901–2908.

(7) Miyazaki, T.; Nishida, K.; Kanaya, T. Contraction and Reexpansion of Polymer Thin Films. *Phys. Rev. E* **2004**, *69* (2), 022801.

(8) Miyazaki, T.; Nishida, K.; Kanaya, T. Thermal Expansion Behavior of Ultrathin Polymer Films Supported on Silicon Substrate. *Phys. Rev. E* **2004**, *69* (6), 061803.

(9) Kanaya, T.; Miyazaki, T.; Inoue, R.; Nishida, K. Thermal Expansion and Contraction of Polymer Thin Films. *Phys. status solidi* **2005**, *242* (3), 595–606.

(10) Mark, J. E. *Polymer Data Handbook*; Oxford University Press, Inc.: New York, 1999.

(11) Mizusawa, M.; Sakurai, K. In-Situ X-Ray Reflectivity Measurement of Polyvinyl Acetate Thin Films during Glass Transition. *IOP Conf. Ser. Mater. Sci. Eng.* **2011**, *24*, 012013.

(12) Sakurai, K.; Mizusawa, M. M. X-Ray Reflectometer and the Measurement Method. 3903184, 2007.

(13) Naudon, A.; Chihab, J.; Goudeau, P.; Mimault, J. New Apparatus for Grazing X-Ray Reflectometry in the Angle-Resolved Dispersive Mode. *J. Appl. Cryst* **1989**, *22*, 460–464.

(14) Tanaka, K.; Takahara, A.; Kajiyama, T. Surface Molecular Aggregation Structure and Surface Molecular Motions of High-Molecular-Weight Polystyrene/Low-Molecular-Weight Poly(Methyl Methacrylate) Blend Films. *Macromolecules* **1998**, *31* (3), 863–869.

(15) Liu, Y.; Sakurai, K. Uniaxial Negative Thermal Expansion of Polyvinyl Acetate Thin Film. *Langmuir* **2018**, *34* (38), 11272–11280.

(16) Liu, Y.; Sakurai, K. Slow Dynamics in Thermal Expansion of Polyvinyl Acetate Thin Film with Interface Layer. *Polym. J.* **2019**.

(17) Liu, Y.; Sakurai, K. Thickness Changes in Temperature-Responsive Poly(N -Isopropylacrylamide) Ultrathin Films under Ambient Conditions . *ACS Omega* **2019**, *4* (7), 12194–12203.

(18) Liu, Y.; Sakurai, K. Thermoresponsive Behavior of Poly(N-Isopropylacrylamide) Solid Ultrathin Film under Ordinary Atmospheric Conditions. *Chem. Lett.* **2017**, *46* (4), 495–498.

(19) Sakurai, K.; Iida, A. Fourier Analysis of Interference Structure in X-Ray Specular Reflection from Thin

Films. *Jpn. J. Appl. Phys.* **1992**, *31* (2), 113–115.

(20) Stoev, K. N.; Sakurai, K. Review on Grazing Incidence X-Ray Spectrometry and Reflectometry. *Spectrochimica acta, Part B: Atomic spectroscopy*. Elsevier Science B.V. January 4, 1999, pp 41–82.

(21) Lvov, Y.; Decher, G.; Mohwald, M. Assembly, Structural Characterization, and Thermal Behavior of Layer-by-Layer Deposited Ultrathin Films of Poly(Vinyl Sulfate) and Poly(Allylamine). *Langmuir* **1993**, *9* (2), 481–486.

(22) Bridou, F.; Pardo, B. Grazing X-Ray Reflectometry Data Processing by Fourier Transform. *J. Xray. Sci. Technol.* **1994**, *4* (3), 200–216.

(23) Bridou, F.; Pardo, B. Use of Fourier Transfoim in Grazing X-Rays Reflectometry. *J. Phys. III* **1994**, *4* (9), 1523–1531.

(24) Parratt, L. G. Surface Studies of Solids by Total Reflection of X-Rays. *Phys. Rev.* **1954**, *95* (2), 359–369.

(25) Miyazaki, T.; Nishida, K.; Kanaya, T. Contraction and Reexpansion of Polymer Thin Films. *Phys. Rev. E - Stat. Nonlinear, Soft Matter Phys.* **2004**, *69* (2 1).

(26) Miyazaki, T.; Nishida, K.; Kanaya, T. Thermal Expansion Behavior of Ultrathin Polymer Films Supported on Silicon Substrate. *Phys. Rev. E - Stat. Physics, Plasmas, Fluids, Relat. Interdiscip. Top.* **2004**, *69* (6), 6.

(27) Mukherjee, M.; Bhattacharya, M.; Sanyal, M. K.; Geue, T.; Grenzer, J.; Pietsch, U. Reversible Negative Thermal Expansion of Polymer Films. *Phys. Rev. E - Stat. Physics, Plasmas, Fluids, Relat. Interdiscip. Top.* **2002**, *66* (6), 4.

(28) Orts, W. J.; Van Zanten, J. H.; Wu, W. L.; Satija, S. K. Observation of Temperature Dependent Thicknesses in Ultrathin Polystyrene Films on Silicon. *Phys. Rev. Lett.* **1993**, *71* (6), 867–870.

(29) Reiter, G. Dewetting of Highly Elastic Thin Polymer Films. *Phys. Rev. Lett.* **2001**, *87* (18), 186101.

(30) Frick, B.; Richter, D.; Ritter, C. Structural Changes near the Glass Transition-Neutron Diffraction on a Simple Polymer. *EPL* **1989**, *9* (6), 557–562.

(31) De Gennes, P. G. Glass Transitions in Thin Polymer Films. *Eur. Phys. J. E* **2000**, *2* (3), 201–205.

(32) Fox, T. G.; Flory, P. J. The Glass Temperature and Related Properties of Polystyrene. Influence of Molecular Weight. *J. Polym. Sci.* **1954**, *14* (75), 315–319.

(33) Miller, A. A. Polymer-Melt Viscosity and the Glass Transition: An Evaluation of the Adam-Gibbs and the Free-Volume Models. *J. Chem. Phys.* **1968**, *49* (3), 1393–1397.

(34) Forrest, J. A.; Dalnoki-Veress, K.; Dutcher, J. R. Interface and Chain Confinement Effects on the Glass Transition Temperature of Thin Polymer Films. *Phys. Rev. E - Stat. Physics, Plasmas, Fluids, Relat. Interdiscip. Top.* **1997**, *56* (5), 5705–5716.

(35) Inoue, R.; Nakamura, M.; Matsui, K.; Kanaya, T.; Nishida, K.; Hino, M. Distribution of Glass Transition Temperature in Multilayered Poly(Methyl Methacrylate) Thin Film Supported on a Si Substrate as Studied by Neutron Reflectivity. *Phys. Rev. E - Stat. Nonlinear, Soft Matter Phys.* **2013**, *88* (3).

(36) Inoue, R.; Kawashima, K.; Matsui, K.; Nakamura, M.; Nishida, K.; Kanaya, T.; Yamada, N. L. Interfacial Properties of Polystyrene Thin Films as Revealed by Neutron Reflectivity. *Phys. Rev. E - Stat. Nonlinear, Soft Matter Phys.* **2011**, *84* (3).

(37) Inoue, R.; Kawashima, K.; Matsui, K.; Kanaya, T.; Nishida, K.; Matsuba, G.; Hino, M. Distributions of Glass-Transition Temperature and Thermal Expansivity in Multilayered Polystyrene Thin Films Studied by Neutron Reflectivity. *Phys. Rev. E - Stat. Nonlinear, Soft Matter Phys.* **2011**, *83* (2).

(38) Kanaya, T.; Miyazaki, T.; Inoue, R.; Nishida, K. Thermal Expansion and Contraction of Polymer Thin Films. *Phys. Status Solidi Basic Res.* **2005**, *242* (3), 595–606.

(39) McKinney, J. E.; Goldstein, M. PVT Relationships for Liquid and Glassy Poly (Vinyl Acetate). *J. Res. NBS-Physics Chem.* **1974**, *78*, 331–353.

Chapter 4

Asymmetric change in Poly(N-isopropylacryl amide) (PNIPAM) ultrathin film with temperature cycle

4.1 Introduction

Poly(*N*-isopropylacrylamide) (PNIPAM) is one of the most attractive thermoresponsive polymers and shows a sharp lower critical solution temperature (LCST)-type transition around 33°C. PNIPAM been widely studied in the aqueous environment. [1–3] Concerning the discussion of the mechanism of LCST-type transitions of PNIPAM aqueous systems, it is general accepted that the Gibbs free energy change arising from the competition between enthalpy and entropy terms can be explained by the changes in hydrogen bonding and hydrophobic interactions with temperature. [4,5] However, further study of the hydrogen bonds during the phase transition processes in PNIPAM has revealed that the LCST transition is more complicated. The hydrogen bonds involved in the LCST transition are not only hydrogen bonds between water and the polymer, but also hydrogen bonds between polymer chains, as well as hydrogen bonds between water molecules, [6–12] which exhibited the different temperature dependence. Or in other words, the transition ability of PNIPAM would be affected by the water amount in surrounding environment and the state of the polymer chain.

In the PNIPAM aqueous system, some water molecules can form hydrogen bonds with the N-H and C=O groups of PNIPAM, and these hydrogen bonds are particularly strong, often surviving after the de-mixing process. On the other hand, some water molecules surrounding the isopropyl groups of PNIPAM

can form hydrogen bonds with each other, thus forming water "cages" when the temperature is below the LCST. However, the latter hydrogen-bonded structure is not as stable as that between water molecules and the hydrophilic groups of PNIPAM. As the temperature increases above the LCST, the water "cage" can collapse with the increase in hydrophobic interactions, resulting in the formation of hydrogen bonds between the amide groups and completing the hydrophilic–hydrophobic transition. Obviously, the bound water and PNIPAM chains play different roles in the phase transition of aqueous PNIPAM with temperature. The transition behavior of PNIPAM is significantly affected by the real environment, such as bound water and state of the polymer chain. In studies of the PNIPAM brush system, a broadening and shift of the LCST of PNIPAM has been reported under various conditions.[13–18] Unlike pure aqueous systems, the mobility of the polymer chains and the hydrogen bonding is significantly influenced by the brush grafting density and the concentration of salt in the solution. Meanwhile, phase transition behavior of PNIPAM has been also observed in thin film systems in environments saturated with water vapor. Müller-Buschbaum and co-workers have investigated the PNIPAM-based copolymer thin film system extensively, [19–24] and found that PNIPAM-based copolymer thin film can absorb and store water from the air, thus causing swelling. In addition, a nonlinear thickness change has been confirmed on heating during the hydrophilic–hydrophobic transition; this is proposed to be influenced by the shape of the polymer chains.

In the first stage in this work, [25] the thermoresponsive behaviors of PNIPAM ultrathin films under the ambient conditions were studied. It has been preliminarily found that the ultrathin films exhibit some temperature response even without a large number of water molecules near the surface. And in the second stage in this work, the asymmetric swelling/shrinking has been confirmed in the PNIPAN ultrathin films with temperature under ambient conditions.[26] different control experiments have been conducted with the time, temperature and humidity. To clarify the mechanism, the changes in the thickness of the PNIPAM ultrathin films with temperature were studied using different strategies, such as (i) discrete monitoring, (ii) in-operando monitory, (iii) moisture control monitoring and (iiii) long-term monitoring. The main experiments involved a customized multichannel X-ray reflectometer [27–29] based on Naudon's method. [30] This device provides essentially the same information as conventional X-ray reflectivity measurements based on $\theta/2\theta$ scanning, including average layer structure information in the z-direction, [31,32] but simultaneous data collection can be realized in an extremely short time without any scanning or motion of the instrument. During discrete monitoring, the thicknesses of PNIPAM ultrathin film were recorded over two months. Continuous recovery and increases in the thickness of the PNIPAM ultrathin films were observed after each individual heating treatment at 70 °C for 3 h. Meanwhile, an asymmetric change in the thickness of the PNIPAM ultrathin film was observed on temperature cycling between 15 and 60 °C using in-operando monitoring. In the cooling process, the thickness of the PNIPAM ultrathin film was initially stable, but then abruptly increased with decreasing temperature. In contrast, in the heating process, the thickness of PNIPAM ultrathin film monotonically decreased with increasing temperature. To clarify the contributions of different kinetic processes, moisture control monitoring, and long-term monitoring were conducted. We have determined that there are changes in the thickness of the PNIPAM

ultrathin film resulting from the sorption of water and the phase transition of PNIPAM, although this asymmetric behavior was only determined based on thermal treatment at ambient conditions with finite-time observation. Finally, a model is postulated based on the inhomogeneity in the polymer ultrathin film system: in our model, the surface layer and interface layer have different phase transition properties, and this difference results in asymmetrical behavior during temperature cycling.

4.2 Preparation of PNIPAM ultrathin films

Commercial PNIPAM powder (Mw = 10,000; Sigma–Aldrich Co., USA) was used for sample preparation. A 1 wt% solution of PNIPAM in ethanol (Wako Chemicals, Japan) was used to prepare PNIPAM ultrathin films on silicon (100) wafers (SUMCO Co., Japan), which were cut to 15 mm × 15 mm and then cleaned with nitric acid. PNIPAM ultrathin films of various thicknesses were obtained by spin coating (SC-400, Oshigane Co., Ltd., Japan) for 20 s at 3000 and 4000 rpm. Subsequently, the samples were annealed at 60–70 °C for at least 3 h under room temperature conditions.

4.3 Thermal treatment strategies for the study of PNIPAM ultrathin films

To clarify the contributions of the different factors in the practical environment, the different control experiments have been conducted as descripted. In this study, the ambient (room) conditions were stable and maintained at 20°C in all experiments. However, although the room RH was kept constant over short periods, such as one day, it fluctuated over the long-term monitoring period (several months) in the range between 20% to 50%. On the other hand, the actual RH experienced by the sample may be different to the measured room RH and may vary with the temperature of the sample, e.g., if the average room RH is constant (around 20%), the actual RH experienced by sample can vary from 27% to 2% with temperature increase from 15 to 60°C in a rough estimation.

4.3.1 *Discrete monitoring*

In the discrete monitoring experiments, the nature of the PNIPAM ultrathin film (approximately 37 nm) was studied under ambient conditions with discrete thermal treatment. After annealing, the PNIPAM ultrathin film was kept at 20 °C for a few days, and the thickness was analyzed using the X-ray reflectivity technique. After the sample had stabilized, the sample was heated to 70 °C for 3 h and, then, allowed to cool to 20 °C again. Then, the thickness monitoring was repeated. In this experiment, the procedure was repeated six times over the following two months. However, the RH in the ambient conditions have not been record in detail in this monitoring.

4.3.2 *Operando monitoring*

For *operando* monitoring, the thickness change of the PNIPAM ultrathin film (approximately 29 nm) was examined with temperature cycling between 15 and 60 °C under ambient conditions by multichannel X-ray reflectometry. After annealing, the PNIPAM ultrathin film was kept on the sample stage at 60 °C for

at least 12 h to stabilize the initial state. Then, data collection was conducted during temperature cycling between 15 and 60 °C. All temperature scan sequences were conducted at 3 °C/step, and each step took 9 min, including the temperature changing stage (about 0.5 min) and the suspending stage (about 8.5 min). At each step, experimental data were collected between 4 and 7 min to avoid the effects of temperature fluctuation. The customized sample stage consisted of a flat copper block and a temperature controller system, which limited the temperature fluctuation to ±0.1 °C.

4.3.3 *Moisture control monitoring*

For moisture control monitoring, the kinetics of the change in the thickness of the PNIPAM ultrathin film (about 28 nm) with RH was studied first. The *operando* monitoring was conducted at 20 °C, and the RH was varied from 5% to 75%. Before the data collection, the PNIPAM ultrathin film was kept on the sample stage at 20 °C with an RH of 5% for at least 12 h to stabilize the initial state. Then, continuous data collection was conducted using multichannel X-ray reflectometry. The acquisition time for each data point was set to 3 min, and, as the data acquisition period reached 9 min, the environmental RH was changed from 5% to 75% immediately. The total measurement took about 90 min.

On the other hand, the equilibrium state of the PNIPAM ultrathin film was also studied with RH scans from 5% to 80% at 20 and 42 °C. Like the above experiments, the PNIPAM ultrathin film was kept on the sample stage at 42 °C at an RH of 5% for at least 12 h to stabilize the initial state. During the measurements, the RH was raised every hour from 5% to 80%, and the X-ray reflectivity curves of PNIPAM ultrathin film were recorded every hour after each change in RH. After the data collection of the PNIPAM ultrathin film at 42 °C with an RH of 80%, the RH was reset to 5% and the temperature was changed to 20 °C. After stabilization for 24 h, an identical second scan was carried out at 20 °C.

Finally, control experiments were conducted under different moisture conditions. The change in thickness of the PNIPAM ultrathin film was examined again with temperature at different RH values (5% and 20% RH in the sample chamber, but 20% RH under ambient conditions).

4.3.4 *Long-term monitoring*

Finally, for long-term monitoring, the equilibrium state of the PNIPAM ultrathin film (approximately 29 nm) was studied by multichannel X-ray reflectometry under ambient conditions over one month. The measurements were conducted using the following strategy: 1) on the 1st day, *operando* measurements were conducted from 60 to 15 to 42 °C; (2) the sample was kept at 42 °C for a few days, and the thickness of the sample was recorded on the 1st, 5th, 7th, 9th, and 12th days; (3) on the 12th day, the sample was heated from 42 from 60 °C, and the thickness was recorded before and after heating; (4) the sample was kept at 60 °C for a few days again, and the thickness of the sample was recorded on the 12th, 15th, and 16th days; (5) on the 16th day, the sample was cooled from 60 from 42 °C, and the thickness was recorded before and after cooling; (6) the sample was kept at 42 °C for nearly two weeks, and the thickness of the sample was recorded on the 16th, 20th, 22nd, 23rd, 26th, 28th, and 29th days; (7) on the 29th day, the sample was heated from 42 from 60 °C again, and the thickness was recorded before and after heating; and (8), finally, on the 29th day, *operando* measurements were conducted from 60 to 15 to 60 °C again. During the monitoring

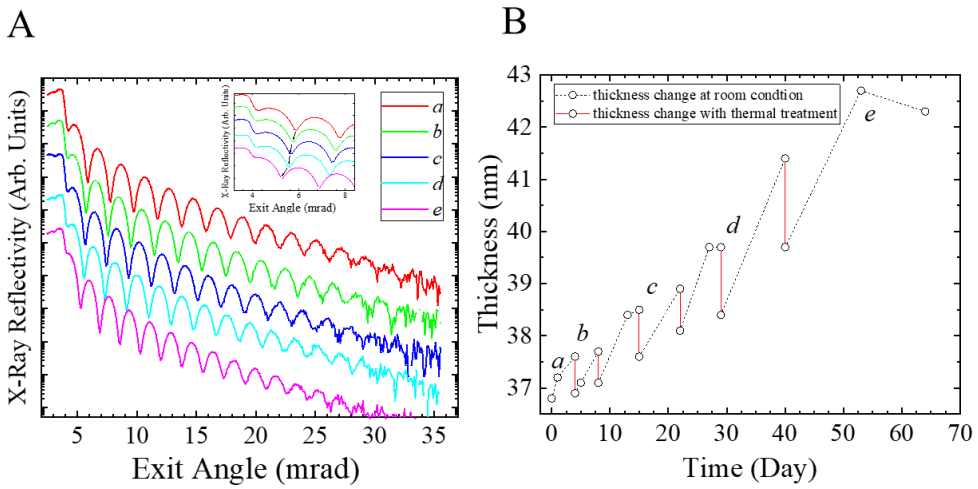

Figure 1. (A) X-ray reflectivity curves of PNIPAM ultrathin film (approximately 37 nm) on the 1st day [a], 4th day [b], 15th day [c], 29th day [d], and 54th day [e] of discrete monitoring. The inset graph shows the magnified X-ray reflectivity data with the exit angles. (B) Thickness change (calculated by the Fourier transform (FT) method) of the PNIPAM ultrathin film (approximately 37 nm) during the discrete monitoring The thickness change under ambient conditions are plotted with dash line, and the thickness change with thermal treatment are plotted with solid line. (ACS omega 4.7 (2019): 12194-12203)

for nearly one month, aside from during the initial and final cycles, the X-ray source was turned off during the rest time to avoid radiation damage. Importantly, there was no mechanical movement of the measurement system over the one-month measurement period.

4.4 Abnormal thermal responsive behaviors in PNIAPM ultrathin films

4.4.1 *Thickness increases during discrete monitoring*

Discrete monitoring of PNIPAM ultrathin films (approximately 37 nm thick) under room temperature conditions for two months confirmed a continuous increase in film thickness with repeated heating at 70 ºC for 3 h. Figure 1A shows some of the discrete raw reflectivity data (each pattern is offset), and Figure 1B shows the calculated thicknesses of the PNIPAM ultrathin film obtained over the two-month monitoring period. Clear Kiessig fringes can be seen in the X-ray reflectivity curves in Figure 1A, and the frequency and amplitude of these provide information about the PNIPAM ultrathin film layer structure. A comparison of X-ray reflectivity curves *a* to *e* in Figure 1(1st day to 54th day) reveals the shift in the minimum of each oscillation towards lower angles, which indicates an increase in the thickness of the single layer structure. In addition, the amplitudes of these oscillations, which are generated by the interference of X-rays reflected from surface and interface, are stable, implying that the sample thickness was stable, even after several thermal treatments over two months. In Figure 1B, an increase in thickness

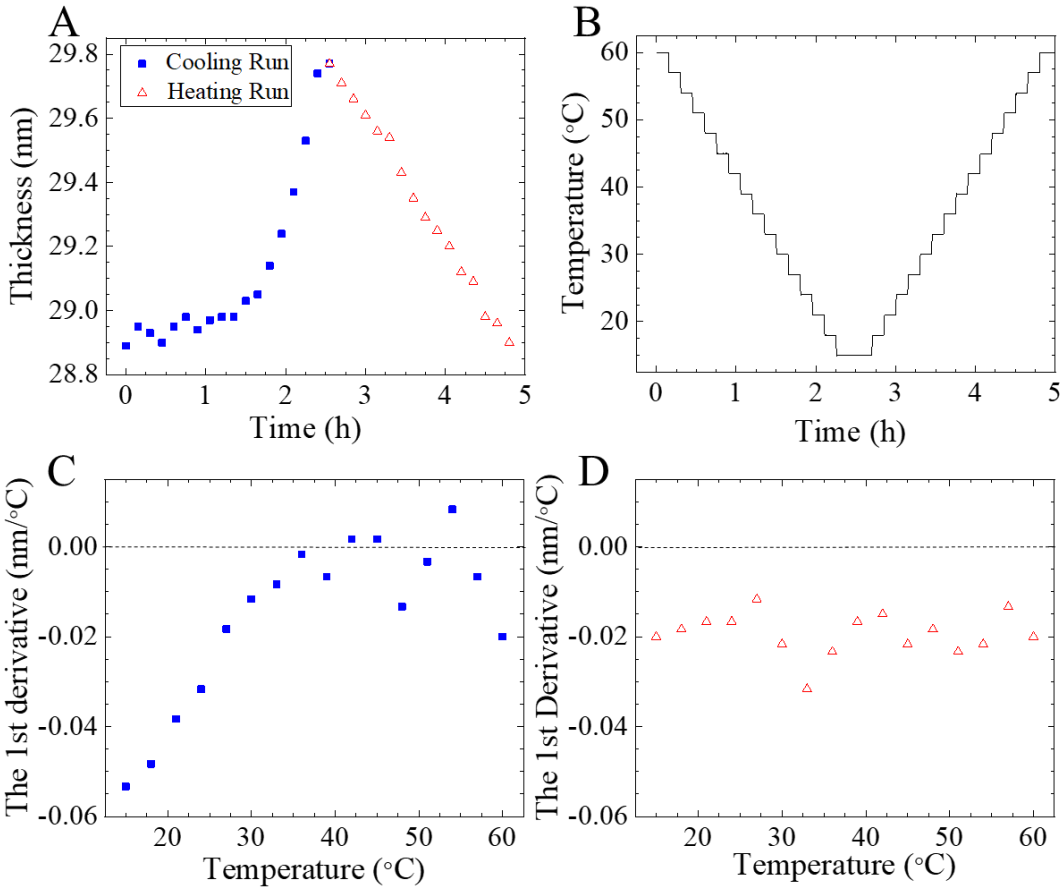

Figure 2. (A) Thickness change (calculated by the FT method) of the PNIPAM ultrathin film (approximately 29 nm) with time during operando monitoring under ambient conditions. (B) Temperature scan during operando monitoring between 15 to 60 ° C (scan rate: 3 ° C/step; each step took 9 min). (C) First derivative of thickness with decreasing temperature in the cooling process. (D) First derivative of thickness with increasing temperature in the heating process. (ACS omega 4.7 (2019): 12194-12203)

can be observed in the first 5 days. Subsequently, the sample was heated at 70 °C for 3 h and then allowed to cool to room temperature. The thickness of the PNIPAM ultrathin film was observed to decrease suddenly just after cooling but, then, continued to increase from the 5th to the 8th day. The same thermal treatment process was repeated six times in two months, and the same trend in changing thickness was observed. Meanwhile, on the basis of the data from the 8th day to the 15th day and the 22nd day to the 29th day, the trend in the thickness increase of the PNIPAM ultrathin film was nonlinear with time. The rate of increase in thickness gradually reduced with time but accelerated after the next thermal treatment. After these experiments, a thickness increase of nearly 16% was observed for the ultrathin PNIPAM films over two months. No doubt, this unexpected increase in thickness cannot be caused only by the structural relaxation of the polymer thin film itself, and we propose that these phenomena may response the swelling in ambient conditions and the memory effect with thermal treatment may also contribute the thickness

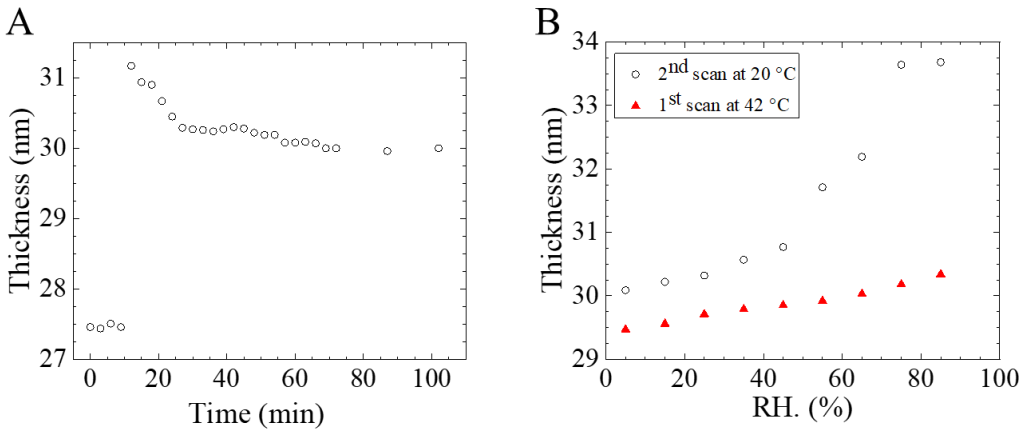

Figure 3. (A) Thickness change (calculated by the FT method) of the PNIPAM ultrathin film (approximately 28 nm) with time as the RH was changed from 5% to 75% at the 9th min. (B) Thickness change (calculated by the FT method) of PNIPAM ultrathin film with RH scan from 5% to 80%. After the first scan, the RH was reset to 5%, and the temperature was changed to 20 ° C immediately. The interval between two scans was more than 24 h. (ACS omega 4.7 (2019): 12194-12203)

increase in 16%. However, since the data collected in this monitoring is not detailed enough, we cannot give further discussion on this hypothesis. Therefore, the control experiments have been conducted in the following work.

4.4.2 *Asymmetric thickness change with temperature cycle operando monitoring*

To reveal the thickness change with temperature under ambient conditions further, *operando* monitoring of the thickness of the PNIPAM ultrathin film (approximately 29 nm) with temperature cycling between 15 to 60 ºC was carried out. In this experiment, an asymmetric change in the thickness of PNIPAM ultrathin films was observed with cooling and heating under ambient conditions. In Figures 2A and B, the thickness of PNIPAM ultrathin film and related temperature profile are presented with time. In the cooling process, the initial thickness of the PNIPAM ultrathin film was stable at around 28.9 nm, showing oscillations of only 0.1 nm initially, but it abruptly increased with further cooling. When the temperature reached 15 ºC, the thickness had increased by 0.9 nm. In the heating process, the thickness just decreased monotonically, and it reached the original thickness of 28.9 nm, when the temperature became 60 ºC. The first derivatives of the thickness with increasing temperature are presented in Figures 2C and D. In the cooling process, the slope was stable around zero first and, then, gradually decreased as the temperature fell below 35 ºC. In contrast, in the heating process, the slope was stable, approximately -0.02 nm/ºC. Undoubtedly, a transition of the PNIPAM ultrathin film occurred around 35 ºC in the cooling process, and it disappeared on heating. Of course, the asymmetric behavior of polymer material with cyclic treatment might be interpreted as the hysteresis of the polymer chains.[33,34] However, in this experiment, the actual kinetic process may be much more complicated. The transition between the hydrophobic state and hydrophilic state may happen in PNIPAM ultrathin film, even though it disappeared during the

Table 1. Coefficient of thickness increase of PNIPAM ultrathin films at RH from 5% to 80% at 20 and 42 °C.

Temperature	Coefficient of thickness increase with RH	
	RH from 5% to 45%	RH from 45% to 80%
20 °C	339 ppm	382 ppm
42 °C	568 ppm	2597 ppm

heating, and if swelling can happen in PNIPAM ultra film, the thickness increase during cooling can be reasonable interpreted. However, in experiments under ambient conditions, the significant factors are always more complicated than we think, e.g. the swelling would be decided by the actual RH experienced by the surface of sample, which can change with temperature of sample, even the RH in the ambient conditions is stable. Therefore, to clarify the temperature contribution in the unusual thickness change in ambient conditions PNIPAM system, the moisture control experiments have to be also solved out.

4.4.3 *Humidity dependence of thickness in moisture control monitoring*

In this section, the kinetics of the thickness change in PNIPAM ultrathin film (approximately 28 nm) was studied with varying RH at 20 °C. In Figure 3A, the change in the thickness of PNIPAM ultrathin film with time is shown with RH change from 5% to 75%. From the start of the measurement to the 9th min, the PNIPAM ultrathin film was kept with an RH of 5% and was stable. However, as the RH changed from 5% to 75% at the 9th min, a significant and immediate thickness change was observed. The thickness of the PNIPAM ultrathin film increased from 27.5 to 31.2 nm in 3 min, subsequently decreasing to 30.3 nm over the next 15 min. Finally, the thickness stabilized. Clearly, the PNIPAM ultrathin film are extremely sensitive to moisture at 20 °C, and this is likely responsible for the thickness increase observed in the previous experiment. The thickness of PNIPAM ultrathin film can increase with swelling at low temperature. On the other hand, on changing the moisture contents, the swelling can be divided into three different kinetic processes: condensation, diffusion, and rearrangement. The first two processes can occur in less than 15 min, even with large changes in RH from 5% to 75%. Therefore, it is proposed that all data collected in the previous experiments, in which the RH changed only slightly, correspond to the rearrangement stage.

In the subsequent experiments, the humidity dependence of the PNIPAM ultrathin film was further studied in a different state. In Figure 3B, the thickness of PNIPAM ultrathin film are shown at RH from 5% to 80% at 20 and 42 °C. As shown in Figure 3B, when the temperature was 42 °C, the thickness increased slightly from 29.5 to 30.3 nm as the RH increased from 5% to 80%. After resetting the RH at 20 °C for 24 h, the thickness decreased but did not recover its original value, remaining at 30.3 to 30.1 nm. Furthermore, during the second RH scan at 20 °C, the thickness increased slightly from 30.1 to 30.8 nm with the RH increase from 5% to 45%, then abruptly increasing and reaching saturation from 30.8 to 33.6

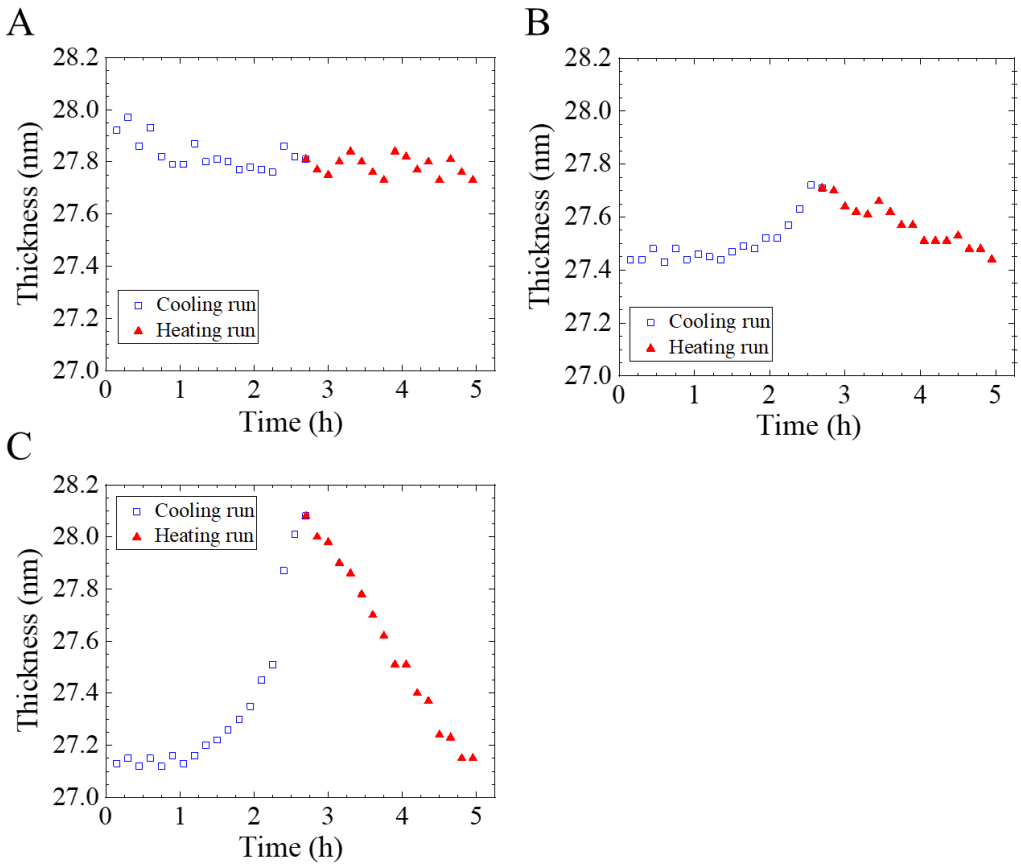

Figure 4. Thickness change (calculated by the FT method) of the PNIPAM ultrathin films (approximately 28 nm) with time during operando monitoring (temperature scan is shown in Figure 2B) with RH of 5% (A) and 20% (B) in the moisture control chamber, and 20% under ambient conditions (C). (ACS omega 4.7 (2019): 12194-12203)

nm with increasing RH from 45% to 80%. As summarized in Table 1, a comparison of the coefficient of thickness increase with RH leads us to some comprehensive conclusions. The swelling at 20 °C is much more efficient than that at 42 °C. In addition, at 20 °C, the swelling under low moisture conditions is significantly different from that under high moisture conditions following the Flory–Huggins model. [33–37] Considering the uncertainty in measurements are less than 0.1 nm, it can propose that PNIPAM ultrathin film showed hydrophobic/hydrophilic transition behavior with temperature, even under low moisture conditions. Meanwhile, unlike the dramatic thickness change under high moisture conditions, the swelling of PNIPAM ultrathin film seems to be insensitive to changes in RH under low moisture conditions.

Now, it is clear that the thickness change of PNIPAM ultrathin film with temperature can related to the swelling of PNIPAM, meanwhile the swelling ability can change with temperature which affect the hydrophobic/hydrophilic state of PNIPAM. Finally, to clarify whether the asymmetric thickness change is caused by the actual RH experienced by the sample, which can change with temperature in the ambient conditions, the thickness change of the PNIPAM ultrathin films with temperature was further studied

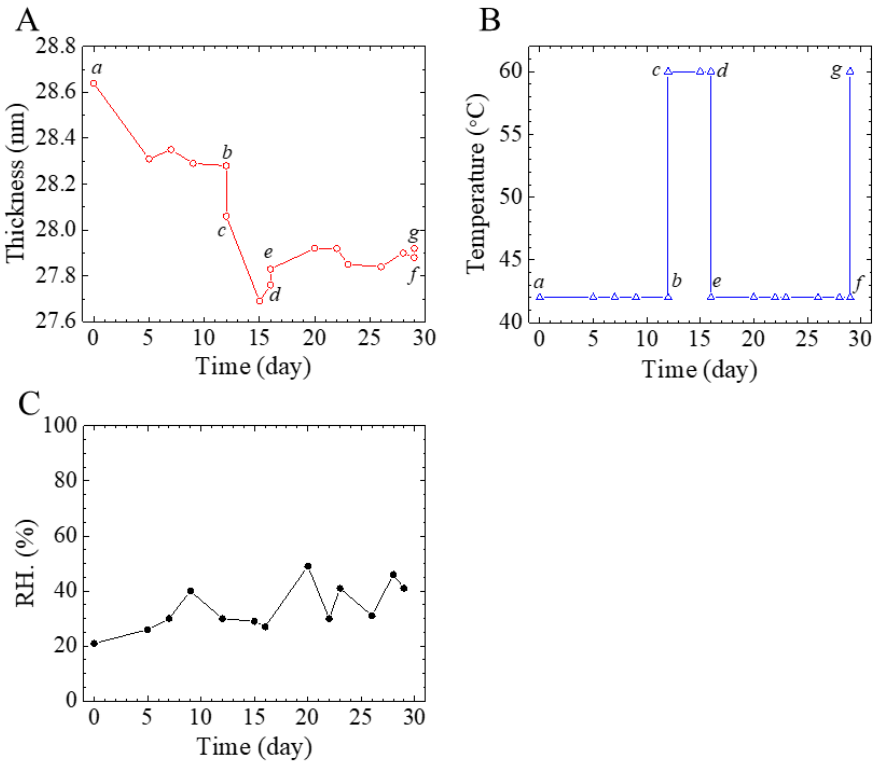

Figure 5. (A) Thickness change (calculated by the FT method) of PNIPAM ultrathin films (approximately 29 nm) in the long- term monitoring [processes (2)－(7)]. (B) Temperature change in the long-term monitoring [processes (2)－(7)]. (C) Relative humidity under ambient conditions in the long-term monitoring [processes (2)－(7)]. The different thermal treatment processes are marked (2) a to b; (3) b to c; (4) c to d; (5) d to e; (6) e to f; and (7) f to g. (ACS omega 4.7 (2019): 12194-12203)

under the moisture control. As shown in Figure 4, *operando* experiments were conducted again at RH of 5% and 20% in the moisture control chamber and at 20% RH under ambient conditions. As shown in Figures 4A and B, at a low RH of 5%, the thickness of PNIPAM ultrathin film was stable with temperature cycling, whereas, when the RH was increased to 20%, an asymmetric change in thickness was observed, although the magnitude was quite small. To confirm this weak asymmetric thickness change in the moisture control system, the same experiment was repeated at an RH of 20% under ambient conditions, as shown in Figure 4C, and the asymmetric thickness change was observed again with a more significant thickness change. Due to the actual RH experienced by the sample will not change with temperature in the moisture chamber, it can be confirmed that the asymmetric changes in the thickness with temperature are influenced by moisture, even at a RH of 20%, but the trend in the asymmetric changes should be independent of the actual RH experienced by the sample under ambient conditions.

4.4.4 *Dynamic equilibrium state of thickness in long-term monitoring*

To confirm whether this asymmetric thickness change is caused by hysteresis in the rearrangement of polymer chains, the equilibrium states of the PNIPAM ultrathin film (approximately 29 nm) during

Table 2. Thermal treatment processes and thicknesses of PNIPAM ultrathin films during long-term monitoring.

Process	Time	Temperature scan	Initial thickness [nm]	Final thickness [nm]
(1)	1st day	60 °C ≥ 15 °C ≥ 42 °C	28.3	28.6
(2)	1st to 12th day	42 °C ≥ 42 °C	28.6	28.3
(3)	12th day	42 °C ≥ 60 °C	28.3	28.1
(4)	12th to 16th day	60 °C ≥ 60 °C	28.1	27.8
(5)	16th day	60 °C ≥ 42 °C	27.8	27.8
(6)	16th to 29th day	42 °C ≥ 42 °C	27.8	27.9
(7)	29th day	42 °C ≥ 60 °C	27.9	27.9
(8)	29th day	60 °C ≥ 15 °C ≥ 60 °C	27.9	28.0

heating were studied using static measurements and different temperature scan sequences over one month. Figure 5 shows the thickness of the PNIPAM ultrathin film and experimental conditions during the one-month monitoring period (processes (2) to (7)). Figures 6 shows the thicknesses of the PNIPAM ultrathin film subjected to temperature cycling in the initial state and the final state, respectively (processes (1) and (8)). Table 2 summarizes the thicknesses of the PNIPAM ultrathin film throughout these thermal treatment processes. As shown in Figure 5, the equilibrium state of the PNIPAM ultrathin film was dominated by temperature, even at temperatures above 33 °C, and the RH change under ambient conditions did not affect the swelling of the PNIPAM ultrathin film during long-term monitoring. After thermal treatment process (1), as shown in Figures 6A and C, the PNIPAM ultrathin film was kept at 42 °C. In Figure 5A, a slow thickness decrease of PNIPAM ultrathin film can be seen over the following 4 days, subsequently becoming stable and being maintained at 28.3 nm on the 12th day in process (2). In process (3) on the 12th day, a decrease in the thickness of the PNIPAM ultrathin film from 28.3 to 28.1 nm was observed with heating from 42 to 60 °C. In aging process (4), the thickness continued to decrease to 27.8 nm over the following 4 days, which can be considered to be caused by the rearrangement of the polymer chains, similar to the observations in process (2). In process (5) on the 16th day, the temperature of the sample was recovered from 60 to 42 °C, and one important finding is that there was no significant thickness change with cooling. In aging process (6), the thickness of PNIPAM ultrathin film was maintained from 27.8 to 27.9 nm at 42 °C from the 16th day to the 29th day, which further confirms the observation that the thickness of PNIPAM ultrathin film does not increase with cooling at temperatures above 33 °C. In process (7) on the 29th day, the sample was heated again from 42 to 60 °C. The second interesting observation is that the thickness of the PNIPAM ultrathin film did not change at all, even though the same procedure as process (3) was used. Finally, temperature cycling process (8) was conducted again on the 29th day. As shown in Figure 6, the asymmetric thickness change with temperature still occurred in the PNIPAM ultrathin film.

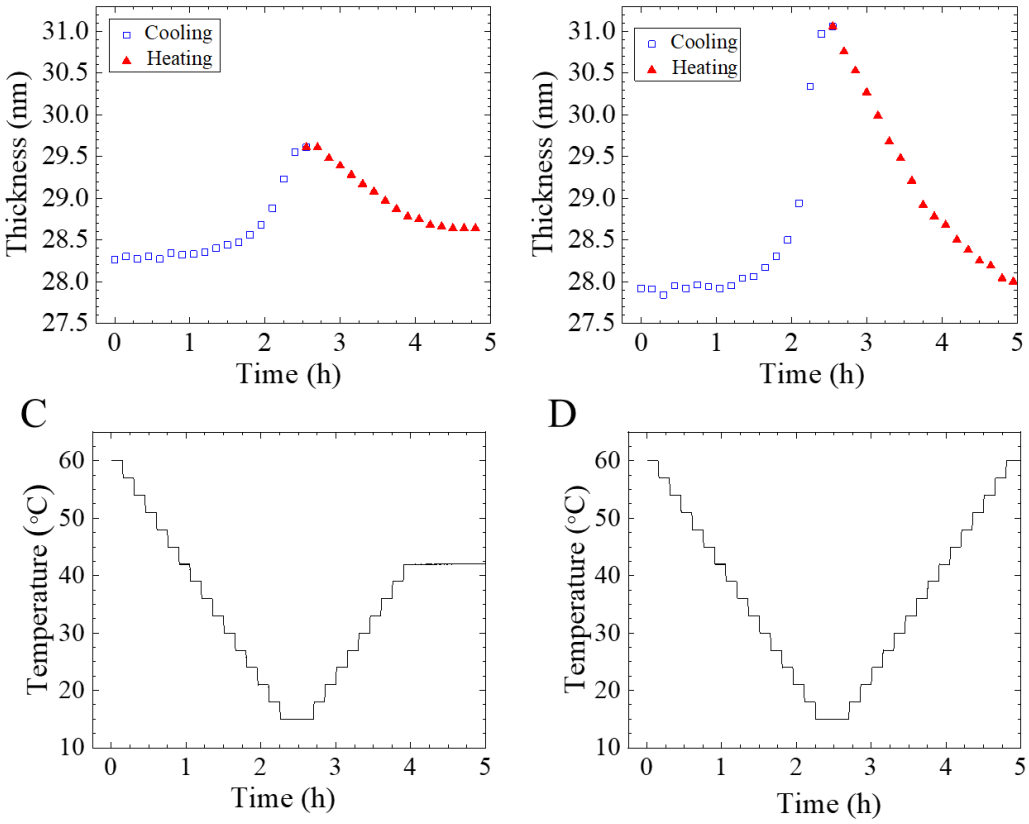

Figure 6. (A) Thickness change (calculated by the FT method) of the PNIPAM ultrathin film (approximately 29 nm) in the long-term monitoring (process (1)). (B) Thickness change (calculated by the FT method) of PNIPAM ultrathin film (approximately 29 nm) in the long-term monitoring (process (8)). (C) Temperature scan during long-term monitoring (process (1)). (C) Temperature scan in the long-term monitoring (process (8)). Scan rate: 3 ° C/step; each step took 9 min. (ACS omega 4.7 (2019): 12194-12203)

Obviously, there is no significant hysteresis in the monotonic thickness decrease with heating, and some irreversible process occurred between processes (3) and (7). It is proposed that, after the absorption of water in the process (1), some bound water may remain in the PNIPAM ultrathin film even the temperature is higher than LCST. Although it seems to contradict the impression of "hydrophobic state" that water should be completely discharged, but when the concentration of water is low, these water molecules would mainly bond with the amide group in PNIPAM and will not contribute the transition of PNIPAM from hydrophilic to hydrophobic state. However, these bound water molecules can further evaporate in processes (3) and (4) with temperature, thus causing the thickness decrease. Then, in processes (5) and (6), temperature was reduced to the initial value, but the thickness of PNIPAM ultrathin film did not change. Clearly, the film did not absorb any moisture in these two weeks. Although this asymmetric behavior is difficult to explain, it is indeed observed in the series experiments in this work. Finally, in process (7), since the moisture in the film has been already evaporated in the process (3) and

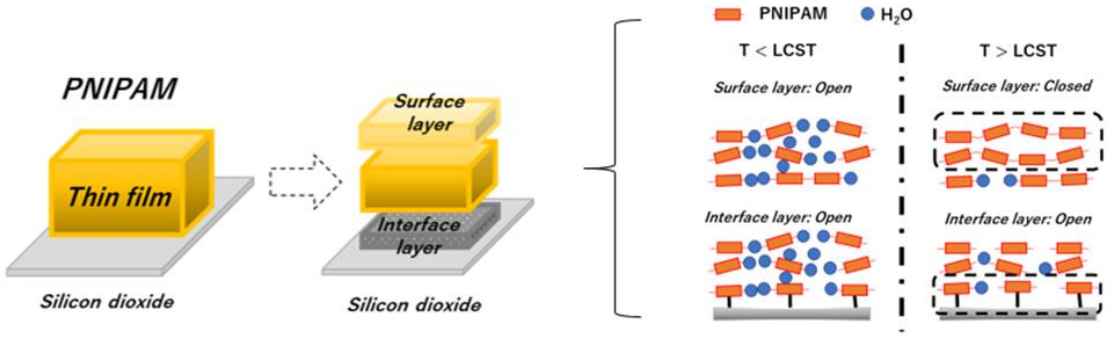

Figure 7. Conceptual sketch of different properties of the surface and interface layers in the PNIPAM ultrathin film system on temperature cycling. When the temperature is below the LCST, water molecules can form hydrogen bonds with the polymer chain in interface layer and surface layer: when the temperature is above the LCST, the polymer chain in surface layer can bond with each other after the evaporation of bound water, whereas the polymer chains in the interface are constrained. (ACS omega 4.7 (2019): 12194-12203)

(4), and no swelling happened in the process (5) and (6), the thickness of PNIPAM ultrathin film has not been able to further decease by the evaporation of water. On the other hand, in Figure 6, it would be noted that the maximum thickness change observed in process (8) was much larger than that in process (1). In Figure 6A, the maximum thickness change is only 4.7%, but, in Figure 6B, the maximum thickness change is 11.2%, indicating that the absorption or swelling became easier after the repeated thermal treatments over one month. This behavior is similar to that observed in Figure 1B, where the thickness of the PNIPAM ultrathin film continued to increase after several thermal treatments which was presumed to be caused by the memory effect in polymer system.

4.5 Asymmetric structure in polymer ultrathin film

To give the final discussion on the asymmetric thickness of PNIPAM ultrathin film with thermal treatments, we propose a boundary condition effect that the mobility of polymer main can be considered inhomogeneous in polymer ultrathin film. Generally, it is understood that the solid PNIPAM bulk does not show hydrophilic/hydrophobic transition unless in contact with liquid water. But in the PNIPAM ultrathin film, the local transition at the surface of sample might become possible due to the free motion of polymer chain which facilitate the formation of hydrogen bonds between amide group during the transition from hydrophilic to hydrophobic state. As shown in Figure 7, the polymer chains in the surface layer of the ultrathin film are highly mobile, and, as the temperature rises, these polymer chains may aggregate with thermal motion to achieve a transition from the hydrophilic to hydrophobic state. In contrast, the polymer chains in the interface layer would be further constrained by interfacial interactions, and the transition would be more difficult than other regions. If the PNIPAM ultrathin film is considered

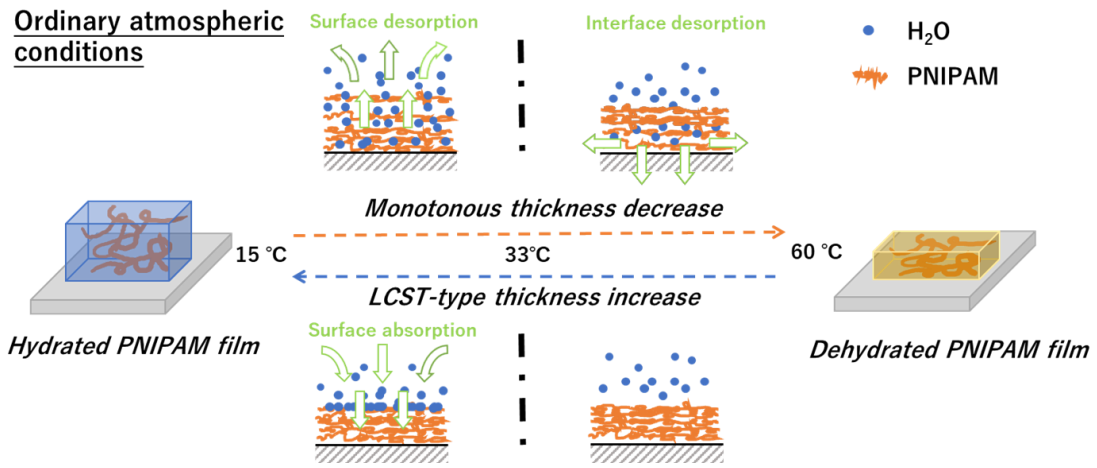

Figure 8. Conceptual model of the asymmetric thickness change of PNIPAM ultrathin film on temperature cycling. In the initial stages of the temperature cycle, water molecules in the air are rejected by the hydrophobic surface layer of the PNIPAM ultrathin film. As the temperature is below LCST, the thickness of PNIPAM ultrathin film can change with absorption and evaporation of water. However, when the temperature rises above LCST again, the evaporative flow would be only still available through the interface layer. (ACS omega 4.7 (2019): 12194-12203)

by analogy to be a room that can store water molecules, then the surface layer would be like an automatic door that can respond to the temperature, whereas the interface layer would be like exit that is always open for evaporation. As shown in Figure 8, in the initial stages of temperature cycling, the water molecules in the air can be rejected by the hydrophobic surface layer of PNIPAM ultrathin film. When the temperature is below the 33 °C, the surface layer becomes hydrophilic, and the water molecules can be absorbed and stored inside the PNIPAM ultrathin film, resulting in swelling with temperature. In the temperature range between 15 and 33 °C, there would be no difference between cooling and heating, and the difference observed in the *operando* monitoring can be explained by the swelling hysteresis. However, when the temperature increases above 33 °C, the evaporation of water is suppressed by the hydrophobic surface layer, but it is possible through the interface layer. Therefore, two different processes can be observed in the same sample in the same temperature range.

Anyway, it should be noted that there is still no experiment data to support the postulated model directly. However, since there are few reports on the behaviors of PNIPAM ultrathin film under the ambient conditions, we believe that it would be important to give some logical assumptions about the unknown mechanism, which can point the direction in the future.

4.6 Conclusion

In this work, the unusual changes in the thickness of PNIPAM ultrathin films with temperature have been symmetrically studied using different strategies. We found that the PNIPAM ultrathin film swells even

under ambient conditions, and this swelling effect can be enhanced by the memory effect after repeated thermal treatment. Furthermore, two distinct behaviors were observed on cooling and heating in one temperature cycle: a swelling process following the LCST transition of the PNIPAM and a monotonic shrinking process. After control experiments with RH and time, we confirmed that this asymmetric behavior is not caused by the fluctuation in the RH at the sample surface or the complex swelling kinetics. Thus, low moisture contents and the boundary conditions are proposed to have significant effects on the PNIPAM ultrathin film system. Under ambient conditions, the surface layer and interface layer are proposed to have different phase transition properties in PNIPAM ultrathin films, which affects the absorption and desorption of water molecules in the temperature cycle, respectively, making the film act like a "smart" pathway for the water vapor flow. However, the proposed model is controversial because of the lack of direct evidence, but the unusual findings concerning PNIPAM ultrathin films reported here indicate the possibility of boundary condition effects in the ultrathin polymer film systems. In the future, these stimuli-responsive ultrathin films may have potential applications based on their asymmetric properties in a microenvironment.

Reference

(1) Schmaljohann, D. Thermo- and PH-Responsive Polymers in Drug Delivery. *Adv. Drug Deliv. Rev.* **2006**, *58* (15), 1655–1670.

(2) Okano, T.; Bae, Y. H.; Jacobs, H.; Kim, S. W. Thermally On-off Switching Polymers for Drug Permeation and Release. *J. Control. Release* **1990**, *11* (1–3), 255–265.

(3) Huffman, A. S.; Afrassiabi, A.; Dong, L. C. Thermally Reversible Hydrogels: II. Delivery and Selective Removal of Substances from Aqueous Solutions. *J. Control. Release* **1986**, *4* (3), 213–222.

(4) Otake, K.; Inomata, H.; Konno, M.; Saito, S. Thermal Analysis of the Volume Phase Transition with N-Isopropylacrylamide Gels. *Macromolecules* **1990**, *23* (1), 283–289.

(5) Wu, C.; Zhou, S. Thermodynamically Stable Globule State of a Single Poly(N-Isopropylacrylamide) Chain in Water. *Macromolecules* **1995**, *28* (15), 5388–5390.

(6) Futscher, M. H.; Philipp, M.; Müller-Buschbaum, P.; Schulte, A. The Role of Backbone Hydration of Poly(N-Isopropyl Acrylamide) Across the Volume Phase Transition Compared to Its Monomer. *Sci. Rep.* **2017**, *7* (1), 1–11.

(7) Sun, B.; Lin, Y.; Wu, P.; Siesler, H. W. A FTIR and 2D-IR Spectroscopic Study on the Microdynamics Phase Separation Mechanism of the Poly(N-Isopropylacrylamide) Aqueous Solution. *Macromolecules* **2008**, *41* (4), 1512–1520.

(8) Kharlampieva, E.; Kozlovskaya, V.; Tyutina, J.; Sukhishvili, S. A. Hydrogen-Bonded Multilayers of Thermoresponsive Polymers. *Macromolecules* **2005**, *38* (25), 10523–10531.

(9) Maeda, Y.; Higuchi, T.; Ikeda, I. Change in Hydration State during the Coil－Globule Transition of Aqueous Solutions of Poly(*N*-Isopropylacrylamide) as Evidenced by FTIR Spectroscopy †. *Langmuir* **2000**, *16* (19), 7503–7509.

(10) Philipp, M.; Kyriakos, K.; Silvi, L.; Lohstroh, W.; Petry, W.; Krüger, J. K.; Papadakis, C. M.; Müller-Buschbaum, P. From Molecular Dehydration to Excess Volumes of Phase-Separating PNIPAM Solutions. *J. Phys. Chem. B* **2014**, *118* (15), 4253–4260.

(11) Ono, Y.; Shikata, T. Hydration and Dynamic Behavior of Poly(N-Isopropylacrylamide)s in Aqueous Solution: A Sharp Phase Transition at the Lower Critical Solution Temperature. *J. Am. Chem. Soc.* **2006**, *128* (31), 10030–10031.

(12) Wang, P. B.; Wang, W.; Xu, D. G.; Li, M.; Toshio, T. Application of IR Digital Controller IRMCF143 in Photovoltaic Inverter System. *Conf. Proc. - 2012 IEEE 7th Int. Power Electron. Motion Control Conf. - ECCE Asia, IPEMC 2012* **2012**, *3*, 2042–2046.

(13) Adam, S.; Koenig, M.; Rodenhausen, K. B.; Eichhorn, K. J.; Oertel, U.; Schubert, M.; Stamm, M.; Uhlmann, P. Quartz Crystal Microbalance with Coupled Spectroscopic Ellipsometry-Study of Temperature-Responsive Polymer Brush Systems. *Appl. Surf. Sci.* **2017**, *421*, 843–851.

(14) Koenig, M.; Rodenhausen, K. B.; Rauch, S.; Bittrich, E.; Eichhorn, K. J.; Schubert, M.; Stamm, M.; Uhlmann, P. Salt Sensitivity of the Thermoresponsive Behavior of PNIPAAm Brushes. *Langmuir* **2018**, *34* (7), 2448–2454.

(15) Bittrich, E.; Burkert, S.; Müller, M.; Eichhorn, K. J.; Stamm, M.; Uhlmann, P. Temperature-Sensitive Swelling of Poly(n-Isopropylacrylamide) Brushes with Low Molecular Weight and Grafting Density. *Langmuir* **2012**, *28* (7), 3439–3448.

(16) Burkert, S.; Bittrich, E.; Kuntzsch, M.; Müller, M.; Eichhorn, K. J.; Bellmann, C.; Uhlmann, P.; Stamm, M. Protein Resistance of PNIPAAm Brushes: Application to Switchable Protein Adsorption. *Langmuir* **2010**, *26* (3), 1786–1795.

(17) Draper, J.; Luzinov, I.; Minko, S.; Tokarev, I.; Stamm, M. Mixed Polymer Brushes by Sequential Polymer Addition: Anchoring Layer Effect. *Langmuir* **2004**, *20* (10), 4064–4075.

(18) Rauch, S.; Eichhorn, K. J.; Oertel, U.; Stamm, M.; Kuckling, D.; Uhlmann, P. Temperature Responsive Polymer Brushes with Clicked Rhodamine B: Synthesis, Characterization and Swelling Dynamics Studied by Spectroscopic Ellipsometry. *Soft Matter* **2012**, *8* (40), 10260–10270.

(19) Wang, W.; Kaune, G.; Perlich, J.; Papadakis, C. M.; Bivigou Koumba, A. M.; Laschewsky, A.; Schlage, K.; Röhlsberger, R.; Roth, S. V.; Cubitt, R.; et al. Swelling and Switching Kinetics of Gold Coated End-Capped Poly(N-Isopropylacrylamide) Thin Films. *Macromolecules* **2010**, *43* (5), 2444–2452.

(20) Wang, W.; Metwalli, E.; Perlich, J.; Troll, K.; Papadakis, C. M.; Cubitt, R.; Müller-Buschbaum, P. Water Storage in Thin Films Maintaining the Total Film Thickness as Probed with in Situ Neutron Reflectivity. *Macromol. Rapid Commun.* **2009**, *30* (2), 114–119.

(21) Wang, W.; Metwalli, E.; Perlich, J.; Papadakis, C. M.; Cubitt, R.; Müller-Buschbaum, P. Cyclic Switching of Water Storage in Thin Block Copolymer Films Containing Poly(N-Isopropylacrylamide). *Macromolecules* **2009**, *42* (22), 9041–9051.

(22) Harms, S.; Rätzke, K.; Faupel, F.; Egger, W.; Ravello, L.; Laschewsky, A.; Wang, W.; Müller-Buschbaum, P. Free Volume and Swelling in Thin Films of Poly(N-Isopropylacrylamide) End-Capped with N-Butyltrithiocarbonate. *Macromol. Rapid Commun.* **2010**, *31* (15), 1364–1367.

(23) Wang, W.; Troll, K.; Kaune, G.; Metwalli, E.; Ruderer, M.; Skrabania, K.; Laschewsky, A.; Roth, S. V.; Papadakis, C. M.; Müller-Buschbaum, P. Thin Films of Poly(N-Isopropylaciylamide) End-Capped with n-Butyltrithiocarbonate. *Macromolecules* **2008**, *41* (9), 3209–3218.

(24) Magerl, D.; Philipp, M.; Qiu, X. P.; Winnik, F. M.; Müller-Buschbaum, P. Swelling and Thermoresponsive Behavior of Linear versus Cyclic Poly(N-Isopropylacrylamide) Thin Films. *Macromolecules* **2015**, *48* (9), 3104–3111.

(25) Liu, Y.; Sakurai, K. Thermoresponsive Behavior of Poly(N-Isopropylacrylamide) Solid Ultrathin Film under Ordinary Atmospheric Conditions. *Chem. Lett.* **2017**, *46* (4), 495–498.

(26) Liu, Y.; Sakurai, K. Thickness Changes in Temperature-Responsive Poly(N -Isopropylacrylamide) Ultrathin Films under Ambient Conditions . *ACS Omega* **2019**, *4* (7), 12194–12203.

(27) Sakurai, K. Japanese Patent No. 3903184; K. Sakurai and M. Mizusawa. *Prep. Publ.*

(28) Sakurai, K.; Mizusawa, M.; Ishii, M.; Kobayashi, S.; Imai, Y. Instrumentation for X-Ray Reflectivity in Micro Area: Present Status and Future Outlook. In *Journal of Physics: Conference Series*; IOP Publishing, 2007; Vol. 83, p 12001.

(29) Mizusawa, M.; Sakurai, K. In-Situ X-Ray Reflectivity Measurement of Polyvinyl Acetate Thin Films

during Glass Transition. In *IOP Conference Series: Materials Science and Engineering*; IOP Publishing, 2011; Vol. 24, p 12013.

(30) Naudon, A.; Chihab, J.; Goudeau, P.; Mimault, J. New Apparatus for Grazing X-Ray Reflectometry in the Angle-Resolved Dispersive Mode. *J. Appl. Cryst* **1989**, *22*, 460–464.

(31) Tolan, M. *X-Ray Scattering from Soft-Matter Thin Films*; Springer-Verlag: Berlin, 1999.

(32) Stoev, K. N.; Sakurai, K. Review on Grazing Incidence X-Ray Spectrometry and Reflectometry. *Spectrochim. acta, Part B At. Spectrosc.* **1999**, *54* (1), 41–82.

(33) Doumenc, F.; Bodiguel, H.; Guerrier, B. Physical Aging of Glassy PMMA/Toluene Films: Influence of Drying/Swelling History. *Eur. Phys. J. E* **2008**, *27* (1), 3–11.

(34) Doumenc, F.; Guerrier, B.; Allain, C. Aging and History Effects in Solvent-Induced Glass Transition of Polymer Films. *Europhys. Lett.* **2006**, *76* (4), 630–636.

(35) Jeromenok, J.; Weber, J. Restricted Access: On the Nature of Adsorption/Desorption Hysteresis in Amorphous, Microporous Polymeric Materials. *Langmuir* **2013**, *29* (42), 12982–12989.

(36) Mukherjee, M.; Souheib Chebil, M.; Delorme, N.; Gibaud, A. Power Law in Swelling of Ultra-Thin Polymer Films. *Polymer (Guildf).* **2013**, *54* (17), 4669–4674.

(37) Singh, A.; Mukherjee, M. Swelling Dynamics of Ultrathin Polymer Films. *Macromolecules* **2003**, *36* (23), 8728–8731.

Chapter 5

The discovering of ultrathin film forming and its property

5.1 Introduction

As we known, Nylon 6 is one of the famous semi-crystalline polyamides, which has been already studied many years.[1,2] Since its excellent physical and chemical properties, it is expected to be used in various material systems.[3,4] However, it is also because of the excellent stable properties that it makes the preparation process of the materials system at nano scale very difficult. In the past decades, although many effort have been devoted to the nano-materials system of Nylon 6, most of the research is still focused on the Nylon 6 nanofiber, and as one interesting finding, its actual structure contained two main crystalline forms that α form and γ form which shown the different properties in the application.[5–9] In the past reports, it is recognized that the α form structure is the thermodynamically stable state, but in the actual Nylon 6 products, the metastable γ form can also exist depending on the kinetic conditions of the preparation process conditions. [10–12]. But so far, it is pity that there are still few reports on the preparation of Nylon 6 thin film, even though it would be one promising material system for the nano-devices such as electronics, optics and sensors.[13–17] Thus, in this work, we have concerned the preparation of the Nylon 6 thin films and engaged in the structure analysis.

Regarding the preparation processing of the polymer ultrathin film, the deposition method would one of the most promising methods for the insoluble matter.[18–21] Different to the sol-gel method, such as the spin-coating, the deposition process can provide a gap-filled coating for nano-device, and the multi-lever

structure would not happen with the evaporation of solvent during the preparation.[13,19] Of course, the deposition of the polymer ultrathin film is not as simple as imagined. Due to different dynamic and kinetic processes, different branches of the deposition method have been developed, such as chemical vapor deposition (CVD), molecular layer deposition (MLD) and physical vapor deposition (PVD), which may contribute the different structure and property even in the same materials system. [21–24] Among them, most of the efforts have focused on CVD and MLD in the past, because the function of polymer thin film can be designed through chemical reactions directly. However, there are also some disadvantages of CVD and MLD that limited their application in practice. The strict chemical reaction environment, such as the high temperature, may distorted the prefabricated structures on the substrate. Meanwhile, the preparation of precursors and the disposal of by-products, which are always expensive or toxic, increased the cost in the process. Furthermore, due to the complex chemical reaction, many parameters must be carefully controlled in the process that makes the control of the thin film structure difficult. On the other hand, some researchers have tried to deposit the polymer thin film by physical means directly. Different to CVD or MLD, one significant advantage of PVD is that it avoids the chemical reaction in the process. In the past, many studies have focused on prepared Teflon AF films by PVD process.[25–27] Although many products have been achieved with the simple evaporation-deposition process, some deficiency of the PVD would have been still considered in the previous research. In the past, in order to promise the efficiency evaporation of polymer source, the PVD also required the high temperature for the sample heating, and as one undesired result, the pyrolyzing always happen during the evaporation process that destroy the chemical structure of virgin source.[28–30] Generally, it is accepted that the pyrolyzing- repolymerizing may happen in the PVD process and the molecular size of polymer would reduce in the final product.[25,26] In the past, few attempts have been made to discuss or control the structure of polymer thin films. Perhaps one of the reasons is that the deposition process of large molecules is much more complicated than that of small molecules.

In this chapter, it introduced the preparation of Nylon 6 thin films, by direct PVD using an MBE apparatus, which not only facilitated the formation of the crystal structure of the thin film but also ensured the state of the surface/interface. Since the MBE setup was mainly used to deposit the small inorganic molecules in the past, it is important to characterize the deposited polymer thin film, and to discuss the relationship between the evaporation-deposition kinetics and thin film morphology. In the experiment, the high-quality Nylon 6 thin films have been prepared with the thickness 10 nm to 100 nm. With the characterization of Raman spectra and X-ray diffraction (XRD) pattern, the same chemical structure as the virgin source was found in the deposited thin films, while only the γ crystalline form was found in the final product, which is suggested to relate to the kinetic of the deposition process. In determining the quality of this thin film, the surface and interface conditions were studied by scanning probe microscopy (SPM) and X-ray reflectivity (XRR) analysis. The good surface morphology of the deposited Nylon 6 thin film has been confirmed by quantitative surface topology analysis, and the interface conditions have been also discussed with the oscillation in the XRR curves. Meanwhile, in the controlled experiments, it was found that the deposition rate greatly contributed to the quality of surface/interface conditions that the

high-quality Nylon 6 thin film can be obtained at the fast deposition rate. Finally, the thickness stability of Nylon 6 thin film was studied by in-operando X-ray reflectivity analysis, with temperature and moisture as variables. It was found that the Nylon 6 thin film is also sensitive to moisture and can swell/shrink under ambient conditions, which can relate to hydration of the amorphous region in the Nylon 6. Furthermore, it is also found that glass transition disappeared in the temperature range from 28 ºC to 70 ºC. It is inferred that the reducing in molecular weight and γ form crystallinity both contributed the mobility of the polymer chain in the Nylon 6 thin film.

5.2 Preparation of Nylon 6 thin film by physical vapor deposition

5.2.1 *Apparatus for physical vapor deposition.*

The apparatus used for the preparation of Nylon 6 thin film was molecular beam epitaxy (MBE) setup, equipped with a substrate-cooling system, that was specifically designed for formation of metallic nano particles.[31] The system has two separated rooms; one is a load-lock chamber for exchanging the samples, and the other one is a main chamber, where the ultra-high vacuum conditions are always maintained. The temperature of the Knudsen (K) cell in the cell container was controlled by electric heating. The temperature sensor was set at the bottom of the sample container touching the K cell, and a rotating shutter was placed on top to control the molecular beam. The XTM/2 deposition monitor (IPN 074-186) was used for monitoring sample growth, and an ionized gauge was used for the pressure monitoring. Two water-cooling systems (around 17 ° C) were set for the vacuum chamber, and the water tank, which tightly touches the sample substrate from the backside during the deposition.

5.2.2 *Materials and Preparation.*

Commercial Nylon 6 bulk granules with molecular weight (MW) of 10032 was used as the sample source. In order to ensure the quality of the deposited film, the pressure in the deposition chamber was reduced to 10^{-6} Pa. Meanwhile, the evaporation temperature was set around 190–210 ° C, lower than the melting point of 220 ° C and the difference is assumed as negligible. During heating, the shutter was used to control the molecular beam, and mass of film deposited, which was observed by the deposition monitor. After deposition, the molecular beam was stopped by the shutter, and the sample was naturally cooled to room temperature. With control of deposition rate and time, a variety of Nylon 6 ultrathin films were prepared.

5.3 Characterization and In-operando analysis of Nylon 6 thin film

5.3.1 *Experimental Process of Characterization and In-operando analysis.*

Raman spectroscopy measurements were performed by laser Raman (Nanophoto Co.). X-ray diffraction spectra and X-ray reflectivity curves were measured on a customized multi-channel X-ray reflectometer.

The X-ray source was equipped with an 18-kW rotating anode copper source (Ultrax 18, Rigaku, typical operation conditions 40 kV, 200 mA). A customized temperature and moisture control system (AHCU-2, Sansyo Co., Ltd.) was used for the in-operando X-ray reflectivity measurements. SPM measurement (SPM-9500J3, Shimadzu Co., Ltd.) was conducted with a dynamic scan model for soft surface morphology analysis, and the result was flattened by plane fitting and curved surface fitting.

5.3.2 *Experimental Process of In-operando analysis.*

The thickness of Nylon 6 thin film was studied by the multi-channel X-ray reflectometer.[32,33] After aging the sample at 10 ° C overnight under ambient conditions, the thickness of Nylon 6 thin film was monitored with the temperature scan from 10 to 70 ° C at 3 ° C intervals. Each step took 9 min, including the heating stage (about 0.5 min) and the static stage (about 8.5 min). At each step, data was collected between 4 and 7 min to avoid the effects of temperature fluctuations. In the moisture control experiment, the thickness change of Nylon 6 thin film was studied with relative humidity (RH) scans from 5 % to 75 % at 20 ° C. Before data collection, the Nylon 6 thin film was maintained with RH of 5 % at 20 ° C at least 12 hours to stabilize the initial state. The RH was raised every hour from 5 % to 80%, and the X-ray reflectivity curves of the Nylon 6 thin film were recorded. Fourier Transform (FT) calculations were preferentially used for the data analysis of the X-ray reflectivity curves. [34,35] Regarding to the error estimates of thickness, the uncertainty in measurement have been studied with different conditions in our previous research.[36] The uncertainty in the determination of layer thickness is within ±0.08 nm. Of course, the uncertainty would be sample state dependent. Thus, in the discussion of thickness change with environment, we are more concerned about the trend of its behavior change, rather than focusing on quantitative analysis.

5.4 Structure of Nylon 6 thin films prepared by physical vapor deposition

As the mentioned above, the structure of the Nylon 6 materials would be varied with the preparation process, and regarding the reports on PVD, there are still many deficiencies in the PVD process of polymer, such as thermal degradation and difficulty in the controlling of the morphology. In this work, the Nylon 6 thin film has been first prepared by the PVD with MBE setup, while there are few reports on the structure of deposited polymer thin film with this preparation process. Therefore, the basic characterization of deposited Nylon 6 thin film, such as chemical structure, physical structure, and surface/interface morphology, have been discussed first in this work. And then, with control experiment on the temperature and moisture, some fundamental properties of the Nylon 6 thin film, such as the swelling/shrinking and glass transition behaviors, have been discussed with its structures.

5.4.1 *Chemical structure of nylon 6 thin film*

In the past, pyrolysis of the PVD deposited polymer has been always observed by the reduction or disappearance of characteristic peaks in the of FTIR / Raman spectra. Since the PVD process requires

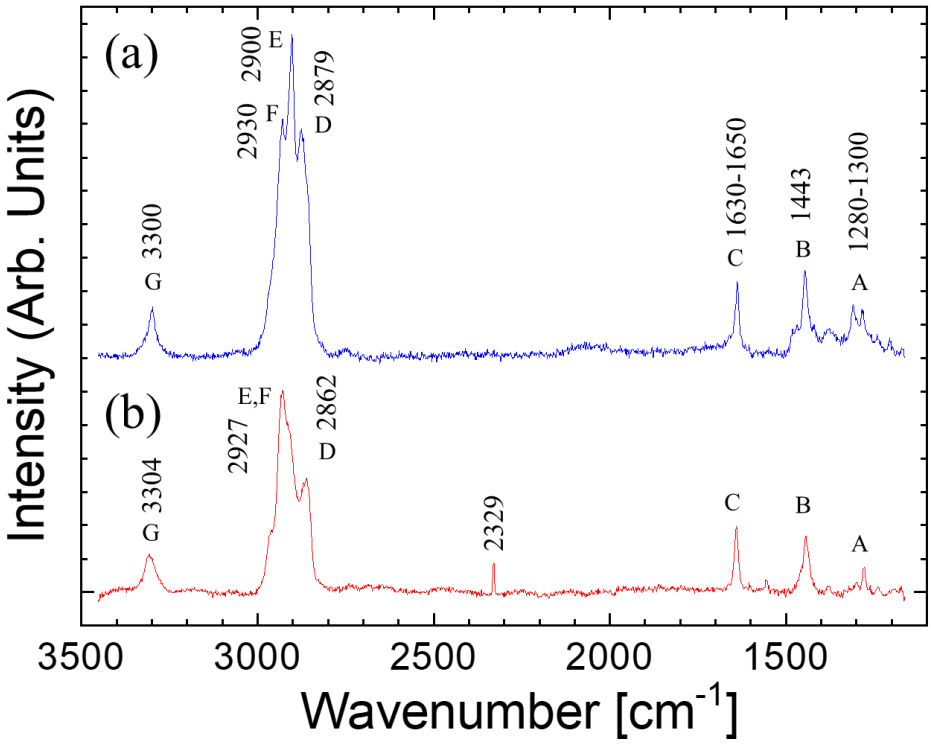

Figure 1. Raman spectroscopy of the Nylon 6 particle (A) and the physically deposited thin film (B). (Publication in progress)

high temperatures to ensure the evaporation of the virgin materials, it is generally accepted that the chemical structure will be inevitably damaged by the evaporation process. However, in this work, we intentionally avoided high temperature evaporation. The heating temperature of virgin Nylon 6 was set around 190–210 ° C, which is lower than the thermal degradation temperature of 400 ° C and the melting point of α form of 220 ° C, but higher than the melting point of γ form of 180 ° C.[28–30] It is suggested that the pyrolysis must be quite limited during the sample preparation.

As shown in Figure 1, the Raman spectra of the virgin Nylon 6 granule and deposited thin film have been compared directly. Figure 1A shows the Raman spectra of the Nylon 6 granule, used as the source for the preparation. The sharp and strong bands at 2879 cm^{-1}, 2900 cm^{-1} and 2930 cm^{-1} are assigned to CH_2 stretching vibration, whereas the band at 1443 cm^{-1} indicates the bending vibration of CH_2 in the Nylon 6 granule. The characteristic absorption of the amide I and amide III bands are observed around 1630 to 1650 cm^{-1} and 1280 to 1300 cm^{-1}, and the band at 3300 cm^{-1} is assigned to the stretching vibration of N-H, which indicate the amide structure in the Nylon 6 granules.[37] Then, as shown in Figure 1B, the observed spectra of the deposited thin film are similar to the Raman spectra of the virgin source, except for the band at 2329 cm^{-1} which is assigned to N_2 from air. The sharp and strong bands at 2862 cm^{-1} and 2927 cm^{-1} can be assigned to the CH_2 stretching vibration. The shift and merge of the peak position may be related to the internal strain in the deposited thin film, which may relate to the packing state of the polymer with the crystalline form in nylon 6.[38] The bands at 1443 cm^{-1}, 1630 to 1650 cm^{-1} and 1280 to

1300 cm^{-1} are also assigned to the bending vibration of CH_2, amide I and amide III as same as the feature in the virgin source. The bands at the 1604 cm^{-1} would shift from 1600 cm^{-1} with the internal stress, indicating the stretching vibration of N-H. Obviously, the deposited film successfully retained the chemical structure of Nylon 6 by MBE setup with low temperature heating, and it proposed that the ultra-high vacuum conditions (below 10^{-6} Pa) facilitates evaporation of polymers at low temperatures.

Regarding the discussion of pyrolysis of deposited polymer, only the study on chemical structure would be not enough, and the discuss on change of molecular weight distribution (MW) during the sample preparation is also important. However, it is pity that the MW of the deposition thin film still cannot be solved out in our experiment directly, although it can be usually obtained by the characteristic peak analysis by FTIR/Raman spectra. Due to the back group of bulk system and ultrathin film system are different, it is difficult to conduct the control experiments in MW in colorimetry. Thus, it would be very tricky to give a discussion on the MW by comparing these two spectra directly. Of course, there are also other ways to estimate MW, such as the gel permeation chromatography (GPC) and instinct viscosity measurement which are usually used to obtain the MW directly. But in this work, it is difficult for us to collect enough samples to obtain the signal in GPC measurement. And, intrinsic viscosity measurement is also difficult for us. Therefore, we also agree the envision that the small polymer chains and small molecules, such as the oligomers, would vaporize and deposit first during the PVD process, and it is difficult to identify the main components in the deposited film directly. But, as a compromise, the ratios of the oligomer in the Nylon 6 thin film has been inferred through other experiment results, such as the XRD pattern and swelling/shrinking behaviors, in this work. It is proposed that the MW of nylon 6 in the deposited thin film may be small, but the ratio of oligomers is limited. The supporting discussion are presented in the following sections.

5.4.2 *Crystalline structure of nylon 6 thin film*

In the previous researches, many efforts have been devoted to the crystal structure of Nylon 6, and two major crystalline forms, α form and γ form, have been confirmed in Nylon 6 system. Generally, it is recognized that the α form is composed of the extend chain where the intramolecular hydrogen bonds are formed between the antiparallel chains, while the γ form is composed of the pleated chains where intermolecular hydrogen bonds are formed between the parallel chains and perpendicular to the intra-sheet of carbon framework.[39,40] It is accepted that the α form should be the thermodynamically stable and the γ form is metastable, which can impart the different properties of the Nylon 6 system. In the past, the γ form has been widely observed in the spun Nylon 6 nanofiber, and. it is proposed that the structure and property of the Nylon 6 can be greatly affected by the kinetic of the preparation process. In this work, the Nylon 6 thin film has been first prepared by the PVD with MBE setup, and the related structure has been discussed with XRD patterns of the virgin Nylon 6 and the deposited thin film.

As shown in Figure 2, the XRD patterns of virgin Nylon 6 granule and deposited thin film are presented. Figure 2 A shows the XRD patterns of virgin Nylon 6 granule. Two peaks at 20 degrees and 23.7 degrees

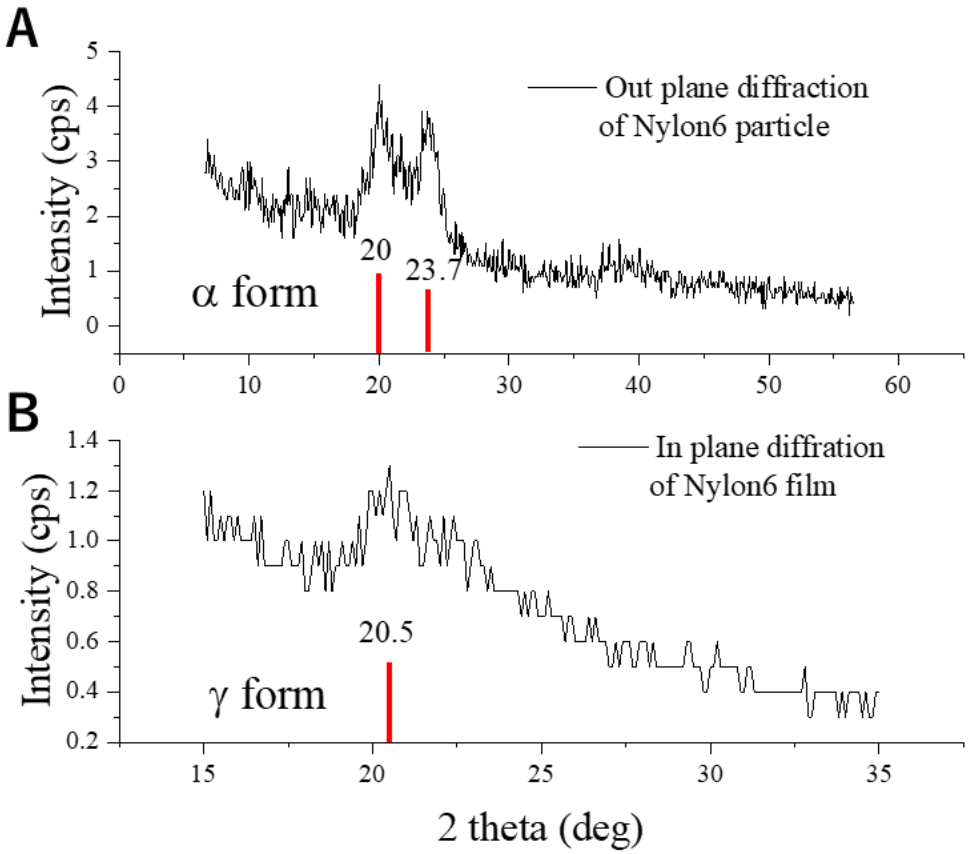

Figure 2. Out plane X-ray diffraction of the Nylon 6 particle (A) and in plane X-ray diffraction of the Nylon 6 thin film (B). (Publication in progress)

are assigned to (200) and (002) reflections, respectively, which are both from α crystalline form in the Nylon 6. But in Figure 2 B, only one broad peak around 20.5 degrees can be observed in the deposited thin film, which is generally assigned to the (200) reflection of γ form in Nylon 6. Although the signal of the Nylon 6 thin film is quite weak, the same pattern has been confirmed in the different deposited Nylon 6 thin film as shown in Support information S1. Thus, it is proposed that the γ form is dominated crystal structure of the deposited Nylon 6 thin film. In the previous research, it has been already known that two distinct different crystalline in nylon 6 would be related the chain conformation, packing and stacking state with hydrogen bonding. Regarding the formation of γ form in these samples, it is proposed that the PVD process and interface interaction have had an impact. During the deposition process, the heating temperature was set around 190 to 220 ° C, which may contribute to rapid crystallization. The interface interaction would suppress the rearrangement of the polymer chain limiting intramolecular hydrogen bonding in the intrasheet, while the stacking of polymer chains would be favored in the deposition process, which can contribute the intermolecular hydrogen bonding in the γ form. On the other hand, regarding the effect of MW on the structure, due to the large amount of oligomers will disrupt the order of the crystalline region resulting to the amorphous structure, it is proposed that the deposited Nylon 6 thin film may contain small molecules, such as oligomer, but its ratio should be limited.

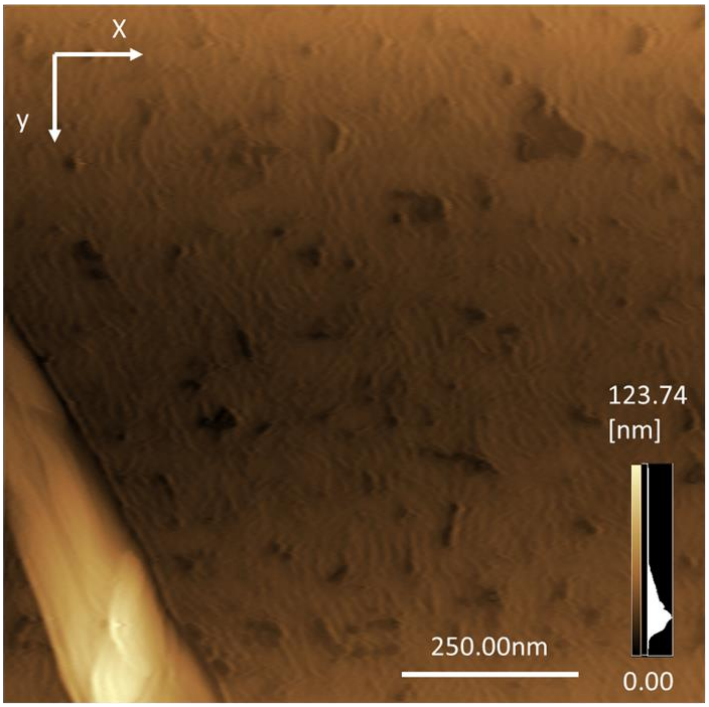

Figure 3. SPM image of physically deposited thin film (of 100 nm). (Publication in progress)

5.4.3 *Surface and interface conditions of nylon 6 thin film*

As we known that, the morphology and structure is important to the properties of materials, especially for thin film systems that the surface/interface conditions can affects its practical performance directly. However, in the past reports on the PVD deposited polymer thin film, few efforts have been devoted to the morphology of the deposited thin films. In this work, in order to make progress in this aspect, MBE equipment, which not only facilitated the formation of the crystal structure of the thin film but also ensured the state of the surface/interface, has been used for the deposition process of the Nylon 6 thin film. Since the MBE setup was mainly used to deposit the small inorganic molecules in the past, the morphology characterization of the deposited polymer thin film has been conducted first. The surface morphology has been confirmed by the SPM image with quantitative surface topology analysis directly, while due to interface morphology cannot be observed directly, XRR analysis has be used to determine the state of the interface conditions.

As shown in Figure 3, surface morphology of nylon 6 thin film (98.5 nm thickness) has been studied by the SPM image, and three main morphologies can be observed in the scanning range of 1 μm * 1 μm. Among them, the most prominent morphological feature is the irregular small holes which are uniformly distributed on the surface. With the profile analysis, it can be found that the relative depth to its edges is mostly less than 8 nm. Considering that the thickness of the sample is close to 100 nm, it is suggested that these shallow holes would only relate to the separation/agglomeration of polymer chains on the surface,

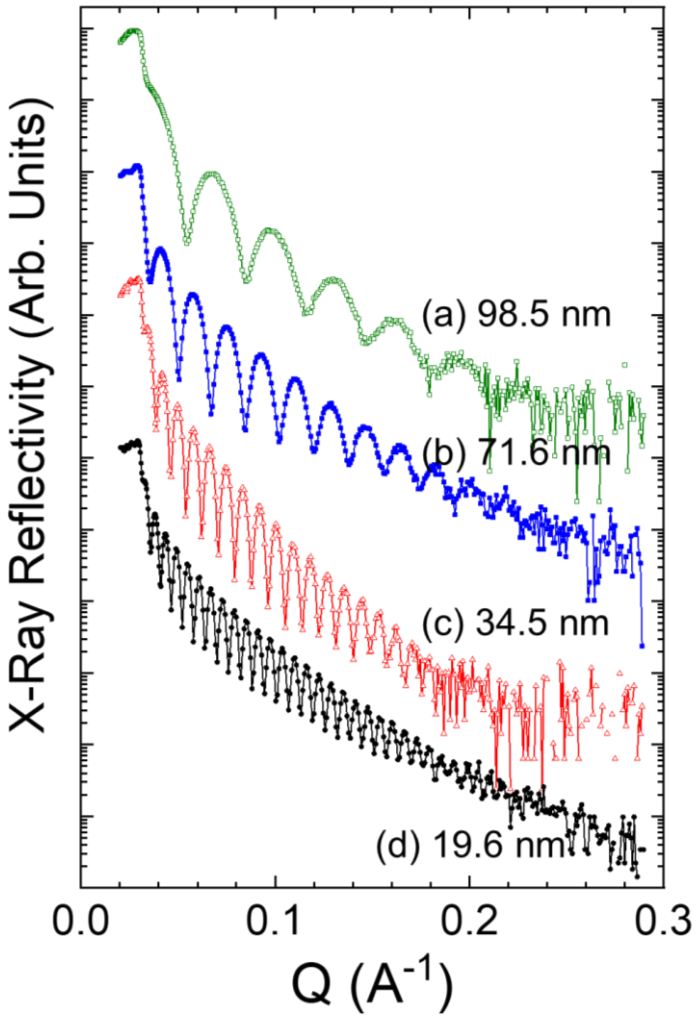

Figure 4. X-ray reflectivity curves of the nylon 6 thin films, which were prepared with the same deposition rate but in different thickness from 98.5 nm to 19.6 nm, (a) to (d). (each pattern is offset)

but not to the dewetting process that always occurred with the internal stress causing the deep hole in the polymer thin film system. On the other hand, between these shallow holes, a flat morphology with regular fine lines can be observed. It is suggested that these fine lines may relate to the nature of the deposited Nylon 6 films, such as the gamma form structure. Finally, a big protrusion at right corner in the scanned range can be observed, its height is about 90 nm relative to its foot. Since the same topographic feature was not observed elsewhere in the image, it is proposed that this protrusion would be the contamination or the detect caused by the preparation process. After the quantitative calculation, it is found that the height distribution range at the surface of the nylon 6 thin film is about 112.9 nm, and the peak position of the distribution is about 33.0 nm with a FWHM of 11.2 nm. After the calculation over the whole image, the RMS roughness of nylon 6 thin film is about 10.3 nm. However, if the effect of this protrusion was neglected, the RMS roughness is about 2.7 nm as shown in the selected area in the Figure 3.

On the other hand, the interface conditions of the Nylon 6 thin films have been studied in different thicknesses and an important parameter of the experimental conditions observed with X-ray reflectivity

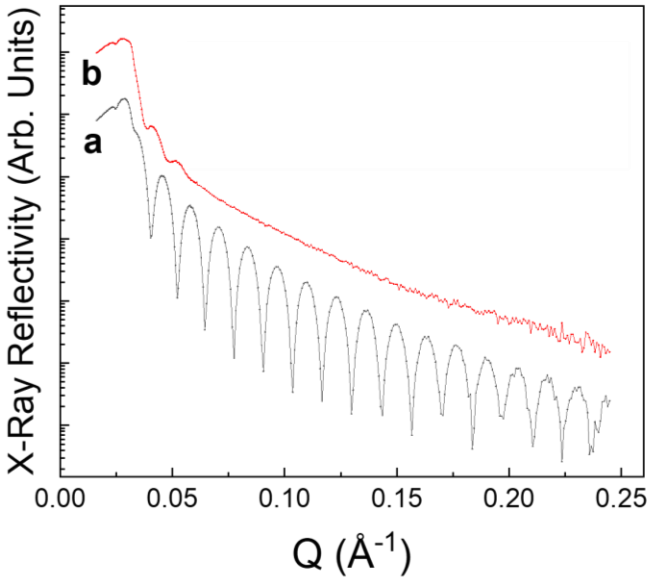

Figure 5. XRR curves the nylon 6 thin film prepared with the deposition rate at (a) 4 nm/min and (b) 0.85/min. (Publication in progress)

data for the sample. The X-ray reflectivity analysis is the study on the interference of the reflected X-ray from each interface with incident angle (or energy).[41] Due to the short wavelength of X-rays, the frequency of the oscillation would be quite sensitive to the thickness of the thin film, and the amplitude can be greatly affected by interface conditions. Figure 4 presents the X-ray reflectivity curves of the samples, which were prepared with the same deposition rate but different deposition times. As shown in (a), (b), (c) and (d) in Figure 4, the single frequencies and clear oscillations indicate good quality of the single layer structure in each thin film, which are consistent with the result from the SPM measurement. After the calculation in FT, it was found that the Nylon 6 thin films with thicknesses of 98.5 nm, 71.6 nm, 34.5nm and 19.6 nm (from high frequency to low frequency) had been successfully prepared by PVD with different deposition times. During the deposition process, although the deposition rate of each sample is difficult to be kept at a constant value, the average deposition rates of the above processes are close and faster than 3nm/min.

To clarify the contribution of deposition rate on the quality of the nylon 6 thin film, different samples have been studied by the X-ray reflectivity curves of the samples, which were prepared with the same expected thickness, but different deposition rates. As shown in Figures 5, the samples were prepared with the average deposition rates at 4 nm/min and 0.85 nm/min, but only the sample (a) in fast deposition shows clear oscillation in the X-ray reflectivity, especially the strong amplitude at the high Q range (larger than 0.2 Å), which indicated the small roughness of only 0.45 nm. In contrast, the calculated roughness of the sample (b), which was prepared in 0.85 nm/min, is more than 16 nm. Obviously, the deposition rate has a great influence on the preparation of polymer thin film by PVD, and the high deposition rate, such as 4 nm/min, is required for good interface conditions. This could indicate the significance of the interaction between the polymer chains in vapor phase, because it has more free energies than the case for the re-arrangement of the polymer chain at the surface of substrate. In the general study of PVD for

inorganic thin films, the discussion will focus on the rearrangement of the small molecules on the surface of the substrate, which mainly involves the surface energy in system and the energy conversion when the molecular beam hits the substrate. For the impact event of the molecular beam, generally, each process is considered as independent, that is unaffected by other molecules. However, in the deposition of polymer chains, the situation would become different in that the polymer chain is much larger than the small molecules. This means that interaction between each molecule can be active within the molecular beam, i.e., the deposition rate has an effect. It is proposed that interaction of the polymer chains during the impacting beam can contribute to the formation of entanglements resulting in the dense layer. Therefore, the formation of good polymer thin film interface is favored with high deposition rates by PVD.

5.5 Thickness stability of Nylon 6 thin films with temperature scan

Finally, to clarify the effect of the structure on the property of the Nylon 6 thin film. The thickness stability of the Nylon 6 thin film have been studied by multi-channel X-ray reflectometer with temperature scan range from 10 to 70 ° C and RH scan range from 5% to 75%, respectively. Figure 6 A demonstrates the thickness change of the Nylon 6 thin film with temperature under ambient conditions, and two abnormal phenomena have been observed. When the temperature is below 28 ° C, the greatest decrease in thickness of 1.7% occurs with heating. While the temperature is above 28 ° C, there is no clear change on the coefficient of thermal expansion, although it is generally recognized that the glass transition of Nylon 6 should happen around 40~50 °C with moisture.[42] For the mechanism of decreasing thickness with temperature, sometimes it would be considered as the negative thermal expansion in the polymer ultrathin film system, which is the additional deformation with internal stress during thermal expansion.[24,34,35] However, in this experiment, such a large change of 1.7% is difficult to be interpreted by the change in structure of polymer film itself. Considering the great number of amide groups in the main chain, the study on humidity-responsive behaviors of the Nylon 6 thin film has been conducted at 20 ° C. However, there is still one point should be noted that the swelling behaviors of materials is be affected by the actual RH directly which is experienced by the surface of sample, and the RH can change with the temperature of the surface of sample, even if the ambient RH is constant. In Figure 6 B, the thickness change of Nylon 6 thin film with RH from 5 % to 75 % is presented, which was conducted in the moisture chamber that promised actual RH can be same to the chamber RH by a dynamic process. It was found that the thickness of Nylon 6 thin film significantly increased as the RH became larger than 45 %. No doubt, the swelling occurred in the Nylon 6 thin film. Then, let us return to the experiment shown in Figure 6 A, it is proposed that the initial state of this sample is already swollen. Because before this experiment, the Nylon 6 thin film has been kept on the sample stage at 10 ° C under ambient conditions (temperature of 20 ° C, RH of ~40%) overnight. And if it is assumed that the ambient conditions are constant, the actual RH experienced by the surface can be estimated about 74%. According to the data shown in Figure 6 B, the Nylon 6 should be swollen before the experiment. Furthermore, with calculation of the actual RH in the Figure 6 A, it is found that the actual RH can greatly drop from 74% to 61% with temperature from 10 ° C

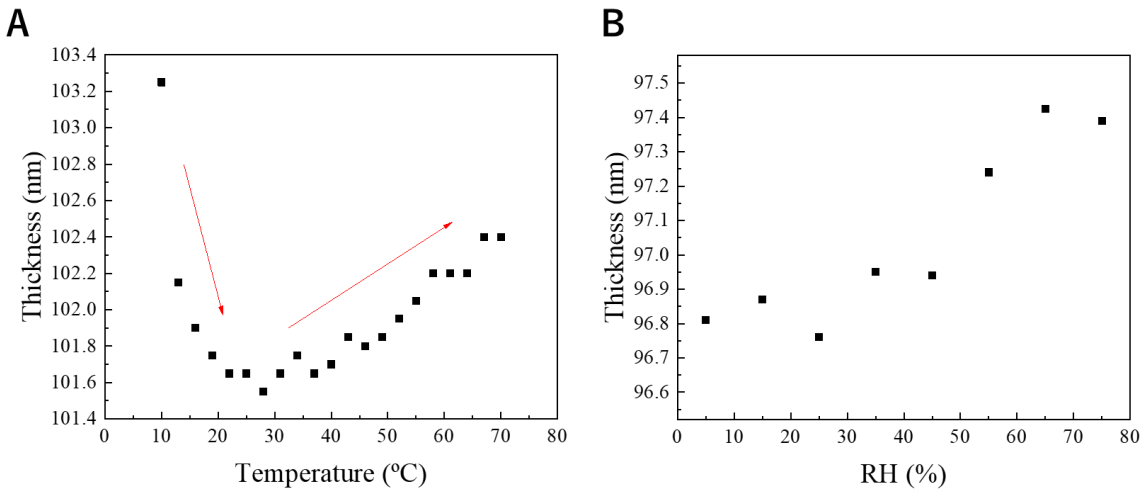

Figure 6. (A) Thickness change of nylon 6 thin film with temperature scan from 10 to 70 ºC under the ambient conditions (with room RH around 40%) and (B) the thickness change of nylon 6 thin film with RH 5 % ~ 75% at 20 ºC. (Publication in progress)

to 13° C causing shrinking which accords with the behaviors shown in Figure 6 B. Of course, considering the kinetic of swelling/shrinking, some numerical differences between the data shown in Figure 6 A and B should be acceptable. Then, regarding to the swelling/shrinking in the Figure 6, it is suggested that only a few amorphous regions swelling in the Nylon 6 thin film. As we known, the crystal construction of Nylon 6 is mainly formed by the hydrogen bonding between the amide bonds in the main chain, and the amide bonds are also the channels for absorption and diffusion of water molecules in the polymer thin film. Therefore, it is not difficult to imagine that the behavior of water molecules can be different in amorphous and crystalline phases in semi-crystalline polymer. In the report from Murthy, the swelling/shrinking of the Nylon 6 have been experimentally studied in the amorphous and crystalline phases.[46] For the swelling process, due to the large number of free amide bonds in the amorphous phase, the absorption and diffusion of water molecules primarily occurred in the amorphous region causing the volume increase. However, in the crystalline regions, due to the strong hydrogen bonding between its crystal structures, only a small amount of water molecules can affect the surface of crystalline lamellae increasing the mobility. Meanwhile, if it is assumed that each amide bonds can bind to one water molecule, the theoretical maximum absorption of Nylon 6 should be about 13.5 wt %. However, as the data shown in Figure 6 B, the thickness change of the Nylon 6 thin film in its swollen state is only about 1-2 %. Thus, it is proposed that the structure of the deposited Nylon 6 thin film is not a low crystalline system, which may relate to the stacking process of PVD by MBE setup. Then, regarding the effect of Mw on the structure, due to the oligomers can contributed the amorphous structure, it is proposed that the amount of the oligomers should be limited in the deposited Nylon 6 thin film. On the other hand, for the disappearance of the glass transition in Nylon 6 thin film, it is suggested that this phenomenon can be related to the structure of Nylon 6 thin film. Generally, it is accepted that the Tg can decrease with the reducing in molecular weight, and the hydration in the amorphous region of Nylon 6 can also increase the mobility of the polymer chain. However, as

shown in Figure 6, if it is assumed the coefficient of thermal expansion (CTE) does not change from 28 ° C to 70 ° C, its value would be about $2*10^{-4}$ K^{-1}. It is suggested that the mobility of the polymer chains was suppressed in the gamma crystalline form in the Nylon 6 thin film. Although it is still difficult to provide a quantity on the ratio between amorphous and gamma form in the thin film system, the low swelling degree, which indicated the ratio of amorphous region, may agree with the low CTE, which indicated the high ratio of crystal region. However, for the polymer thin film system, the interface interaction is also an important factor that can restrict the mobility of polymer chain. In the reports from Kanaya, an increasing on the Tg have been experimentally proved in the polymer ultrathin film system, and the influence of the interface action is only in the interface layer with a few nanometers.[47–49] Considering the thickness of this sample of 100 nm in Figure 6, it is suggested that the effect of the interface action may limited.

5.6 Conclusion

In the present study, Nylon 6 thin film has been successfully prepared with thicknesses ranging from 10 nm to 100 nm by PVD. This preparation process not only avoids damage to chemical structure, but also ensures a high-quality thin film. The Raman and X-ray diffraction (XRD) spectra confirm the granules' chemical structure as Nylon 6 containing the γ crystalline form in the deposited thin film. With SPM imaging and X-ray reflectivity analysis, flat surface and interface conditions with low roughness have also been confirmed. One important experimental condition established by the study is that the formation of high-quality Nylon 6 thin film is favorable during fast deposition. Regarding the thickness stability of the Nylon 6 thin film, it was found that the Nylon 6 thin film is also sensitive to moisture and can swell under ambient conditions, which is related the amorphous region ratio in the thin film. In addition, glass transition does not occur at temperatures ranging from 28 ° C to 70 ° C. Although the experimental data is not sufficient to interpret everything in this study, it can still be inferred that the interface interaction and the kinetic of preparation process contribute to formation of γ phase in the Nylon 6 thin film, and the reducing in molecular weight and γ crystalline form both contributed the mobility of the polymer chain in the Nylon 6 thin film.

Reference

(1) Kyotani, M.; Mitsuhashi, S. Journal of Polymer Science Part A-2 Polymer Physics. *Artic. J. Polym. Sci. Part A-2 Polym. Phys.* **1972**, *10* (8), 1497–1508.

(2) Murthy, N. S.; Curran, S. A.; Aharoni, S. M.; Minor, H. Premelting Crystalline Relaxations and Phase Transitions in Nylon 6 and 6,6. *Macromolecules* **1991**, *24*, 3215–3220.

(3) Takele, H.; Greve, H.; Pochstein, C.; Zaporojtchenko, V.; Faupel, F. Plasmonic Properties of Ag Nanoclusters in Various Polymer Matrices. *Nanotechnology* **2006**, *17* (14), 3499–3505.

(4) Katoh, Y.; Okamoto, M. Crystallization Controlled by Layered Silicates in Nylon 6-Clay Nano-Composite. *Polymer (Guildf).* **2009**, *50* (19), 4718–4726.

(5) Gianchandani, J.; Spruiell, J. E.; Clark, E. S. Polymorphism and Orientation Development in Melt Spinning, Drawing, and Annealing of Nylon - 6 Filaments. *J. Appl. Polym. Sci.* **1982**, *27* (9), 3527–3551.

(6) Murthy, N. S.; Bray, R. G.; Correale, S. T.; Moore, R. A. F. Drawing and Annealing of Nylon-6 Fibres: Studies of Crystal Growth, Orientation of Amorphous and Crystalline Domains and Their Influence on Properties. *Polymer (Guildf).* **1995**, *36* (20), 3863–3873.

(7) Li, Y.; Goddard, W. A. Nylon 6 Crystal Structures, Folds, and Lamellae from Theory. *Macromolecules* **2002**, *35* (22), 8440–8455.

(8) Yang, Z.; Peng, H.; Wang, W.; Liu, T. Crystallization Behavior of Poly(ε -Caprolactone)/Layered Double Hydroxide Nanocomposites. *J. Appl. Polym. Sci.* **2010**, *116* (5), 2658–2667.

(9) Loo, L. S.; Gleason, K. K. Insights into Structure and Mechanical Behavior of α and γ Crystal Forms of Nylon-6 at Low Strain by Infrared Studies. *Macromolecules* **2003**, *36* (16), 6114–6126.

(10) Kwak, S. Y.; Kim, J. H.; Kim, S. Y.; Jeong, H. G.; Kwon, I. H. Microstructural Investigation of High-Speed Melt-Spun Nylon 6 Fibers Produced with Variable Spinning Speeds. *J. Polym. Sci. Part B Polym. Phys.* **2000**, *38* (10), 1285–1293.

(11) Liu, Y.; Cui, L.; Guan, F.; Gao, Y.; Hedin, N. E.; Zhu, L.; Fong, H. Crystalline Morphology and Polymorphic Phase Transitions in Electrospun Nylon-6 Nanofibers. *Macromolecules* **2007**, *40* (17), 6283–6290.

(12) Murase, S.; Kashima, M.; Kudo, K.; Hirami, M. Structure and Properties of High-Speed Spun Fibers of Nylon 6. *Macromol. Chem. Phys.* **1997**, *198* (2), 561–572.

(13) Chow, R.; Loomis, G. E.; Ward, R. L. Optical Multilayer Films Based on an Amorphous Fluoropolymer. *Cit. J. Vac. Sci. Technol. A* **1996**, *14* (1), 63–68.

(14) Wang, C.; Dong, H.; Hu, W.; Liu, Y.; Zhu, D. Semiconducting π-Conjugated Systems in Field-Effect Transistors: A Material Odyssey of Organic Electronics. *Chemical Reviews*. April 11, 2012, pp 2208–2267.

(15) Wang, C.; Dong, H.; Hu, W.; Liu, Y.; Zhu, D. Semiconducting π-Conjugated Systems in Field-Effect Transistors: A Material Odyssey of Organic Electronics. *Chem. Rev.* **2012**, *112* (4), 2208–2267.

(16) Yan, H.; Chen, Z.; Zheng, Y.; Newman, C.; Quinn, J. R.; Dötz, F.; Kastler, M.; Facchetti, A. A High-Mobility Electron-Transporting Polymer for Printed Transistors. *Nature* **2009**, *457*, 679–686.

(17) Iwamori, S.; Tanabe, T.; Yano, S.; Noda, K. Adsorption Properties of Fluorocarbon Thin Films Prepared by Physical Vapor Deposition Methods. *Surf. Coatings Technol.* **2010**, *204* (16–17), 2803–2807.

(18) Nason, T. C.; Moore, J. A.; Lu, T. M. Deposition of Amorphous Fluoropolymer Thin Films by Thermolysis of Teflon Amorphous Fluoropolymer. *Appl. Phys. Lett.* **1992**, *60* (15), 1866–1868.

(19) Biswas, A.; Aktas, O. C.; Kanzow, J.; Saeed, U.; Strunskus, T.; Zaporojtchenko, V.; Faupel, F. Polymer-Metal Optical Nanocomposites with Tunable Particle Plasmon Resonance Prepared by Vapor Phase Co-Deposition. *Mater. Lett.* **2004**, *58* (9), 1530–1534.

(20) Chow, R.; Loomis, G. E.; Ward, R. L. Optical Multilayer Films Based on an Amorphous Fluoropolymer. *J. Vac. Sci. Technol. A Vacuum, Surfaces, Film.* **1996**, *14* (1), 63–68.

(21) Maier, G. Low Dielectric Constant Polymers for Microelectronics. *Progress in Polymer Science (Oxford)*. February 2001, pp 3–65.

(22) Li, X.; Lushington, A.; Sun, Q.; Xiao, W.; Liu, J.; Wang, B.; Ye, Y.; Nie, K.; Hu, Y.; Xiao, Q.; et al. Safe and Durable High-Temperature Lithium–Sulfur Batteries via Molecular Layer Deposited Coating. *Nano Lett.* **2016**, *16* (6), 3545–3549.

(23) Jeong, H.; Shepard, K. B.; Purdum, G. E.; Guo, Y.; Loo, Y. L.; Arnold, C. B.; Priestley, R. D. Additive Growth and Crystallization of Polymer Films. *Macromolecules* **2016**, *49* (7), 2860–2867.

(24) Yamazaki, T.; Mahapun, C.; Usui, S. Vapor Deposition Polymerization of a Polyimide Containing Perylene Units Characterized by Displacement Current Measurement. *Japanese J. Appl. Phys. To* **2005**, *44*, 2810–2814.

(25) Yoon, H.; Koh, Y. P.; Simon, S. L.; McKenna, G. B. An Ultrastable Polymeric Glass: Amorphous Fluoropolymer with Extreme Fictive Temperature Reduction by Vacuum Pyrolysis. *Macromolecules* **2017**, *50* (11), 4562–4574.

(26) Nason, T. C.; Lu, T. M. Thermoplastic and Spectroscopic Properties of Amorphous Fluoropolymer Thin Films. *Thin Solid Films* **1994**, *239* (1), 27–30.

(27) Ding, S. J.; Zaporojtchenko, V.; Kruse, J.; Zekonyte, J.; Faupel, F. Investigation of the Interaction of Evaporated Aluminum with Vapor Deposited Teflon AF Films via X-Ray Photoelectron Spectroscopy. *Appl. Phys. A Mater. Sci. Process.* **2003**, *76* (5), 851–856.

(28) Kubono, A.; Okui, N. Polymer Thin Films Prepared by Vapor Deposition. *Prog. Polym. Sci.* **1994**, *19* (3), 389–438.

(29) Usui, H. Preparation of Polymer Thin Films by Physical Vapor Deposition. In *Functional Polymer Films*; Wiley-VCH, 2011; Vol. 1, pp 287–318.

(30) Philip J. *SFPE Handbook of Fire Protection Engineering Third Edition Editorial Staff The Following Are Registered Trademarks of the National Fire Protection Association: National Electrical Code ® and NEC ® National Fire Codes ® Life Safety Code ® and 101 ® Nationa*; Hughes Associates, Inc, 2002.

(31) Jerab, M.; Sakurai, K. Structures of Yb Nanoparticle Thin Films Grown by Deposition in He and N 2 Gas Atmospheres: AFM and x-Ray Reflectivity Studies. *J. Phys. Condens. Matter* **2010**, *22*, 474010–474023.

(32) Sakurai, K.; Mizusawa, M. X-Ray Reflectometer and the Measurement Method. 3903184, 2007.

(33) Sakurai, K.; Mizusawa, M.; Ishii, M. Recent Novel X-Ray Reflectivity Techniques: Moving Towards Quicker Measurement to Observe Changes at Surface and Buried Interfaces. *Trans. Res. Soc. Japan* **2007**, *32* (001), 181–187.

(34) Sakurai, K.; Mizusawa, M.; Ishii, M. Significance of Frequency Analysis in X-Ray Reflectivity: Towards Analysis Which Does Not Depend Too Much on Models. *Trans. Mater. Res. Soc. Japan* **2008**, *33* (3), 523–528.

(35) Sakurai, K.; Iida, A. Fourier Analysis of Interference Structure in X-Ray Specular Reflection from Thin Films. *Jpn. J. Appl. Phys.* **1992**, *31* (2), 113–115.

(36) Liu, Y.; Sakurai, K. Thickness Changes in Temperature-Responsive Poly(N -Isopropylacrylamide) Ultrathin Films under Ambient Conditions . *ACS Omega* **2019**, *4* (7), 12194–12203.

(37) Stuart, B. H. A Fourier Transform Raman Study of Water Sorption by Nylon 6. *Polym. Bull.* **1994**, *33* (6), 681–686.

(38) Li, Y.; Goddard, W. A. Nylon 6 Crystal Structures, Folds, and Lamellae from Theory. *Macromolecules* **2002**, *35* (22), 8440–8455.

(39) Matyi, R. J.; Crist, B. Small-Angle x-Ray Scattering by Nylon 6. *J. Polym. Sci. Polym. Phys. Ed.* **1978**, *16* (8), 1329–1354.

(40) Arabnejad, S.; Manzhos, S. Defects in Alpha and Gamma Crystalline Nylon6: A Computational Study. *AIP Adv.* **2015**, *5* (10), 107123–107130.

(41) Stoev, K. N.; Sakurai, K. Review on Grazing Incidence X-Ray Spectrometry and Reflectometry. *Spectrochim. acta, Part B At. Spectrosc.* **1999**, *54* (1), 41–82.

(42) Khanna, Y. P.; Kuhn, W. P. Reliable Measurements of the Nylon 6 Glass Transition Made Possible by the New Dynamic DSC. *Macromolecules* **1995**, *28*, 2644–2646.

(43) Liu, Y.; Sakurai, K. Uniaxial Negative Thermal Expansion of Polyvinyl Acetate Thin Film. *Langmuir* **2018**, *34* (38), 11272–11280.

(44) Mukherjee, M.; Bhattacharya, M.; Sanyal, M. K.; Geue, T.; Grenzer, J.; Pietsch, U. Reversible Negative Thermal Expansion of Polymer Films. *Phys. Rev. E - Stat. Physics, Plasmas, Fluids, Relat. Interdiscip. Top.* **2002**, *66* (6), 061801–061804.

(45) Miyazaki, T.; Nishida, K.; Kanaya, T. Contraction and Reexpansion of Polymer Thin Films. *Phys. Rev. E - Stat. Nonlinear, Soft Matter Phys.* **2004**, *69* (2), 022801–022804.

(46) Murthy, N. S.; Stamm, M.; Sibilia, J. P.; Krimm, S. Structural Changes Accompanying Hydration in Nylon 6. *Macromolecules* **1989**, *22* (3), 1261–1267.

(47) Inoue, R.; Kawashima, K.; Matsui, K.; Nakamura, M.; Nishida, K.; Kanaya, T.; Yamada, N. L. Interfacial Properties of Polystyrene Thin Films as Revealed by Neutron Reflectivity. *Phys. Rev. E - Stat. Nonlinear, Soft Matter Phys.* **2011**, *84* (3), 31802–31808.

(48) Inoue, R.; Kawashima, K.; Matsui, K.; Kanaya, T.; Nishida, K.; Matsuba, G.; Hino, M. Distributions of Glass-Transition Temperature and Thermal Expansivity in Multilayered Polystyrene Thin Films Studied by Neutron Reflectivity. *Phys. Rev. E - Stat. Nonlinear, Soft Matter Phys.* **2011**, *83* (2), 31802–31808.

(49) Inoue, R.; Nakamura, M.; Matsui, K.; Kanaya, T.; Nishida, K.; Hino, M. Distribution of Glass Transition Temperature in Multilayered Poly(Methyl Methacrylate) Thin Film Supported on a Si Substrate as Studied by Neutron Reflectivity. *Phys. Rev. E - Stat. Nonlinear, Soft Matter Phys.* **2013**, *88* (3), 32601–32606.

Overall Conclusion

Although the polymer materials have been already studied for many years, there are only few researches on the change in the performance of the polymer materials from bulk to ultrathin film. In this PhD program, we have tried to clarify the change in the fundamental properties of the polymer ultrathin films with their structures by in-operando X-ray reflectivity analysis. We mainly studied the temperature-responsive changes in layers structures of different polymer ultrathin film systems, such as polyvinyl acetate thin film and poly(N-isopropylacrylamide) ultrathin film. Meanwhile we have also developed the new method for the preparation of polymer ultrathin film and implement the similar study on the new nylon 6 ultrathin film. After series control experiments, many abnormal physical and chemical phenomena have been confirmed in the ultrathin film systems.

Uniaxial Negative Thermal Expansion of Polyvinyl Acetate (PVAc) Thin Film. In the PVAc ultrathin film system, two different instances of negative thermal expansion (NTE) has been confirmed. When the temperature is higher than the glass transition temperature (T_g), a slow thickness can be observed even after the annealing, and when the temperature is lower than the T_g, a reversible NTE can be observed with temperature. On the other hand, it is also found that these NTEs can not only be thickness dependent but also vary with the temperature strategies. In the postulated model, the contribution of the constrained interface layer has been proposed. The different mobility of polymer chain between the interface layer and transition layer would contribute the internal stress with the dynamic motion, causing the additional structure in the ultrathin film system.

Asymmetric Change in Poly(N-isopropylacrylamide) (PNIPAM) Ultrathin Film with Temperature Cycle. In the PNIPAM ultrathin film system, the asymmetric thickness change has been confirmed during

the cooling and heating at the same temperature range under ambient conditions. One switching in the thickness decrease was found with cooling, while linear thickness increase was observed with heating. It is found that the thickness change is caused by the swelling and shrinking with the transition of PNIPAM between hydrophobic and hydrophilic state in temperature cycle. Considering the different activity energy of the polymer chain in the boundary layers, it is proposed that the transition ability of PNIPAM would be different at the surface and interface layer, which result in the asymmetric behaviors in temperature cycle.

The Discovering of Ultrathin Film Forming and Its Property. In this work, we have developed the physical method for the preparation of polymer ultrathin film which is difficult to be prepared with the sol-gel process. The nylon 6 ultrathin film has been prepared by physical vapor deposition (PVD) method. In the related characterization, the γ form crystalline has been confirmed in this ultrathin film, and it is proposed to be related to the mobility of the polymer chain on the surface of substrate, during the deposition. One the other hand, in the study of the thickness stability of the nylon 6 thin films, it is found that the swelling can happen in the nylon 6 thin film at the room conditions, and glass transition does not occur at temperatures ranging from 10 °C to 70 °C. It is suggested that the interface interaction and γ phase structure contracture to this property in nylon 6 ultrathin film.

In the doctoral program, although in-operando X-ray reflectivity analysis have been only conducted in the three general polymer ultrathin film system, these new finding would represent the unknown area in our knowledge. We believe that this nature should be also widely existed in different polymer ultrathin film system, such as the distribution/orientation and the activity energy of polymer chain with the effect of interface interaction. Meanwhile, the structure control in the preparation of semi-crystal polymer ultrathin film would be another interesting topic for the industry and academic. Undoubtedly, with the revolution of the in-operando X-ray reflectivity analysis technique, more and more new phenomena will be discovered as well, and these valuable experimental data will help us further explore the potential of ultra-thin film applications in the future.